USGS
science for a changing world

Prepared in cooperation with Bureau of Reclamation
acting as fiscal agent for the Middle Rio Grande Endangered Species Collaborative Program

Groundwater Hydrology and Estimation of Horizontal Groundwater Flux from the Rio Grande at Selected Locations in Albuquerque, New Mexico, 2009–10

Scientific Investigations Report 2016–5021

U.S. Department of the Interior
U.S. Geological Survey

Cover, Upstream view of the Rio Grande from a location about 1 mile southwest of the Montaño Bridge. Photograph was taken January 24, 2016, by Nathan Myers.

Groundwater Hydrology and Estimation of Horizontal Groundwater Flux from the Rio Grande at Selected Locations in Albuquerque, New Mexico, 2009–10

By Dale R. Rankin, Gretchen P. Oelsner, Kurt J. McCoy, Geoff J.M. Moret, Jeffrey A. Worthington, and Kimberly M. Bandy-Baldwin

Prepared in cooperation with Bureau of Reclamation
acting as fiscal agent for the Middle Rio Grande Endangered Species Collaborative Program

Scientific Investigations Report 2016–5021

U.S. Department of the Interior
U.S. Geological Survey

U.S. Department of the Interior
SALLY JEWELL, Secretary

U.S. Geological Survey
Suzette M. Kimball, Director

U.S. Geological Survey, Reston, Virginia: 2016

Suggested citation:
Rankin, D.R., Oelsner, G.P., McCoy, K.J., Moret, G.J.M., Worthington, J.A., and Bandy-Baldwin, K.M., 2016, Groundwater hydrology and estimation of horizontal groundwater flux from the Rio Grande at selected locations in Albuquerque, New Mexico, 2009–10: U.S. Geological Survey Scientific Investigations Report 2016–5021, 89 p., http://dx.doi.org/10.3133/sir20165021.

ISSN 2328-0328 (online)

Acknowledgments

The authors would like to recognize the efforts of others who contributed to the completion of this study. The City of Albuquerque's Open Space Division granted permission for the U.S. Geological Survey (USGS) to install and maintain piezometers in the Rio Grande riparian area along the river. The Middle Rio Grande Conservancy District granted permission for the USGS to install and maintain surface-water gages at various locations in the Corrales, Atrisco, and Albuquerque Riverside Drains. The Bernalillo County Commission granted permission for the USGS to install and maintain piezometers at various locations near the I-25 bridge and the Barelas Bridge.

The authors wish to recognize the support of committees associated with the Middle Rio Grande Endangered Species Collaborative Program, including the Executive Committee, the Science Subcommittee, and, in particular, members of the Species and Water Management Committee. We wish to acknowledge the assistance and guidance provided by Charles Fischer and Valda Terauds of the Bureau of Reclamation. In addition, we would like to thank the U.S. Army Corps of Engineers for the initial funding of the monitoring network, the installation of which preceded the interpretive work done in cooperation with the Bureau of Reclamation and the Middle Rio Grande Endangered Species Collaborative Program.

We would also like to acknowledge the technical assistance provided by Jeb Brown and Anthony Cox, hydrologic technicians in the USGS New Mexico Water Science Center, who performed the discharge measurements for the seepage investigation.

Contents

Abstract 1
Introduction 2
Purpose and Scope 13
Description of the Study Area 13
Inner Valley Alluvial Aquifer 13
Santa Fe Group Aquifer 13
Previous Investigations 13
Methods of Data Collection and Analysis 14
Piezometer Installation and Core Descriptions 14
Water-Level and Temperature Data 24
Slug Tests 24
Horizontal Hydraulic Gradients 25
Darcy Flux 27
Suzuki-Stallman Method for Estimating Heat Flux 27
Limitations and Assumptions of Suzuki-Stallman Method 29
Range of Applicability 29
Flow Direction 29
Aquifer Heterogeneity 29
Variable Recharge 29
Spatial Aliasing 29
Surface-Temperature Variations 30
Temperature Dependence of Hydraulic Conductivity 30
Uncertainty in Thermal Properties 30
Data Error 30
Groundwater Hydrology 30
Groundwater Levels and Temperatures 31
Horizontal Hydraulic Gradients 67
Hydraulic Conductivity 68
Estimation of Horizontal Groundwater Flux from the Rio Grande 71
Darcy Flux 71
Heat-Flux Modeling 74
Horizontal Groundwater-Flux Model Comparison 81
Riverside Drain Seepage Investigations 81
Variability of Horizontal Hydraulic Gradients and Groundwater Fluxes 84
Summary 86
References 87

Figures

1. Map showing location of study area and transects in the Albuquerque area, New Mexico 3
2. Map showing potentiometric-elevation contours, 2002, in the Santa Fe Group aquifer in the Albuquerque area and estimated groundwater-level declines from 1960 to 2002 4
3. Aerial photographs showing location of piezometer nests and surface-water gages, hydraulic head and water-table contours based on data collected during 2009, and the direction of groundwater flow at the *A*, Alameda (August 15, 2009); *B*, Paseo del Norte (September 26, 2009); *C*, Montaño (August 15, 2009); *D*, Central (August 15, 2009); *E*, Barelas (March 15, 2009); *F*, Rio Bravo (August 15, 2009); *G*, Pajarito (July 26, 2009); and *H*, I-25 (July 26, 2009) transects 5
4. Diagram showing how piezometer triangles were defined to compute daily mean hydraulic gradients on the west side of the Rio Grande at the I-25 transect 26
5. Graph showing type curves developed using equations 8 and 9 showing values of the parameters a and b as a function of specific flux, q_s 28
6. Hydrographs showing daily mean water-level altitude for stage of the Rio Grande and riverside drains and for groundwater levels in piezometers at *A*, Alameda transect 1; *B*, Alameda transect 2; *C*, Paseo del Norte transect 1; *D*, Paseo del Norte transect 2; *E*, Montaño transect 1; *F*, Montaño transect 2; *G*, Central transect 1; *H*, Central transect 2; *I*, Barelas transect 1; *J*, Barelas transect 2; *K*, Rio Bravo transect 1; *L*, Rio Bravo transect 2; *M*, Pajarito transect 1; *N*, Pajarito transect 2; *O*, I-25 transect 1; and *P*, I-25 transect 2 32
7. Daily mean water temperatures in the Rio Grande and riverside drains and daily mean groundwater temperatures in piezometers at *A*, Alameda transect 1; *B*, Alameda transect 2; *C*, Paseo del Norte transect 1; *D*, Paseo del Norte transect 2; *E*, Montaño transect 1; *F*, Montaño transect 2; *G*, Central transect 1; *H*, Central transect 2; *I*, Barelas transect 1; *J*, Barelas transect 2; *K*, Rio Bravo transect 1; *L*, Rio Bravo transect 2; *M*, Pajarito transect 1; *N*, Pajarito transect 2; *O*, I-25 transect 1; and *P*, I-25 transect 2 49
8. Graphs showing monthly vertical temperature profiles in piezometers, 2008–9 65
9. Boxplots of hydraulic conductivities estimated from slug tests conducted at selected locations in the Rio Grande inner valley alluvial aquifer, Albuquerque, New Mexico 70
10. Graphs showing daily mean Darcy flux calculated from daily mean hydraulic gradients and slug-test derived hydraulic conductivities, daily mean Darcy flux calculated from daily mean hydraulic gradients and a plausible range of hydraulic conductivities, and daily mean Rio Grande stage for the Alameda, Paseo del Norte, Montaño, and Central transects and the Barelas, Rio Bravo, Pajarito, and I-25 transects, Rio Grande inner valley alluvial aquifer, 2009–10 72
11. Boxplots showing summary of annual Darcy flux through the Rio Grande inner valley alluvial aquifer, Albuquerque, New Mexico, calculated using the Suzuki-Stallman method. 80

Tables

1. Site data for piezometers and surface-water data collection sites, Rio Grande inner valley alluvial aquifer, Albuquerque, New Mexico 15
2. Annual mean magnitude of groundwater horizontal hydraulic gradient and direction of groundwater flow at piezometer transects, Rio Grande inner valley alluvial aquifer, Albuquerque, New Mexico, 2009–10 67
3. Summary of slug-test results from piezometers in the Rio Grande inner valley alluvial aquifer, Albuquerque, New Mexico 68
4. Annual flux between individual time-series pairs and depths in the Rio Grande inner valley alluvial aquifer, Albuquerque, New Mexico, 2009–10 75
5. Comparison of Darcy's Law and Suzuki-Stallman method results for horizontal-groundwater flux in the Rio Grande inner valley alluvial aquifer, Albuquerque, Mexico 81
6. Seepage investigation discharge measurements and estimated uncertainty in Rio Grande riverside drains, Albuquerque, New Mexico, February 10–12, 2010 82
7. Comparison of annual mean horizontal hydraulic gradient and annual median flux at selected locations calculated for Report 1 (2003–9) and Report 2 (the current report, 2009–10) 85

Conversion Factors

Inch/Pound to International System of Units

Multiply	By	To obtain
	Length	
inch (in.)	2.54	centimeter (cm)
inch (in.)	25.4	millimeter (mm)
foot (ft)	0.3048	meter (m)
mile (mi)	1.609	kilometer (km)
	Area	
square mile (mi^2)	2.590	square kilometer (km^2)
	Volume	
cubic foot (ft^3)	0.02832	cubic meter (m^3)
	Flow rate	
foot per day (ft/d)	0.3048	meter per day (m/d)
cubic foot per second (ft^3/s)	0.02832	cubic meter per second (m^3/s)
cubic foot per day (ft^3/d)	0.02832	cubic meter per day (m^3/d)
	Thermal Conductivity	
British thermal unitIT per hour foot degree Fahrenheit (BTUIT hr-1 ft-1 °F-1)	1.730	watt per meter Kelvin (W m-1 K-1)
	Volumetric Heat Capacity	
British thermal unit IT cubic foot degree Fahrenheit (BTUIT ft-3 °F-1)	67,070	joule per cubic meter Kelvin (J m-3 K-1)

Temperature in degrees Celsius (°C) may be converted to degrees Fahrenheit (°F) as °F = (1.8 × °C) + 32.

Temperature in degrees Fahrenheit (°F) may be converted to degrees Celsius (°C) as °C = (°F – 32) / 1.8.

Datum

Vertical coordinate information is referenced to the North American Vertical Datum of 1988 (NAVD 88) or National Geodetic Vertical Datum of 1929 (NGVD 29).

Horizontal coordinate information is referenced to the North American Datum of 1983 (NAD 83).

Groundwater Hydrology and Estimation of Horizontal Groundwater Flux from the Rio Grande at Selected Locations in Albuquerque, New Mexico, 2009–10

By Dale R. Rankin,[1] Gretchen P. Oelsner,[1] Kurt J. McCoy,[2] Geoff J.M. Moret,[3] Jeffrey A. Worthington,[1] and Kimberly M. Bandy-Baldwin[4]

Abstract

The Albuquerque area of New Mexico has two principal sources of water: (1) groundwater from the Santa Fe Group aquifer system, and (2) surface water from the Rio Grande. From 1960 to 2002, pumping from the Santa Fe Group aquifer system caused groundwater levels to decline more than 120 feet while water-level declines along the Rio Grande in Albuquerque were generally less than 40 feet. These differences in water-level declines in the Albuquerque area have resulted in a great deal of interest in quantifying the river-aquifer interaction associated with the Rio Grande.

In 2003, the U.S. Geological Survey, in cooperation with the Bureau of Reclamation, acting as fiscal agent for the Middle Rio Grande Endangered Species Collaborative Program, and the U.S. Army Corps of Engineers, began a study to characterize the hydrogeology of the Rio Grande inner valley alluvial aquifer in the Albuquerque area of New Mexico. The study provides hydrologic data in order to enhance the understanding of rates of water leakage from the Rio Grande to the alluvial aquifer, groundwater flow through the aquifer, and discharge of water from the aquifer to riverside drains. The study area extends about 20 miles along the Rio Grande in the Albuquerque area. Piezometers and surface-water gages were installed in paired transects at eight locations. Nested piezometers, completed at various depths in the alluvial aquifer, and surface-water gages, installed in the Rio Grande and riverside drains, were instrumented with pressure transducers. Water-level and water-temperature data were collected from 2009 to 2010.

Water levels from the piezometers indicated that groundwater movement was usually away from the river towards the riverside drains. Annual mean horizontal groundwater gradients in the inner valley alluvial aquifer ranged from 0.0024 (I-25 East) to 0.0144 (Pajarito East). The median hydraulic conductivity values of the inner valley alluvial aquifer, determined from slug tests, ranged from 30 feet per day (ft/d) (Montaño) to 120 ft/d (Central) for paired transects, with a median hydraulic conductivity for all transects of 50 ft/d. Daily mean groundwater fluxes from the river through the inner valley alluvial aquifer computed using Darcy's Law and the slug test results ranged from about 0.01 ft/d (Montaño West) to between 1.0 and 2.0 ft/d (Central East). Median annual groundwater fluxes from the river through the inner valley alluvial aquifer determined using the Suzuki-Stallman method was greatest at Alameda East (0.50 ft/d) and lowest at Alameda West (0.25 ft/d). The results from both methods agreed reasonably well.

Seepage investigations conducted by measuring discharge in the east and west riverside drains provided information for computing changes in flow within the drains and for evaluating results from Darcy's Law and Suzuki-Stallman method flux calculations. Discharge measured in the east riverside drain between the Barelas Bridge and the I-25 bridge indicated that the flow in the east riverside drain increased by an average of 56.5 cubic feet per day per linear foot ($ft^3/d/ft$) of drain. Discharge measured in the west riverside drain between the Central bridge and the I-25 bridge indicated that flow increased between west drain miles 0 and 4, an average of 53.8 $ft^3/d/ft$ of drain, and that flow increased between west drain miles 7 and 10, an average of 44.9 $ft^3/d/ft$ of drain. In comparison to the seepage measurement results, the groundwater fluxes from the river through the inner valley alluvial aquifer calculated from Darcy's Law (q_{slug}) and by the Suzuki-Stallman method (q_{heat}) would account for 20–36 percent or 53–95 percent, respectively, of the total flow in the east riverside drain and 22–31 percent or 19–26 percent, respectively, of the total flow in the west drain. These results indicate that the drains likely also receive water from outside the inner valley.

[1]U.S. Geological Survey, New Mexico Water Science Center, 5338 Montgomery Blvd. NE, Albuquerque, NM, 87059.

[2]U.S. Geological Survey, Virginia Water Science Center, 1730 East Parham Road, Richmond, VA, 23228.

[3]University of Idaho, Department of Fish and Wildlife Resources, P.O. Box 441136, Moscow, ID, 83844.

[4]Colorado School of Mines, Department of Geology and Geological Engineering, 1516 Illinois St., Golden, CO, 80401.

The spatial variability of horizontal hydraulic gradients and groundwater fluxes can be primarily attributed to variability in the distances between the river and riverside drains throughout the study area and geologic heterogeneities in the alluvial aquifer. Temporal variability in the water levels, which control the horizontal hydraulic gradients and fluxes between the Rio Grande and the riverside drains, can be primarily attributed to seasonal fluctuations in river stage and irrigation practices.

Introduction

The Albuquerque area (fig. 1) is the major population center in New Mexico and covers about 400 square miles (mi^2). With a population of about 535,000 people in 2000, the Albuquerque area accounts for 29 percent of the State's population (U.S. Census Bureau, 2000). Currently (2015), there are two principal sources of water for municipal, domestic, commercial, and industrial uses in this area: (1) groundwater from the Santa Fe Group aquifer system, and (2) surface water from the Rio Grande. The Rio Grande, which flows from north to south through New Mexico, is the principal source of water for irrigated agriculture in the State (McAda, 1996). Estimates indicated that from 1960 to 2002, pumping from the Santa Fe Group aquifer system caused groundwater levels in eastern Albuquerque to decline more than 120 feet (ft) while water-level declines along the Rio Grande in Albuquerque were generally less than 40 ft (Bexfield and Anderholm, 2002; fig. 2). These differences in water-level declines in the Albuquerque area have resulted in a great deal of interest in quantifying the river-aquifer interaction associated with the Rio Grande.

The aquifer system in the Albuquerque area consists of the Santa Fe Group (middle Tertiary to Quaternary age) and the post-Santa Fe Group (Quaternary age) alluvium and is hereafter referred to as the "Santa Fe Group aquifer system." The Rio Grande is hydraulically connected to the Santa Fe Group aquifer system (McAda, 1996) where fluvial gravel, sand, silt, and clay deposits of the post-Santa Fe Group alluvium form a thin but extensive aquifer zone below the Rio Grande flood plain (Hawley and Whitworth, 1996), referred to as the "inner valley alluvial aquifer" in this report. The inner valley alluvial aquifer is composed of channel, flood-plain, and tributary deposits that are as much as 120 ft thick. Previous researchers have used streambed permeameters (Gould, 1994), the transient response of the aquifer to a flood pulse (Roark, 2001), vertical profiles of temperature measurements (Bartolino and Niswonger, 1999), and calibrated numerical models (Kernodle and others, 1995; Tiedeman and others, 1998; McAda and Barroll, 2002) to estimate the flux between the Rio Grande and the Santa Fe Group aquifer system. Currently, basin-scale groundwater models are used for water-resource administration purposes (Barroll, 2001) and for assessing stream depletion (Tiedeman and others, 1998; Barroll, 2001; McAda and Barroll, 2002). As compared to previous more regional-scale studies, this study was designed to focus on the shallow part (about the upper 50 ft) of the inner valley alluvial aquifer and provide spatially detailed information about the amount of water that discharges from the Rio Grande to the adjacent aquifer in the Albuquerque area.

In 2003, the U.S. Geological Survey (USGS), in cooperation with the Bureau of Reclamation (BOR), acting as fiscal agent for the Middle Rio Grande Endangered Species Collaborative Program (MRGESCP), and the U.S. Army Corps of Engineers (USACE), began a study to characterize the hydrogeology of the Rio Grande inner valley alluvial aquifer in the Albuquerque area of New Mexico. Study results provide hydrologic data and enhance the understanding of rates of water leakage from the Rio Grande to the inner valley alluvial aquifer, groundwater flow through the aquifer, and discharge of water from the aquifer to the riverside drains. Beginning in late 2003 through 2008, a total of 16 east-west trending hydrologic transects were installed along both sides of the Rio Grande through the Albuquerque area at 8 selected locations (fig. 1). Each location consists of paired transects of piezometers installed between the river and riverside drains to evaluate the rate of leakage from the river to riverside drains. In some cases (fig. 3*A–H*), piezometers were installed at various distances outside the drains. Surface-water gages also were installed in the river and in the east and west riverside drains. Lithologic information collected during drilling and hourly groundwater-level and water-temperature data and vertical temperature profile data collected during the study were used to define a conceptual model of flow in the Rio Grande inner valley alluvial aquifer adjacent to the river.

As part of the ongoing study of water leakage from the Rio Grande to the inner valley alluvial aquifer, the USGS, in cooperation with BOR acting as fiscal agent for the MRGESCP, used two methods to quantify groundwater flux at depths less than 30 ft below land surface (bls) with data collected during 2009 and 2010. In the first method, Darcy's Law and estimates of hydraulic conductivity from slug tests and the literature are used to assess the variability in river leakage attributed to temporal changes in hydraulic gradient. In the second method, the Suzuki-Stallman one-dimensional analytical solution to the heat-transport equation (Suzuki, 1960; Stallman, 1965) is used to model annual groundwater-temperature changes within the aquifer that result from river leakage. Temperature models provide additional detail on groundwater flux with depth and distance from the river in the Albuquerque area.

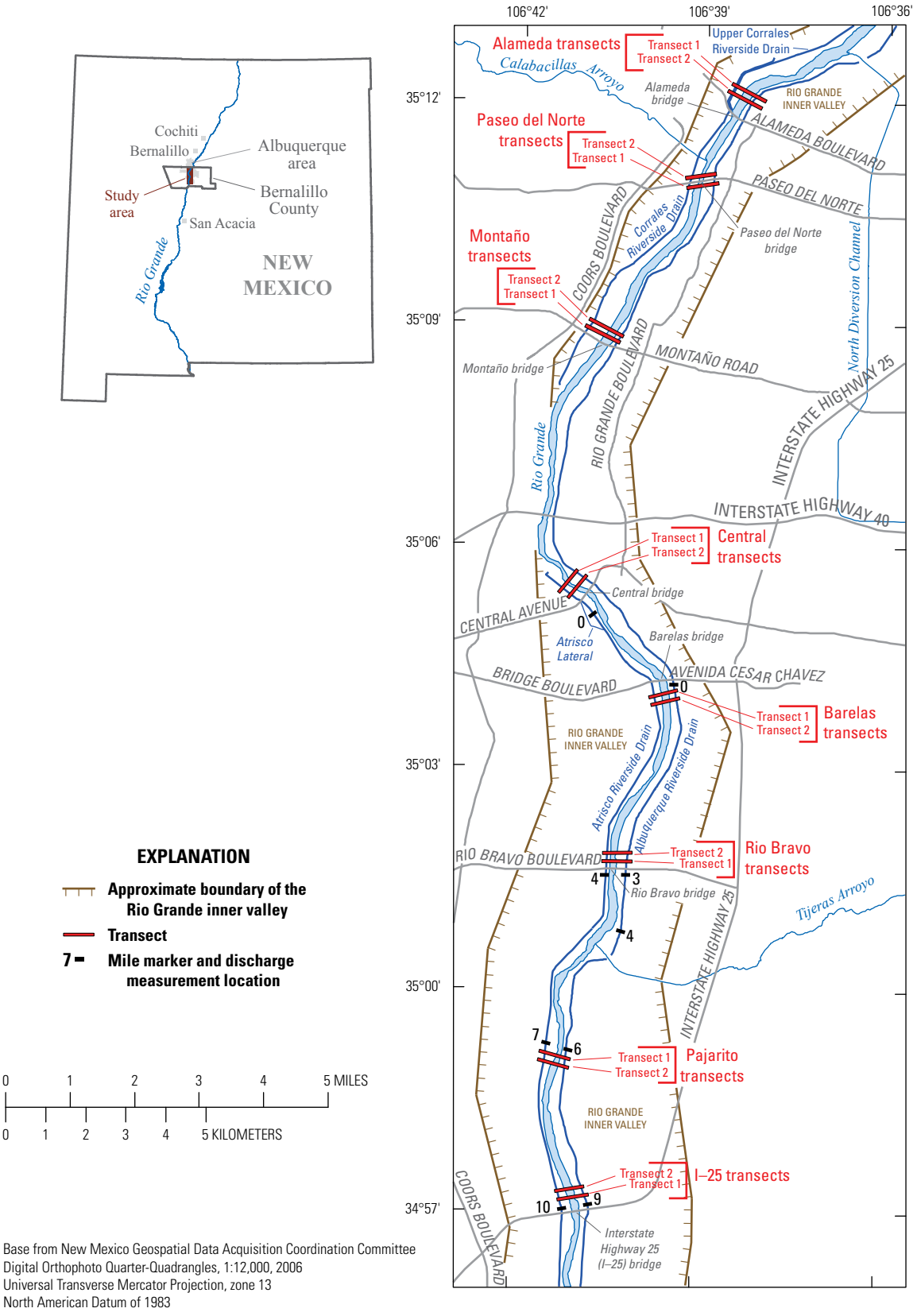

Base from New Mexico Geospatial Data Acquisition Coordination Committee
Digital Orthophoto Quarter-Quadrangles, 1:12,000, 2006
Universal Transverse Mercator Projection, zone 13
North American Datum of 1983

Figure 1. Location of study area and transects in the Albuquerque area, New Mexico.

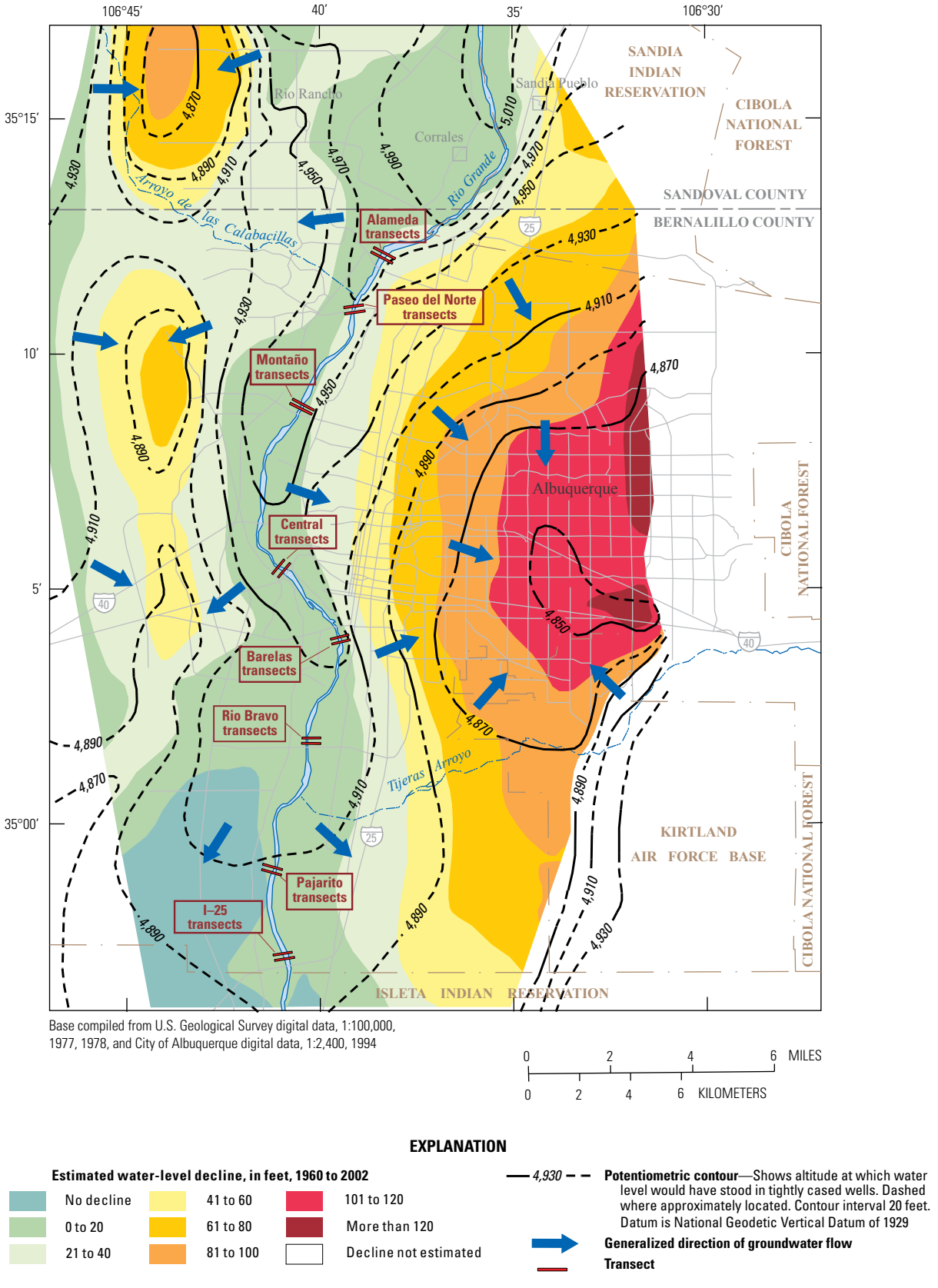

Figure 2. Potentiometric-elevation contours, 2002, in the Santa Fe Group aquifer in the Albuquerque area and estimated groundwater-level declines from 1960 to 2002 (modified from Bexfield and Anderholm, 2002).

Figure 3. Location of piezometer nests and surface-water gages, hydraulic head and water-table contours based on data collected during 2009, and the direction of groundwater flow at the *A*, Alameda (August 15, 2009); *B*, Paseo del Norte (September 26, 2009); *C*, Montaño (August 15, 2009); *D*, Central (August 15, 2009); *E*, Barelas (March 15, 2009); *F*, Rio Bravo (August 15, 2009); *G*, Pajarito (July 26, 2009); and *H*, I-25 (July 26, 2009) transects.

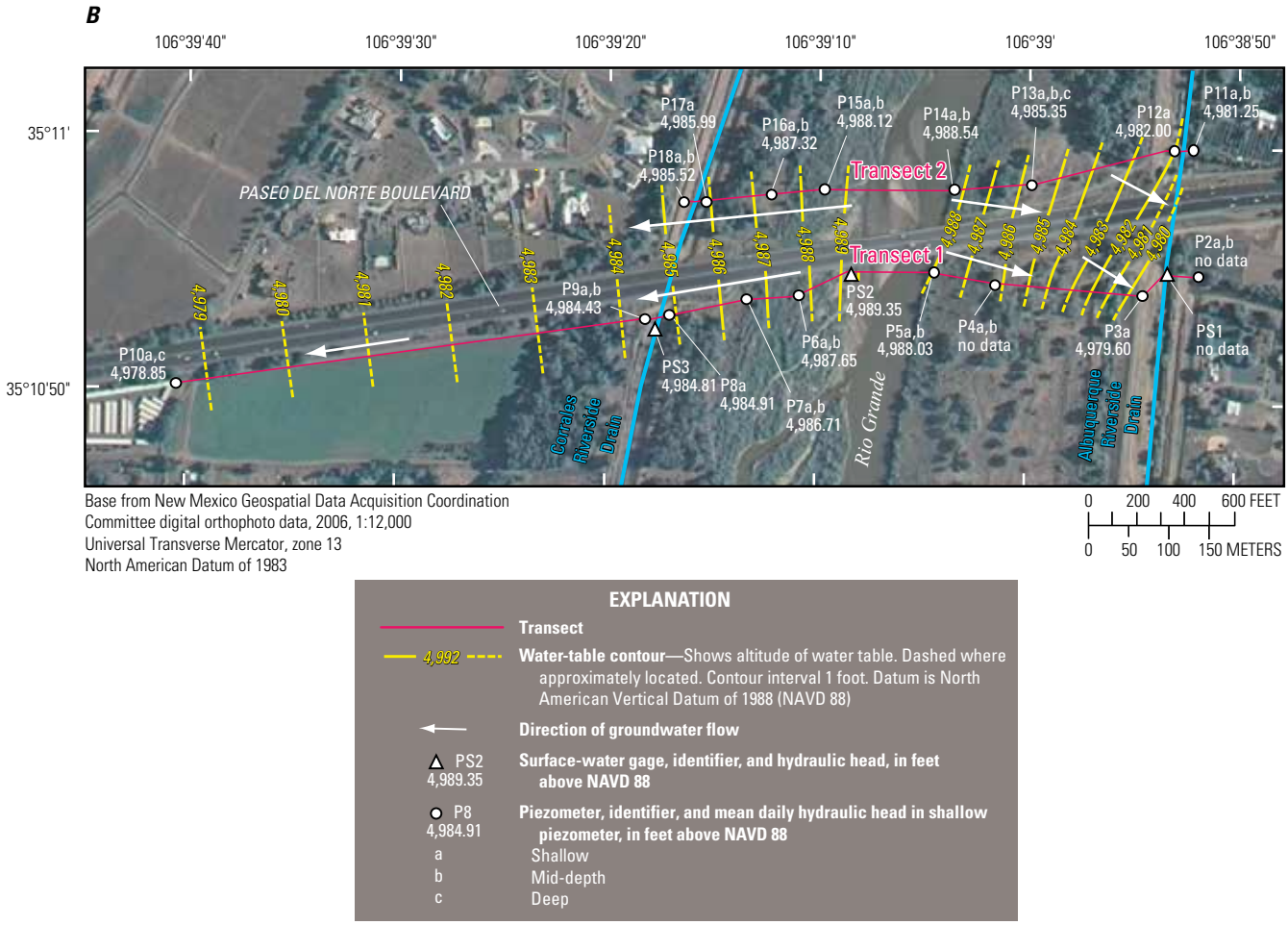

Figure 3. Location of piezometer nests and surface-water gages, hydraulic head and water-table contours based on data collected during 2009, and the direction of groundwater flow at the *A*, Alameda (August 15, 2009); *B*, Paseo del Norte (September 26, 2009); *C*, Montaño (August 15, 2009); *D*, Central (August 15, 2009); *E*, Barelas (March 15, 2009); *F*, Rio Bravo (August 15, 2009); *G*, Pajarito (July 26, 2009); and *H*, I-25 (July 26, 2009) transects.—Continued

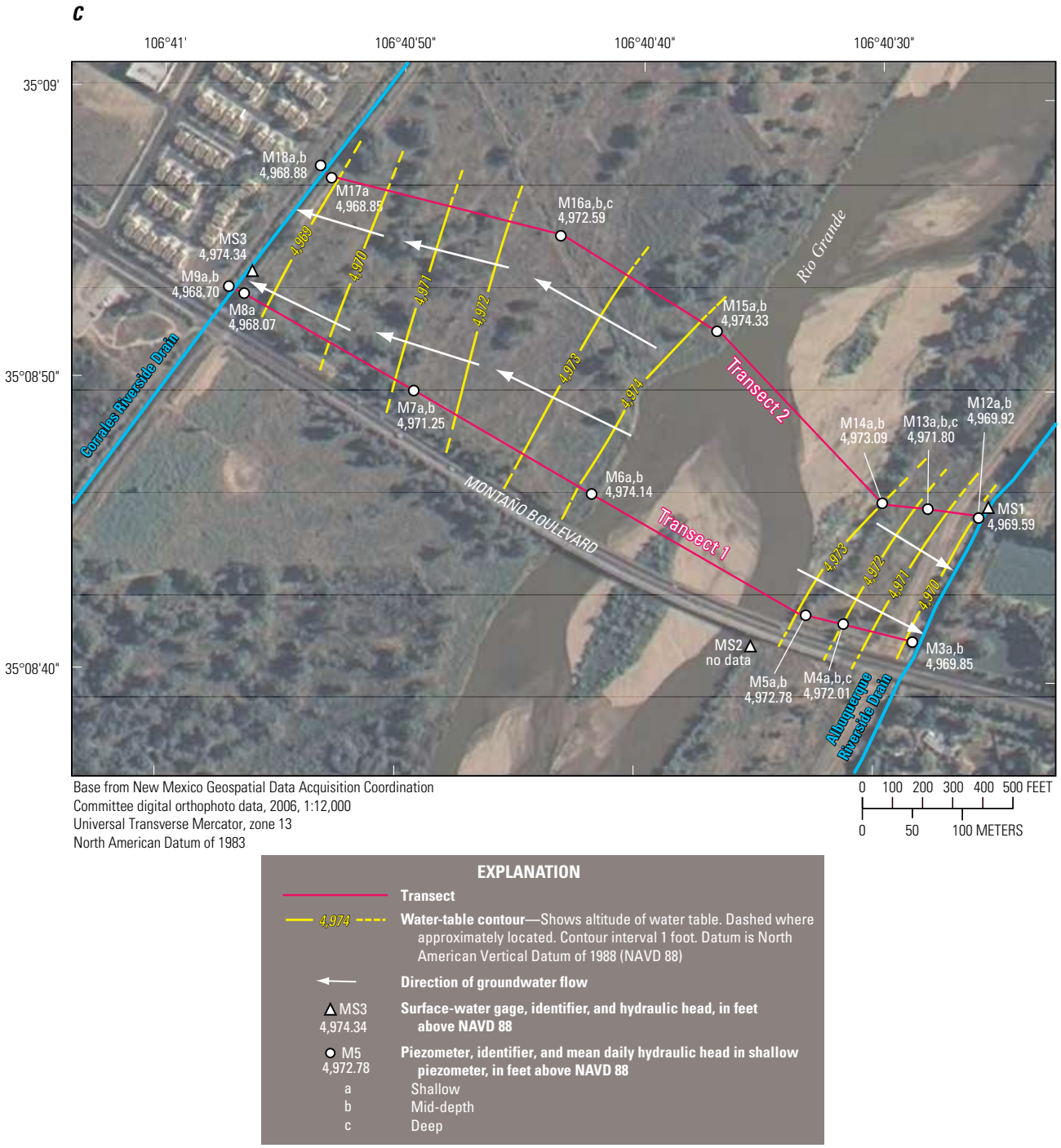

Figure 3. Location of piezometer nests and surface-water gages, hydraulic head and water-table contours based on data collected during 2009, and the direction of groundwater flow at the *A*, Alameda (August 15, 2009); *B*, Paseo del Norte (September 26, 2009); *C*, Montaño (August 15, 2009); *D*, Central (August 15, 2009); *E*, Barelas (March 15, 2009); *F*, Rio Bravo (August 15, 2009); *G*, Pajarito (July 26, 2009); and *H*, I-25 (July 26, 2009) transects.—Continued

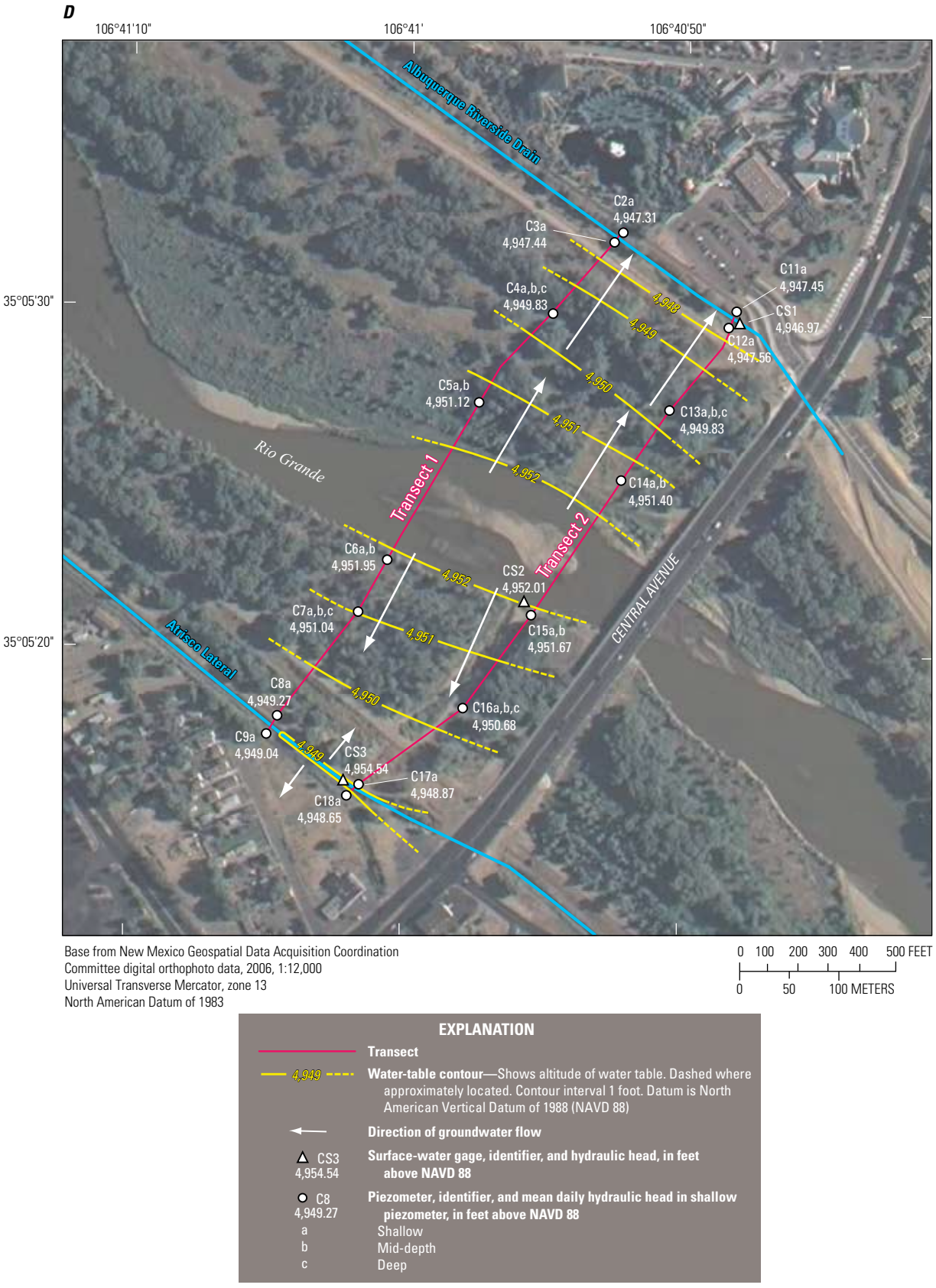

Figure 3. Location of piezometer nests and surface-water gages, hydraulic head and water-table contours based on data collected during 2009, and the direction of groundwater flow at the *A*, Alameda (August 15, 2009); *B*, Paseo del Norte (September 26, 2009); *C*, Montaño (August 15, 2009); *D*, Central (August 15, 2009); *E*, Barelas (March 15, 2009); *F*, Rio Bravo (August 15, 2009); *G*, Pajarito (July 26, 2009); and *H*, I-25 (July 26, 2009) transects.—Continued

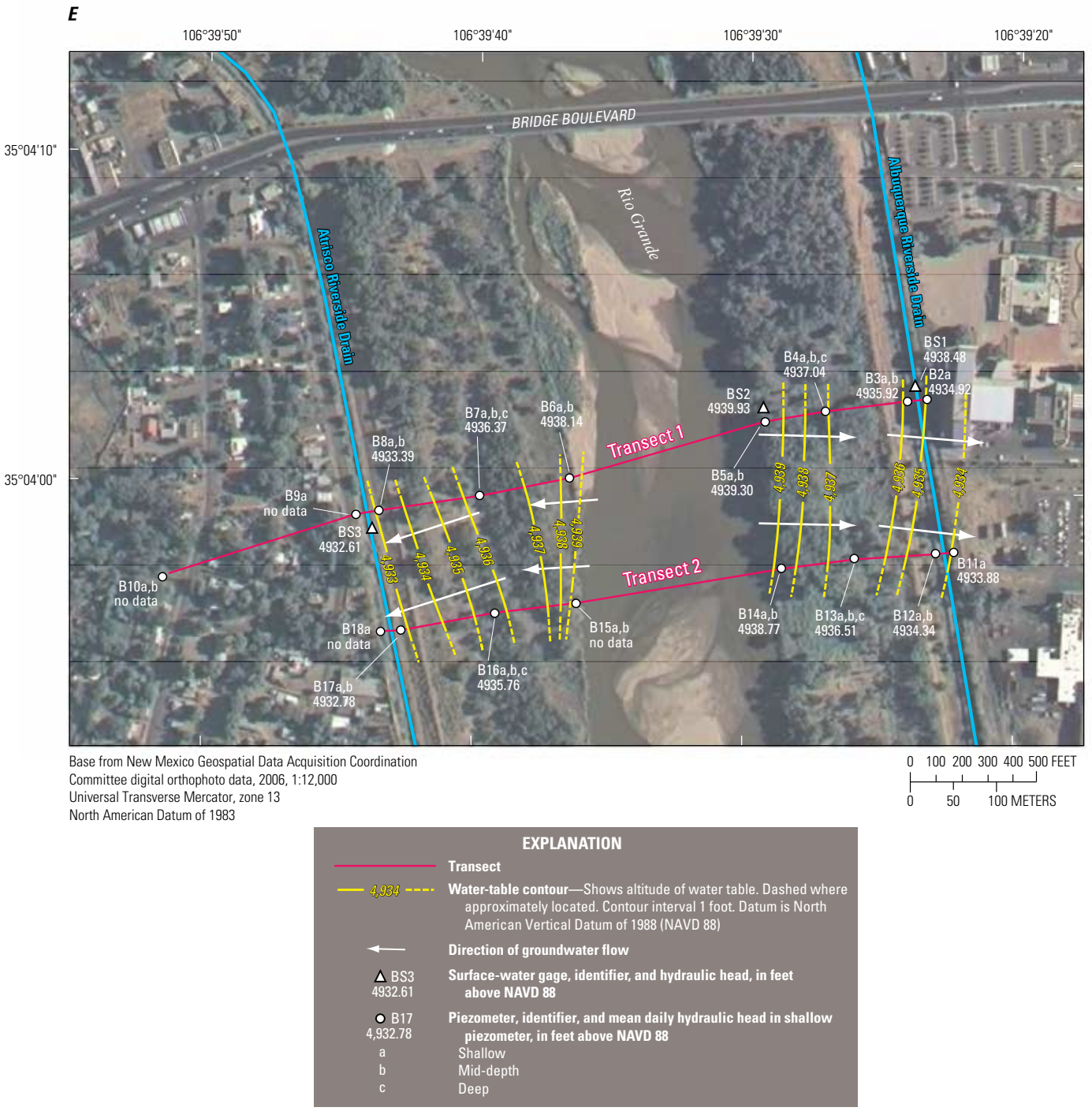

Figure 3. Location of piezometer nests and surface-water gages, hydraulic head and water-table contours based on data collected during 2009, and the direction of groundwater flow at the *A*, Alameda (August 15, 2009); *B*, Paseo del Norte (September 26, 2009); *C*, Montaño (August 15, 2009); *D*, Central (August 15, 2009); *E*, Barelas (March 15, 2009); *F*, Rio Bravo (August 15, 2009); *G*, Pajarito (July 26, 2009); and *H*, I-25 (July 26, 2009) transects.—Continued

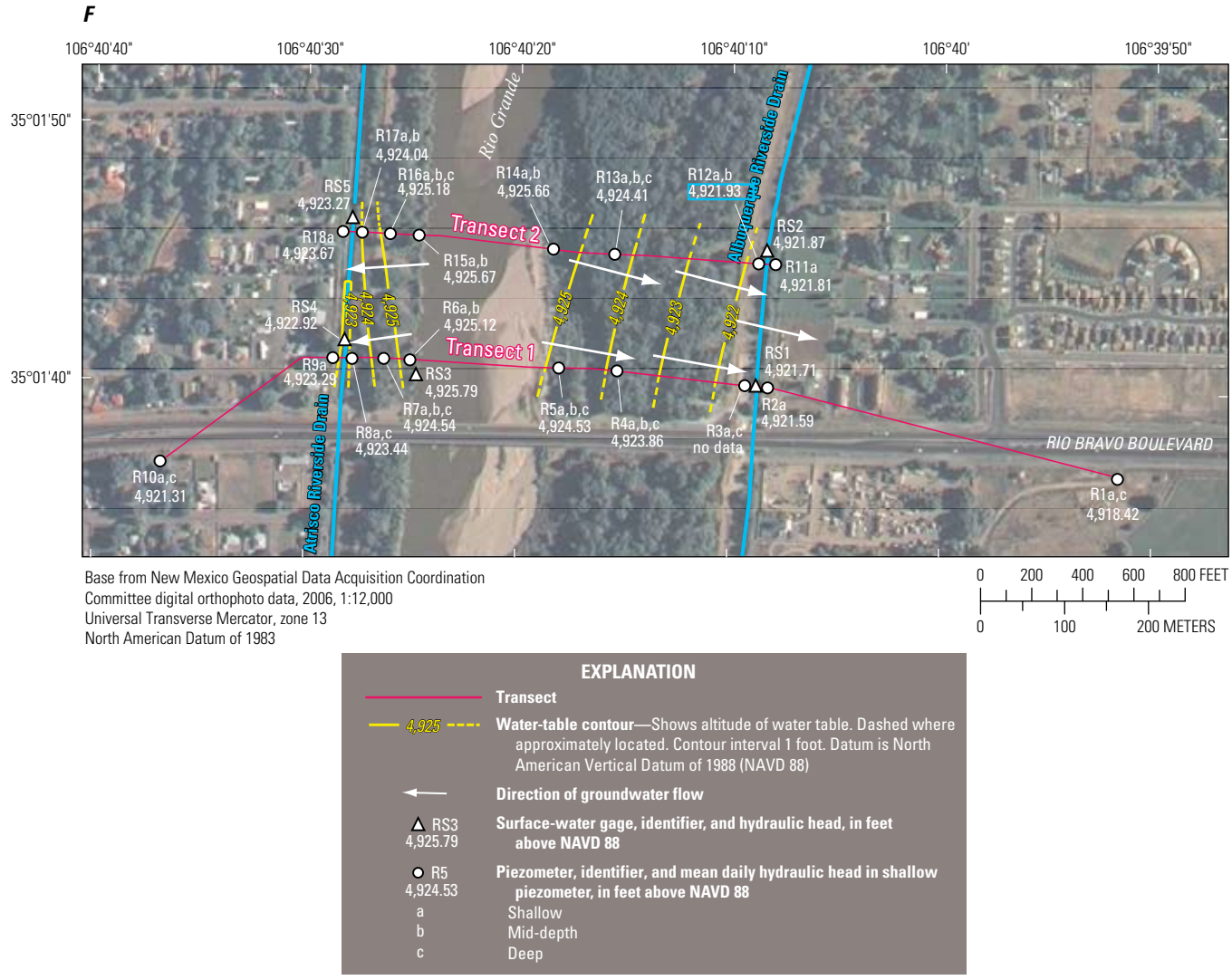

Figure 3. Location of piezometer nests and surface-water gages, hydraulic head and water-table contours based on data collected during 2009, and the direction of groundwater flow at the *A*, Alameda (August 15, 2009); *B*, Paseo del Norte (September 26, 2009); *C*, Montaño (August 15, 2009); *D*, Central (August 15, 2009); *E*, Barelas (March 15, 2009); *F*, Rio Bravo (August 15, 2009); *G*, Pajarito (July 26, 2009); and *H*, I-25 (July 26, 2009) transects.—Continued

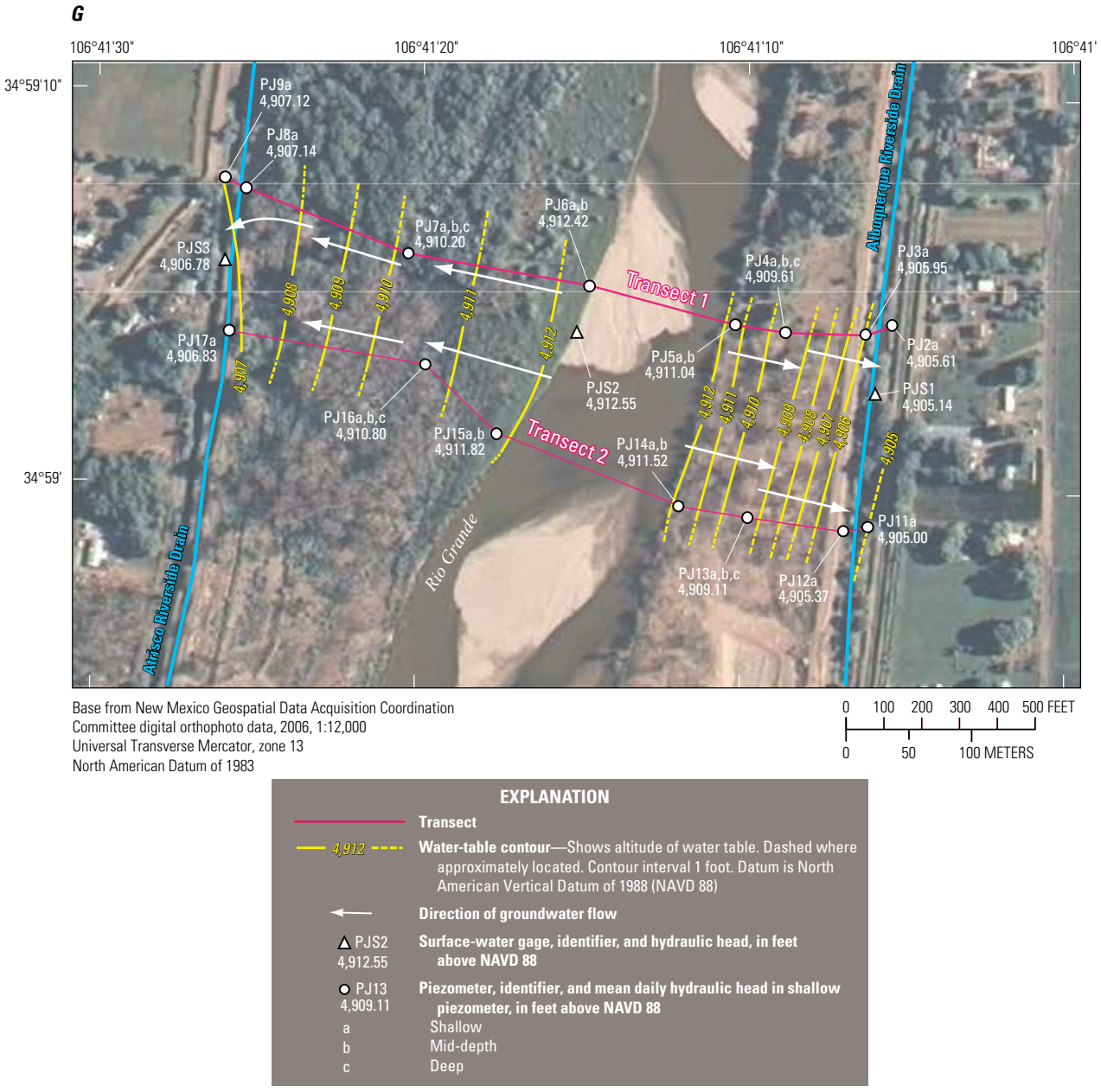

Figure 3. Location of piezometer nests and surface-water gages, hydraulic head and water-table contours based on data collected during 2009, and the direction of groundwater flow at the *A*, Alameda (August 15, 2009); *B*, Paseo del Norte (September 26, 2009); *C*, Montaño (August 15, 2009); *D*, Central (August 15, 2009); *E*, Barelas (March 15, 2009); *F*, Rio Bravo (August 15, 2009); *G*, Pajarito (July 26, 2009); and *H*, I-25 (July 26, 2009) transects.—Continued

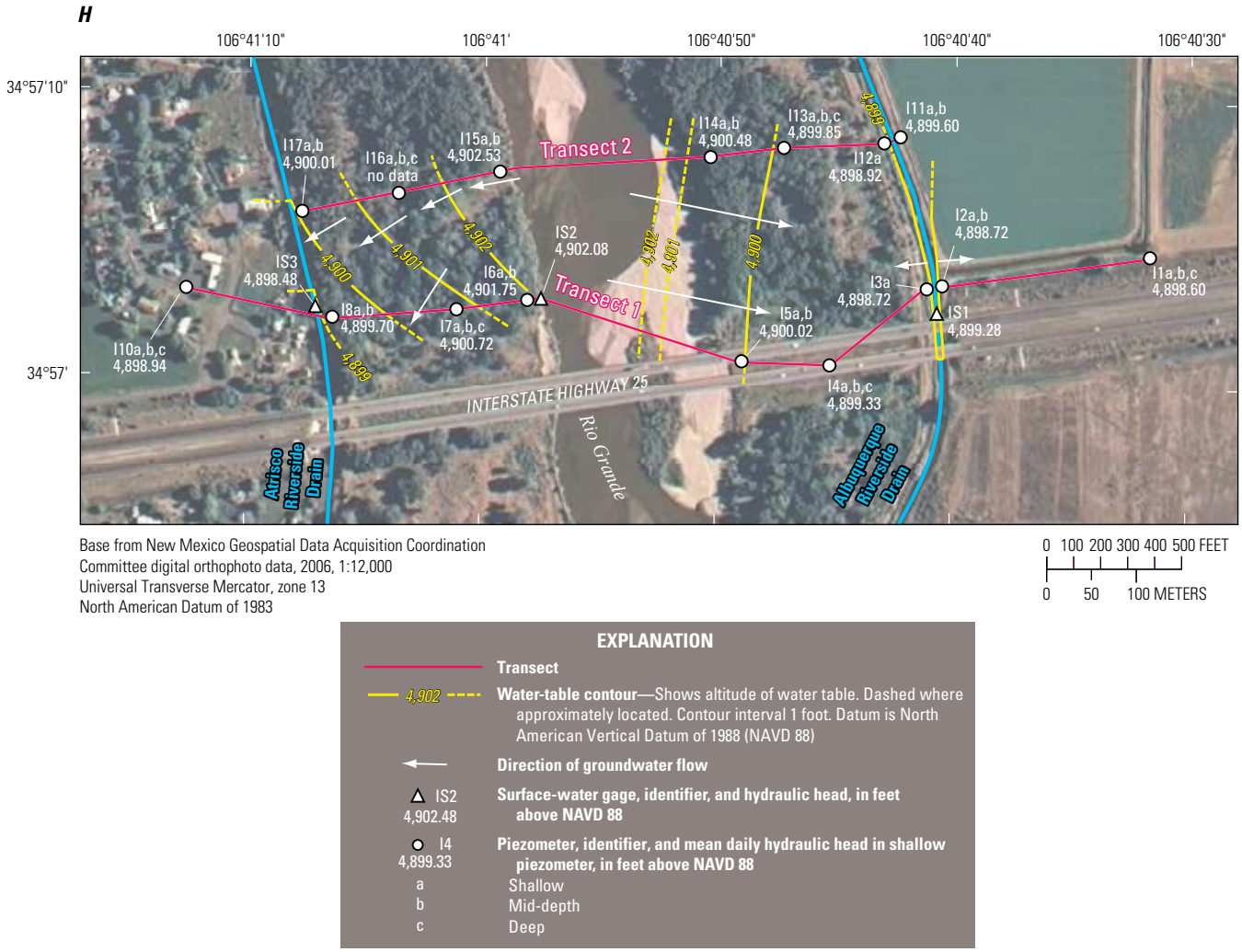

Figure 3. Location of piezometer nests and surface-water gages, hydraulic head and water-table contours based on data collected during 2009, and the direction of groundwater flow at the *A*, Alameda (August 15, 2009); *B*, Paseo del Norte (September 26, 2009); *C*, Montaño (August 15, 2009); *D*, Central (August 15, 2009); *E*, Barelas (March 15, 2009); *F*, Rio Bravo (August 15, 2009); *G*, Pajarito (July 26, 2009); and *H*, I-25 (July 26, 2009) transects.—Continued

Purpose and Scope

This report documents the groundwater hydrology of the Rio Grande inner valley alluvial aquifer based on groundwater and surface-water data collected from February 2009 to February 2010 in the Albuquerque area of New Mexico. Horizontal groundwater flux from the Rio Grande to the inner valley alluvial aquifer was estimated using two methods: (1) Darcy's Law, and (2) the Suzuki-Stallman method of heat transport. The scope of this study included collection of data from 16 transects at 8 locations in the Albuquerque area: the Alameda, Paseo del Norte, Montaño, Central, Barelas, and Rio Bravo bridges, Pajarito, and the I-25 bridge (fig. 1). Data collected from the first 10 paired transects installed at the Paseo del Norte, Montaño, Barelas, Rio Bravo, and I-25 bridges between December 2003 and February 2009 are presented in Rankin and others (2013) (hereafter referred to as "Report 1"). Report 1 also presented a simple conceptual model of groundwater flow and groundwater-flux results. This report presents groundwater and surface-water levels, temperature, slug-test data, and seepage measurements collected from February 2009 through February 2010 at all 16 transects. Additionally, this report compares the results from Report 1 to the results presented in this report for February 2009 through February 2010.

Description of the Study Area

The study area extends about 20 miles (mi) along the Rio Grande in the Albuquerque area from the Alameda bridge to the I-25 bridge (fig. 1). The Rio Grande inner valley (fig. 1) is approximately 2–3 mi wide and slopes about 5–6 feet per mile (ft/mi) southward through the Albuquerque area. The east and west edges of the study area are limited to areas within the inner valley adjacent to the Upper Corrales, Corrales, Albuquerque, and Atrisco Riverside Drains (fig. 1). The Rio Grande has a densely vegetated riparian area that supports a variety of biological communities. The riverside drains are ditches located east and west of the river, are generally separated from the river by levees, and are designed to intercept lateral groundwater flow from the river and prevent waterlogged-soil conditions east and west of the river in the inner valley. Seepage to the riverside drains constitutes one of the main sources of groundwater discharge from the inner valley alluvial aquifer (Kernodle and others, 1995). Snowmelt runoff and irrigation seasons influence the hydrology of the study area. There are roughly four hydrologic seasons in the study area: (1) snowmelt and irrigation (March–April), (2) post snowmelt and irrigation (May–June), (3) monsoon and irrigation (July–October), and (4) nonirrigation (November–February).

Inner Valley Alluvial Aquifer

The inner valley alluvial aquifer consists of post-Santa Fe Group river-valley and basin-fill sediments that underlie the present-day Rio Grande flood plain (Hawley and Haase, 1992). In the Albuquerque area, the alluvium consists of unconsolidated to poorly consolidated, fine- to coarse-grain sand and rounded gravel with subordinate, discontinuous lens-shaped interbeds of fine-grain sand, silt, and clay (Connell and others, 2007). These deposits represent the last cut-and-fill cycle of the expansion of the Rio Grande fluvial system (Connell and others, 2007) and form an extensive shallow aquifer along the Rio Grande in the Albuquerque area. Hawley and Haase (1992) indicate that these channel and flood-plain deposits may be as much as 130-ft thick with an average thickness of 80 ft. Connell and others (2007) suggest that the inner valley probably was excavated during the Pleistocene epoch (about 1.8 million to 11,500 years before present) and subsequently was filled to near its present level by the middle Holocene epoch (about 8,000 to 5,000 years before present).

Santa Fe Group Aquifer

The middle Tertiary to Quaternary-age Santa Fe Group aquifer, which underlies the inner valley alluvial aquifer, is composed primarily of gravel, sand, silt, and clay. Most of these sediments were transported into fault-bounded basins of the Rio Grande by rivers and drainages from surrounding areas (Bartolino and Cole, 2002). The spatial distribution of sedimentary facies in these deposits tends to be complex and three-dimensional rather than a simple, layered system (Bartolino and Cole, 2002; Engdahl and others, 2010).

Approximately 14,000-ft thick in parts of the basin, the Santa Fe Group is divided into upper, middle, and lower hydrostratigraphic units (Hawley and Haase, 1992). Sediments in the upper Santa Fe unit were deposited during the development of the ancestral Rio Grande and contain intertongued piedmont-slope and fluvial basin-floor deposits as thick as 1,200 ft (Hawley and Haase, 1992). Coarse-grain sediments compose the ancestral Rio Grande axial-channel deposits contained in the upper unit of the Santa Fe Group. Sediments in the middle Santa Fe unit include piedmont-slope deposits, fluvial basin-floor deposits, and basin-floor playa deposits (Hawley and Haase, 1992). This middle unit contains the largest accumulation of sediment and is as much as 10,000-ft thick. Sediments in the lower Santa Fe unit are predominantly piedmont-slope, eolian, and basin-floor playa deposits and are as much as 3,500-ft thick (Hawley and Haase, 1992).

Previous Investigations

The interaction of groundwater and surface water in the Albuquerque area has been the focus of a number of investigations. McAda (1996) described the components of the Rio Grande and Santa Fe Group aquifer system in the Albuquerque area and prioritized activities to better understand groundwater and surface-water interaction. Peter (1987) compared differences in the configuration of the water table near the Rio Grande in the Albuquerque area from 1936

to 1986 and briefly described groundwater and surface-water interaction. Engdahl and others (2010) examined the effects of lithologic heterogeneity on the exchange of water between the surface and subsurface near the Rio Bravo bridge. Using the same dataset and high-resolution groundwater-flow modeling, Engdahl and Weissmann (2010) showed that the rate of simulated contaminant transport in heterogeneous realizations of the alluvial aquifer is dependent on the direction of groundwater flow relative to bedding and is sensitive to scale. Bartolino (2003) used groundwater levels and temperature data to evaluate groundwater fluxes in a single piezometer transect near the Paseo del Norte bridge. Bartolino and Niswonger (1999) measured groundwater levels and vertical temperature profiles near the Paseo del Norte and Rio Bravo bridges to simulate vertical groundwater flux and estimate vertical hydraulic conductivity. Bartolino and Sterling (2000) delineated specific areas on both sides of the river between the Paseo del Norte bridge and Rio Bravo bridge that contain hydrologically significant clay-rich layers. Moret (2007), using an analytical method developed by Suzuki (1960) and Stallman (1965), estimated groundwater flux from the river to the aquifer near the Paseo del Norte bridge to be 1.2-1.6 cubic meters per day per meter of riverbank (12.9 to 17.2 cubic feet per day per linear foot [ft^3/d/ft] of riverbank).

The projected movement of groundwater in the Albuquerque area has been described by Kernodle and others (1995) and Bexfield and McAda (2003); these authors simulated historic and hypothetical groundwater flow in the Santa Fe Group aquifer system. The direction of groundwater flow prior to widespread development of the Santa Fe Group aquifer (about 1961) in the Albuquerque area generally was from north-northeast to south-southwest (Bexfield and Anderholm, 2000). Water-level declines and directions of groundwater flow resulting from development of the Santa Fe Group aquifer since 1961 have been estimated by Bexfield and Anderholm (2002), Falk and others (2011), and Powell and McKean (2014); the authors reported groundwater declines in the Albuquerque area of as much as 120 ft and shifts in groundwater-flow direction away from the Rio Grande and towards clusters of supply wells in the east, north, and west of the area shown in figure 2.

McAda and Barroll (2002) simulated groundwater flow using a three-dimensional groundwater-flow model of the Santa Fe Group aquifer system from Cochiti to San Acacia. Sanford and others (2003) used environmental tracers to estimate aquifer parameters for a predevelopment groundwater-flow model in the Middle Rio Grande Basin.

Kues (1986) described the movement of shallow groundwater near the Rio Grande between the Barelas Bridge and the I-25 bridge based on water-level measurements from 44 wells. Anderholm and Bullard (1987) described the installation of piezometers in the Albuquerque area and provided lithologic descriptions from monitoring wells drilled along Rio Bravo Boulevard and Montaño Road. Roark (2001) evaluated river flood pulses to estimate hydraulic characteristics of the Santa Fe Group aquifer system.

In general, the studies discussed above have been conducted at either a local scale (Kues, 1986; Bartolino and Niswonger, 1999) or basin scale (McAda and Barroll, 2002). The study described in this report was designed to develop hydrogeologic data and interpretations at an intermediate scale with higher spatial and temporal resolution over a longer reach of the Rio Grande than has been provided by previous studies. Additionally, this study focuses on the hydrogeology of the shallow part of the alluvial aquifer.

Methods of Data Collection and Analysis

Groundwater-level, temperature, and slug-test data along with stream-stage data were collected along 16 transects in the Albuquerque area from February 2009 to February 2010, and the data were used to estimate horizontal groundwater flux from the Rio Grande to the inner valley alluvial aquifer using Darcy's Law and the Suzuki-Stallman method of heat transport.

Piezometer Installation and Core Descriptions

Piezometers and surface-water gages were installed in paired transects at eight locations in the Albuquerque area (fig. 1; table 1). Each transect included nested piezometers (multiple monitoring wells with screened intervals at different depths) and surface-water gages (stage only) configured in roughly straight lines and oriented perpendicular to the river and riverside drains (fig. 3*A–H*). At each location, transects extended from the Rio Grande to just outside the riverside drains on both sides of the river and were spaced about 500 ft apart. The paired-transect configuration was chosen to facilitate definition of horizontal and vertical gradients at each location.

Piezometer nests generally were installed with the deep piezometer screen at 45–50 ft bls and the mid-depth piezometer screen at 30–35 ft bls. The shallow piezometer screen typically was installed at 5–10 ft bls to intersect the expected range of seasonal depths to the water table. The deep piezometer of each nest was installed first. The water level measured in the deep piezometer was then used to determine the depths for the mid-depth and shallow piezometer screens. Each piezometer is labeled according to the following convention of (1) the capital letter and number indicate location, and (2) the small letter indicates piezometer depth (a, shallow; b, mid-depth; and c, deep). Each surface-water gage is labeled according to the following convention of (1) the first capital letter and number indicate location, and (2) the second capital letter (S) indicates a surface-water gage (fig. 3*A–H*).

Table 1. Site data for piezometers and surface-water data collection sites, Rio Grande inner valley alluvial aquifer, Albuquerque, New Mexico.

[NAVD 88, North American Vertical Datum of 1988; A, Alameda; a, shallow; b, mid-depth; c, deep; S, surface-water stage gage; NA, not applicable; P, Paseo del Norte; M, Montaño; C, Central; B, Barelas; R, Rio Bravo; PJ, Pajarito; I, I-25]

Other identifier		Piezometer depth	Screened interval	Land surface[1] or measuring-point[2] elevation	Period of record presented in this report		Type of transducer in well for period of this report or for period indicated	
(figs. 3*A*–*H*)	Site identifier	(feet below land surface, rounded to nearest foot)	(feet below land surface, rounded to nearest foot)	(feet above NAVD 88)	Start date	End date	Vented	Nonvented
A2a	351205106381201	20	10–15	4,999.71	02/17/09	02/28/10	No	Yes
A3a	351205106381202	20	10–15	4,998.05	02/17/09	02/28/10	No	Yes
A4a	351204106381601	14	4–9	5,001.36	02/17/09	02/28/10	No	Yes
A4b	351204106381602	29	19–24	5,001.36	02/17/09	02/28/10	No	Yes
A4c	351204106381603	49	39–44	5,001.36	02/17/09	02/28/10	No	Yes
A5a	351205106381601	14	4–9	5,002.32	02/17/09	02/28/10	No	Yes
A5b	351205106381602	29	19–24	5,002.32	02/17/09	02/28/10	No	Yes
A5c	351205106381603	46	36–41	5,002.32	02/17/09	02/28/10	No	Yes
A6a	351208106382701	14	4–9	5,001.51	02/13/09	02/28/10	No	Yes
A6b	351208106382702	29	19–24	5,001.51	02/13/09	02/28/10	No	Yes
A7a	351209106383001	14	4–9	5,000.95	02/13/09	02/28/10	No	Yes
A7b	351209106383002	29	19–24	5,000.95	02/13/09	02/28/10	No	Yes
A7c	351209106383003	44	34–39	5,000.95	02/13/09	02/28/10	No	Yes
A8a	351211106383301	20	10–15	5,000.68	02/13/09	02/28/10	No	Yes
A9a	351211106383501	20	10–15	4,998.41	02/13/09	02/28/10	No	Yes
A11a	351200106381601	20	10–15	4,998.79	02/17/09	02/28/10	No	Yes
A12a	351200106381701	20	10–15	4,996.07	02/17/09	02/28/10	No	Yes
A13a	351159106381901	14	4–9	5,001.63	02/17/09	02/28/10	No	Yes
A13b	351159106381902	29	19–24	5,001.63	02/17/09	02/28/10	No	Yes
A13c	351159106381903	45	35–40	5,001.63	02/17/09	02/28/10	No	Yes
A14a	351200106382001	14	4–9	5,002.14	02/17/09	02/28/10	No	Yes
A14b	351200106382002	29	19–24	5,002.14	02/17/09	02/28/10	No	Yes
A15a	351203106383001	14	4–9	5,001.23	02/13/09	02/28/10	No	Yes
A15b	351203106383002	29	19–24	5,001.23	02/13/09	02/28/10	No	Yes
A16a	351204106383201	14	4–9	4,999.98	02/13/09	02/28/10	No	Yes
A16b	351204106383202	29	19–24	4,999.98	02/13/09	02/28/10	No	Yes
A16c	351204106383203	49	39–44	4,999.98	02/13/09	02/28/10	No	Yes
A17a	351205106383601	20	10–15	5,000.45	02/13/09	02/28/10	No	Yes
A18a	351206106383801	20	10–15	4,996.51	02/13/09	02/28/10	No	Yes
AS1	351202106381601	NA	NA	4,992.72	02/17/09	02/28/10	No	Yes
AS2	351208106382601	NA	NA	5,001.41	02/13/09	02/28/10	No	Yes
AS3	351207106383501	NA	NA	5,001.26	02/13/09	02/28/10	No	Yes
AS4	351208106383601	NA	NA	4,998.17	02/13/09	02/28/10	No	Yes

Table 1. Site data for piezometers and surface-water data collection sites, Rio Grande inner valley alluvial aquifer, Albuquerque, New Mexico.—Continued

[NAVD 88, North American Vertical Datum of 1988; A, Alameda; a, shallow; b, mid-depth; c, deep; S, surface-water stage gage; NA, not applicable; P, Paseo del Norte; M, Montaño; C, Central; B, Barelas; R, Rio Bravo; PJ, Pajarito; I, I-25]

Other identifier		Piezometer depth	Screened interval	Land surface[1] or measuring-point[2] elevation	Period of record presented in this report		Type of transducer in well for period of this report or for period indicated	
(figs. 3*A*–*H*)	Site identifier	(feet below land surface, rounded to nearest foot)	(feet below land surface, rounded to nearest foot)	(feet above NAVD 88)	Start date	End date	Vented	Nonvented
P2b	351055106385102	40	30–35	4,994.53	02/01/09	02/28/10	Yes	No
P3a	351054106385401	25	15–20	4,992.11	02/01/09	02/28/10	Yes	No
P4a	351054106390101	16	6–11	4,993.29	02/01/09	02/28/10	Yes	No
P4b	351054106390102	35	25–30	4,993.29	02/01/09	02/28/10	Yes	No
P5a	351054106390401	16	6–11	4,993.53	02/01/09	02/28/10	Yes	No
P5b	351054106390402	35	25–30	4,993.53	02/01/09	02/28/10	Yes	No
P6a	351055106391101	16	6–11	4,992.03	02/01/09	02/28/10	No	Yes
P6b	351055106391102	31	21–26	4,992.03	02/01/09	02/28/10	No	Yes
P7a	351054106391301	16	6–11	4,993.47	02/01/09	02/28/10	No	Yes
P7b	351054106391302	31	21–26	4,993.47	02/01/09	02/28/10	No	Yes
P8a	351052106391701	16	6–11	4,990.86	02/01/09	02/28/10	No	Yes
P9a	351053106391701	23	13–18	4,996.34	02/01/09	02/28/10	No	Yes
P9b	351053106391702	27	17–22	4,996.34	02/01/09	02/28/10	No	Yes
P10a	351050106394001	22	12–17	4,991.09	02/01/09	02/28/10	Yes	No
P10c	351050106394002	46	36–41	4,991.09	12/22/09	02/28/10	Yes	No
P11a	351059106385201	22	12–17	4,991.37	02/01/09	02/28/10	No	Yes
P11b	351059106385202	37	27–32	4,991.37	02/01/09	02/28/10	No	Yes
P12a	351059106385301	22	12–17	4,991.77	02/01/09	02/28/10	No	Yes
P13a	351058106385901	17	7–12	4,993.36	02/01/09	02/28/10	No	Yes
P13b	351058106385902	32	22–27	4,993.36	02/01/09	02/28/10	No	Yes
P13c	351058106385903	52	42–47	4,993.36	02/01/09	02/28/10	No	Yes
P14a	351058106390301	15	5–10	4,993.76	02/01/09	02/28/10	No	Yes
P14b	351058106390302	30	20–25	4,993.76	02/01/09	02/28/10	No	Yes
P15a	351058106391001	16	6–11	4,992.33	02/01/09	02/28/10	No	Yes
P15b	351058106391002	31	21–26	4,992.33	02/01/09	02/28/10	No	Yes
P16a	351058106391101	16	6–11	4,993.26	02/01/09	02/28/10	No	Yes
P16b	351058106391102	40	30–35	4,993.26	02/01/09	02/28/10	No	Yes
P17a	351058106391501	16	6–11	4,989.73	02/01/09	02/28/10	01/25/10–02/28/10	02/01/09–01/25/10
P18a	351058106391601	20	10–15	4,991.50	02/01/09	02/28/10	No	Yes
P18b	351058106391602	35	25–30	4,991.50	02/01/09	02/28/10	12/21/09–02/28/10	02/01/09–12/21/09
PS1	351054106385310	NA	NA	4,984.21	02/01/09	02/28/10	No	Yes
PS2	351055106390810	NA	NA	4,993.49	02/01/09	02/28/10	No	Yes

Table 1. Site data for piezometers and surface-water data collection sites, Rio Grande inner valley alluvial aquifer, Albuquerque, New Mexico.—Continued

[NAVD 88, North American Vertical Datum of 1988; A, Alameda; a, shallow; b, mid-depth; c, deep; S, surface-water stage gage; NA, not applicable; P, Paseo del Norte; M, Montaño; C, Central; B, Barelas; R, Rio Bravo; PJ, Pajarito; I, I-25]

Other identifier		Piezometer depth	Screened interval	Land surface[1] or measuring-point[2] elevation	Period of record presented in this report		Type of transducer in well for period of this report or for period indicated	
(figs. 3*A*–*H*)	Site identifier	(feet below land surface, rounded to nearest foot)	(feet below land surface, rounded to nearest foot)	(feet above NAVD 88)	Start date	End date	Vented	Nonvented
PS3	351053106391710	NA	NA	4,989.62	02/01/09	02/28/10	No	Yes
M3a	350843106402801	17	7–12	4,974.14	02/01/09	02/28/10	No	Yes
M3b	350843106402802	31	21–26	4,974.14	12/22/09	02/28/10	Yes	No
M4a	350842106403101	15	5–10	4,978.85	02/01/09	02/28/10	No	Yes
M4b	350842106403102	30	20–25	4,978.85	02/01/09	02/28/10	No	Yes
M4c	350842106403103	49	39–44	4,978.85	02/01/09	02/28/10	No	Yes
M5a	350842106403201	15	5–10	4,978.20	02/01/09	02/28/10	No	Yes
M5b	350842106403202	32	22–27	4,978.20	02/01/09	02/28/10	No	Yes
M6a	350848106404703	13	3–8	4,978.86	02/01/09	02/28/10	No	Yes
M6b	350848106404704	28	18–23	4,978.86	02/01/09	02/28/10	No	Yes
M7a	350848106404701	15	5–10	4,977.89	02/01/09	02/28/10	No	Yes
M7b	350848106404702	30	20–25	4,977.89	02/01/09	02/28/10	No	Yes
M8a	350852106405601	16	6–11	4,980.23	02/01/09	02/28/10	No	Yes
M9a	350853106405701	15	5–10	4,977.39	02/01/09	02/28/10	No	Yes
M9b	350853106405702	30	20–25	4,977.39	02/01/09	02/28/10	01/27/10–02/28/10	06/13/05–01/27/10
M12a	350847106402501	17	7–12	4,977.26	02/01/09	02/28/10	No	Yes
M12b	350847106402502	32	22–27	4,977.26	02/01/09	02/28/10	Yes	No
M13a	350846106402801	16	6–11	4,977.37	02/01/09	02/28/10	Yes	No
M13b	350846106402802	31	21–26	4,977.37	02/01/09	02/28/10	No	Yes
M13c	350846106402803	47	37–42	4,977.37	02/01/09	02/28/10	No	Yes
M14a	350846106402804	18	8–13	4,979.83	02/01/09	02/28/10	Yes	No
M14b	350846106402805	33	23–28	4,979.83	02/01/09	02/28/10	02/01/09–06/12/09	06/12/09–02/28/10
M15a	350851106403801	13	3–8	4,977.80	02/01/09	02/28/10	Yes	No
M15b	350851106403802	28	18–23	4,977.80	02/01/09	02/28/10	Yes	No
M16a	350854106404201	17	7–12	4,978.62	02/01/09	02/28/10	Yes	No
M16b	350854106404202	32	22–27	4,978.62	02/01/09	02/28/10	Yes	No
M16c	350854106404203	46	36–41	4,978.62	02/01/09	02/28/10	Yes	No
M17a	350855106405401	18	8–13	4,978.65	02/01/09	02/28/10	No	Yes
M18a	350857106405401	18	8–13	4,978.17	02/01/09	02/28/10	Yes	No
M18b	350857106405402	33	23–28	4,978.17	02/01/09	02/28/10	Yes	No
MS1	350846106402510	NA	NA	4,972.61	02/01/09	02/28/10	Yes	No
MS2	350841106403510	NA	NA	4,978.52	04/15/09	02/28/10	Yes	No

Table 1. Site data for piezometers and surface-water data collection sites, Rio Grande inner valley alluvial aquifer, Albuquerque, New Mexico.—Continued

[NAVD 88, North American Vertical Datum of 1988; A, Alameda; a, shallow; b, mid-depth; c, deep; S, surface-water stage gage; NA, not applicable; P, Paseo del Norte; M, Montaño; C, Central; B, Barelas; R, Rio Bravo; PJ, Pajarito; I, I-25]

Other identifier		Piezometer depth	Screened interval	Land surface[1] or measuring-point[2] elevation	Period of record presented in this report		Type of transducer in well for period of this report or for period indicated	
(figs. 3*A*–*H*)	Site identifier	(feet below land surface, rounded to nearest foot)	(feet below land surface, rounded to nearest foot)	(feet above NAVD 88)	Start date	End date	Vented	Nonvented
MS3	350854106405610	NA	NA	4,979.11	02/01/09	02/28/10	Yes	No
C2a	350534106405502	22	12–17	4,956.23	02/18/09	02/28/10	No	Yes
C3a	350534106405501	22	12–17	4,954.70	02/18/09	02/28/10	No	Yes
C4a	350531106405801	16	6–11	4,956.13	02/18/09	02/28/10	No	Yes
C4b	350531106405802	31	21–26	4,956.13	02/18/09	02/28/10	No	Yes
C4c	350531106405803	51	41–46	4,956.13	02/18/09	02/28/10	No	Yes
C5a	350529106410401	16	6–11	4,957.29	02/18/09	02/28/10	No	Yes
C5b	350529106410402	31	21–26	4,957.29	02/18/09	02/28/10	No	Yes
C6a	350524106410401	16	6–11	4,956.66	02/19/09	02/28/10	No	Yes
C6b	350524106410402	31	21–26	4,956.66	02/19/09	02/28/10	No	Yes
C7a	350522106410501	16	6–11	4,955.70	02/19/09	02/28/10	No	Yes
C7b	350522106410502	31	21–26	4,955.70	02/19/09	02/28/10	No	Yes
C7c	350522106410503	51	41–46	4,955.70	02/19/09	02/28/10	No	Yes
C8a	350520106410701	22	12–17	4,958.09	02/19/09	02/28/10	No	Yes
C9a	350519106410701	22	12–17	4,957.82	02/19/09	02/28/10	No	Yes
C11a	350530106404802	22	12–17	4,954.78	02/18/09	02/28/10	No	Yes
C12a	350530106404801	22	12–17	4,955.44	02/18/09	02/28/10	No	Yes
C13a	350527106405101	16	6–11	4,954.70	02/18/09	02/28/10	No	Yes
C13b	350527106405102	31	21–26	4,954.70	02/18/09	02/28/10	No	Yes
C13c	350527106405103	51	41–46	4,954.70	02/18/09	02/28/10	No	Yes
C14a	350525106405301	16	6–11	4,956.19	02/18/09	02/28/10	No	Yes
C14b	350525106405302	31	21–26	4,956.19	02/18/09	02/28/10	No	Yes
C15a	350521106405501	16	6–11	4,954.32	02/19/09	02/28/10	No	Yes
C15b	350521106405502	31	21–26	4,954.32	02/19/09	02/28/10	No	Yes
C16a	350519106405701	16	6–11	4,957.11	02/19/09	02/28/10	No	Yes
C16b	350519106405702	31	21–26	4,957.11	02/19/09	02/28/10	No	Yes
C16c	350519106405703	49	39–44	4,957.11	02/19/09	02/28/10	No	Yes
C17a	350516106410001	22	12–17	4,956.90	02/19/09	02/28/10	No	Yes
C18a	350516106410002	22	12–17	4,957.78	02/19/09	02/28/10	No	Yes
CS1	350530106404803	NA	NA	4,951.72	02/18/09	02/28/10	No	Yes
CS2	350521106405503	NA	NA	4,955.09	02/19/09	02/28/10	No	Yes
CS3	350516106410003	NA	NA	4,956.98	02/19/09	02/28/10	No	Yes
B2a	350403106392201	16	6–11	4,940.68	02/01/09	02/28/10	No	Yes

Table 1. Site data for piezometers and surface-water data collection sites, Rio Grande inner valley alluvial aquifer, Albuquerque, New Mexico.—Continued

[NAVD 88, North American Vertical Datum of 1988; A, Alameda; a, shallow; b, mid-depth; c, deep; S, surface-water stage gage; NA, not applicable; P, Paseo del Norte; M, Montaño; C, Central; B, Barelas; R, Rio Bravo; PJ, Pajarito; I, I-25]

Other identifier		Piezometer depth	Screened interval	Land surface[1] or measuring-point[2] elevation	Period of record presented in this report		Type of transducer in well for period of this report or for period indicated	
(figs. 3*A*–*H*)	Site identifier	(feet below land surface, rounded to nearest foot)	(feet below land surface, rounded to nearest foot)	(feet above NAVD 88)	Start date	End date	Vented	Nonvented
B3a	350403106392301	15	5–10	4,941.86	02/01/09	02/28/10	No	Yes
B3b	350403106392302	30	20–25	4,941.86	02/01/09	02/28/10	No	Yes
B4a	350402106392601	16	6–11	4,942.18	02/01/09	02/28/10	No	Yes
B4b	350402106392602	31	21–26	4,942.18	Uninstrumented	NA	NA	NA
B4c	350402106392603	52	42–47	4,942.18	02/01/09	02/28/10	No	Yes
B5a	350402106392901	15	5–10	4,943.08	02/01/09	02/28/10	No	Yes
B5b	350402106392902	30	20–25	4,943.08	Uninstrumented	NA	NA	NA
B6a	350400106393701	17	7–12	4,942.40	02/01/09	02/28/10	No	Yes
B6b	350400106393702	32	22–27	4,942.40	02/01/09	02/28/10	No	Yes
B7a	350359106393901	17	7–12	4,943.03	02/01/09	02/28/10	No	Yes
B7b	350359106393902	32	22–27	4,943.03	Uninstrumented	NA	NA	NA
B7c	350359106393903	52	42–47	4,943.03	02/01/09	02/28/10	No	Yes
B8a	350359106394401	16	6–11	4,940.23	02/01/09	02/28/10	No	Yes
B8b	350359106394402	34	24–29	4,940.23	Uninstrumented	NA	NA	NA
B9a	350359106394501	20	10–15	4,943.21	12/21/09	02/28/10	Yes	No
B10a	350354106395201	17	7–12	4,940.77	02/01/09	02/28/10	No	Yes
B10b	350354106395202	32	22–27	4,940.77	02/01/09	02/28/10	No	Yes
B10c	350354106395203	48	38–43	4,940.77	02/01/09	02/28/10	No	Yes
B11a	350358106392201	16	6–11	4,939.91	02/01/09	02/28/10	No	Yes
B12a	350358106392301	16	6–11	4,939.88	02/01/09	02/28/10	Yes	No
B12b	350358106392302	31	21–26	4,939.88	02/01/09	02/28/10	Yes	No
B13a	350358106392601	15	5–10	4,941.91	02/01/09	02/28/10	Yes	No
B13b	350358106392602	30	20–25	4,941.91	02/01/09	02/28/10	Yes	No
B13c	350358106392603	40	30–35	4,941.91	02/01/09	02/28/10	Yes	No
B14a	350357106392901	15	5–10	4,943.41	02/01/09	02/28/10	Yes	No
B14b	350357106392902	30	20–25	4,943.41	02/01/09	02/28/10	Yes	No
B15a	350356106393601	16	6–11	4,943.14	02/01/09	02/28/10	Yes	No
B15b	350356106393602	31	21–26	4,943.14	02/01/09	02/28/10	Yes	No
B16a	350356106393901	16	6–11	4,943.59	02/01/09	02/28/10	Yes	No
B16b	350356106393902	31	21–26	4,943.59	02/01/09	02/28/10	Yes	No
B16c	350356106393903	51	41–46	4,943.59	02/01/09	02/28/10	Yes	No
B17a	350354106394201	16	6–11	4,939.60	02/01/09	02/28/10	Yes	No
B17b	350354106394202	31	21–26	4,939.60	02/01/09	02/28/10	Yes	No

Table 1. Site data for piezometers and surface-water data collection sites, Rio Grande inner valley alluvial aquifer, Albuquerque, New Mexico.—Continued

[NAVD 88, North American Vertical Datum of 1988; A, Alameda; a, shallow; b, mid-depth; c, deep; S, surface-water stage gage; NA, not applicable; P, Paseo del Norte; M, Montaño; C, Central; B, Barelas; R, Rio Bravo; PJ, Pajarito; I, I-25]

Other identifier		Piezometer depth	Screened interval	Land surface[1] or measuring-point[2] elevation	Period of record presented in this report		Type of transducer in well for period of this report or for period indicated	
(figs. 3*A*–*H*)	Site identifier	(feet below land surface, rounded to nearest foot)	(feet below land surface, rounded to nearest foot)	(feet above NAVD 88)	Start date	End date	Vented	Nonvented
B18a	350353106394301	20	10–15	4,943.14	02/01/09	02/28/10	Yes	No
BS1	350403106392410	NA	NA	4,942.04	02/01/09	02/28/10	Yes	No
BS2	350402106392810	NA	NA	4,942.86	02/01/09	02/28/10	Yes	No
BS3	350359106394410	NA	NA	4,935.89	02/01/09	02/28/10	Yes	No
R1a	350137106395101	27	17–22	4,931.35	02/01/09	02/28/10	12/18/09–02/28/10	12/11/03–12/18/09
R1c	350137106395102	59	49–54	4,931.35	02/01/09	02/28/10	No	Yes
R2a	350141106400701	16	6–11	4,927.27	02/01/09	02/28/10	No	Yes
R3a	350141106400801	17	7–12	4,927.51	02/01/09	02/28/10	No	Yes
R3c	350141106400802	57	47–52	4,927.51	02/01/09	02/28/10	No	Yes
R4a	350138106401102	22	12–17	4,929.91	02/01/09	02/28/10	No	Yes
R4b	350138106401104	30	20–25	4,929.91	02/01/09	02/28/10		
R4c	350140106401701	56	46–51	4,929.91	02/01/09	02/28/10	No	Yes
R5a	350140106401704	19	9–14	4,930.49	02/01/09	02/28/10	No	Yes
R5b	350140106401703	30	20–25	4,930.49	02/01/09	02/28/10	No	Yes
R5c	350140106401702	54	44–49	4,930.49	02/01/09	02/28/10	12/18/09–02/28/10	12/12/03–12/18/09
R6a	350143106402401	15	5–10	4,928.75	02/01/09	02/28/10	12/04/09–02/28/10	07/12/05–12/04/09
R6b	350143106402402	30	20–25	4,928.62	02/01/09	02/28/10	12/04/09–02/28/10	10/05/05–12/04/09
R7a	350143106402503	15	5–10	4,928.79	02/01/09	02/28/10	12/04/09–02/28/10	07/12/05–12/04/09
R7b	350143106402501	35	25–30	4,928.99	02/01/09	02/28/10	12/04/09–02/28/10	12/17/03–12/04/09
R7c	350143106402502	54	44–49	4,928.99	02/01/09	02/28/10	12/04/09–02/28/10	12/17/03–12/04/09
R8a	350142106402701	15	5–10	4,928.32	02/01/09	02/28/10	12/04/09–02/28/10	12/17/03–12/04/09
R8c	350142106402702	50	40–45	4,928.32	02/01/09	02/28/10	12/04/09–02/28/10	12/17/03–12/04/09
R9a	350142106402801	14	4–9	4,927.73	02/01/09	02/17/10	No	Yes
R10a	350137106403501	30	20–25	4,925.90	02/01/09	02/28/10	No	Yes
R10c	350137106403502	49	39–44	4,925.90	02/01/09	02/28/10	No	Yes
R11a	350144106400703	18	8–13	4,926.48	02/01/09	02/28/10	No	Yes
R12a	350144106400701	16	6–11	4,929.06	02/01/09	02/28/10	Yes	No

Table 1. Site data for piezometers and surface-water data collection sites, Rio Grande inner valley alluvial aquifer, Albuquerque, New Mexico.—Continued

[NAVD 88, North American Vertical Datum of 1988; A, Alameda; a, shallow; b, mid-depth; c, deep; S, surface-water stage gage; NA, not applicable; P, Paseo del Norte; M, Montaño; C, Central; B, Barelas; R, Rio Bravo; PJ, Pajarito; I, I-25]

Other identifier		Piezometer depth	Screened interval	Land surface[1] or measuring-point[2] elevation	Period of record presented in this report		Type of transducer in well for period of this report or for period indicated	
(figs. 3*A*–*H*)	Site identifier	(feet below land surface, rounded to nearest foot)	(feet below land surface, rounded to nearest foot)	(feet above NAVD 88)	Start date	End date	Vented	Nonvented
R12b	350144106400702	31	21–26	4,929.06	02/01/09	02/28/10	Yes	No
R13a	350144106401101	15	5–10	4,929.13	02/01/09	02/28/10	No	Yes
R13b	350144106401102	30	20–25	4,929.13	02/01/09	02/28/10	No	Yes
R13c	350144106401103	56	46–51	4,929.13	02/01/09	02/28/10	No	Yes
R14a	350146106401801	15	5–10	4,929.92	02/01/09	02/28/10	No	Yes
R14b	350146106401802	30	20–25	4,929.69	02/01/09	02/28/10	No	Yes
R15a	350147106402601	15	5–10	4,929.77	02/01/09	02/28/10	12/04/09–02/28/10	10/05/05–12/04/09
R15b	350147106402602	30	20–25	4,929.77	02/01/09	02/28/10	12/04/09–02/28/10	06/02/05–12/04/09
R16a	350147106402501	15	5–10	4,928.70	02/01/09	02/28/10	12/04/09–02/28/10	10/05/05–12/04/09
R16b	350147106402502	30	20–25	4,928.70	02/01/09	02/28/10	12/04/09–02/28/10	06/02/05–12/04/09
R16c	350147106402503	54	44–49	4,928.70	02/01/09	02/28/10	12/04/09–02/28/10	06/02/05–12/04/09
R17a	350147106402801	16	6–11	4,928.18	02/01/09	02/28/10	12/04/09–02/28/10	10/05/05–12/04/09
R17b	350147106402802	31	21–26	4,928.18	02/01/09	02/28/10	12/04/09–02/28/10	10/05/05–12/04/09
R18a	350147106402701	15	5–10	4,929.11	02/01/09	02/28/10	12/04/09–02/28/10	10/29/08–12/04/09
RS1	350141106400810	NA	NA	4,925.22	02/01/09	02/28/10	Yes	No
RS2	350145106400810	NA	NA	4,926.52	02/01/09	02/28/10	Yes	No
RS3	350143106402301	NA	NA	4,934.74	02/01/09	02/28/10	No	Yes
RS4	350142106402810	NA	NA	4,927.49	02/01/09	02/28/10	Yes	No
RS5	350147106402810	NA	NA	4,928.69	02/01/09	02/28/10	Yes	No
PJ2a	345904106410501	20	10–15	4,909.79	02/19/09	02/28/10	No	Yes
PJ3a	345904106410601	20	10–15	4,912.53	02/20/09	02/28/10	No	Yes
PJ4a	345904106410901	14	9–14	4,915.55	02/23/09	02/28/10	No	Yes
PJ4b	345904106410902	29	19–24	4,915.55	02/23/09	02/28/10	No	Yes
PJ4c	345904106410903	49	39–44	4,915.55	02/23/09	02/28/10	No	Yes
PJ5a	345904106411001	14	4–9	4,916.21	02/23/09	02/28/10	No	Yes
PJ5b	345904106411002	29	19–24	4,916.21	02/23/09	02/28/10	No	Yes
PJ6a	345905106411501	14	4–9	4,915.80	02/20/09	02/28/10	No	Yes

Table 1. Site data for piezometers and surface-water data collection sites, Rio Grande inner valley alluvial aquifer, Albuquerque, New Mexico.—Continued

[NAVD 88, North American Vertical Datum of 1988; A, Alameda; a, shallow; b, mid-depth; c, deep; S, surface-water stage gage; NA, not applicable; P, Paseo del Norte; M, Montaño; C, Central; B, Barelas; R, Rio Bravo; PJ, Pajarito; I, I-25]

Other identifier		Piezometer depth	Screened interval	Land surface[1] or measuring-point[2] elevation	Period of record presented in this report		Type of transducer in well for period of this report or for period indicated	
(figs. 3*A*–*H*)	Site identifier	(feet below land surface, rounded to nearest foot)	(feet below land surface, rounded to nearest foot)	(feet above NAVD 88)	Start date	End date	Vented	Nonvented
PJ6b	345905106411502	29	19–24	4,915.80	02/20/09	02/28/10	No	Yes
PJ7a	345906106412001	14	4–9	4,915.91	02/20/09	02/28/10	No	Yes
PJ7b	345906106412002	29	19–24	4,915.91	02/20/09	02/28/10	No	Yes
PJ7c	345906106412003	49	39–44	4,915.91	02/20/09	02/28/10	No	Yes
PJ8a	345908106412501	20	10–15	4,913.60	02/19/09	02/28/10	No	Yes
PJ9a	345908106412601	25	15–20	4,916.32	02/19/09	02/28/10	No	Yes
PJ11a	345859106410601	20	10–15	4,911.19	02/19/09	02/28/10	No	Yes
PJ12a	345859106410701	20	10–15	4,913.10	02/20/09	02/28/10	No	Yes
PJ13a	345859106411001	14	4–9	4,915.12	02/23/09	02/28/10	No	Yes
PJ13b	345859106411002	29	19–24	4,915.12	02/23/09	02/28/10	No	Yes
PJ13c	345859106411003	45	35–40	4,915.12	02/23/09	02/28/10	No	Yes
PJ14a	345900106411201	14	4–9	4,915.91	02/23/09	02/28/10	No	Yes
PJ14b	345900106411202	29	19–24	4,915.91	02/23/09	02/28/10	No	Yes
PJ15a	345901106411801	14	4–9	4,915.27	02/20/09	02/28/10	No	Yes
PJ15b	345901106411802	29	19–24	4,915.27	02/20/09	02/28/10	No	Yes
PJ16a	345903106412001	14	4–9	4,915.56	02/20/09	02/28/10	No	Yes
PJ16b	345903106412002	29	19–24	4,915.56	02/20/09	02/28/10	No	Yes
PJ16c	345903106412003	49	39–44	4,915.56	02/19/09	02/28/10	No	Yes
PJ17a	345904106412601	20	10–15	4,913.34	02/20/09	02/28/10	No	Yes
PJS1	345902106410701	NA	NA	4,909.47	02/20/09	02/28/10	No	Yes
PJS2	345904106411501	NA	NA	4,916.41	02/20/09	02/28/10	No	Yes
PJS3	345906106412601	NA	NA	4,909.48	02/19/09	02/28/10	No	Yes
I1a	350358106391301	16	6–11	4,904.92	02/01/09	02/28/10	No	Yes
I1b	350358106391302	31	21–26	4,904.92	Uninstrumented	NA	NA	NA
I1c	350358106391303	56	46–51	4,904.92	02/01/09	02/28/10	03/02/10–02/28/10	06/01/05–03/02/10
I2a	345703106403901	16	6–11	4,902.76	02/01/09	02/28/10	No	Yes
I2b	345703106403902	31	21–26	4,902.76	02/01/09	02/28/10	Yes	No
I3a	345703106404001	16	6–11	4,902.35	02/01/09	02/28/10	No	Yes
I4a	345701106404501	14	4–9	4,903.47	02/01/09	02/28/10	No	Yes
I4b	345701106404502	29	19–24	4,903.47	02/01/09	02/28/10	No	Yes
I4c	345701106404503	54	44–49	4,903.47	Uninstrumented	NA	NA	NA
I5a	345701106404601	14	4–9	4,904.60	02/01/09	02/28/10	No	Yes
I5b	345701106404602	29	19–24	4,904.60	02/01/09	02/28/10	No	Yes

Table 1. Site data for piezometers and surface-water data collection sites, Rio Grande inner valley alluvial aquifer, Albuquerque, New Mexico.—Continued

[NAVD 88, North American Vertical Datum of 1988; A, Alameda; a, shallow; b, mid-depth; c, deep; S, surface-water stage gage; NA, not applicable; P, Paseo del Norte; M, Montaño; C, Central; B, Barelas; R, Rio Bravo; PJ, Pajarito; I, I-25]

Other identifier		Piezometer depth	Screened interval	Land surface[1] or measuring-point[2] elevation	Period of record presented in this report		Type of transducer in well for period of this report or for period indicated	
(figs. 3*A*–*H*)	Site identifier	(feet below land surface, rounded to nearest foot)	(feet below land surface, rounded to nearest foot)	(feet above NAVD 88)	Start date	End date	Vented	Nonvented
I6a	345707106410101	14	4–9	4,905.91	02/01/09	02/28/10	No	Yes
I6b	345707106410102	29	19–24	4,905.91	12/18/09	02/28/10	Yes	No
I7a	345706106410201	14	4–9	4,905.12	02/01/09	02/28/10	No	Yes
I7b	345706106410202	29	19–24	4,905.12	02/01/09	02/28/10	09/25/09–02/28/10	06/01/05–09/25/09
I7c	345706106410203	49	39–44	4,905.12	09/25/09	02/28/10	No	Yes
I8a	345704106410701	15	5–10	4,901.90	02/01/09	02/28/10	No	Yes
I8b	345704106410702	30	20–25	4,901.90	02/01/09	02/28/10	No	Yes
I10a	345703106411201	13	3–8	4,900.97	02/01/09	02/28/10	No	Yes
I10b	345703106411202	28	18–23	4,900.97	Uninstrumented	NA	NA	NA
I10c	345703106411203	48	38–43	4,900.97	02/01/09	02/28/10	No	Yes
I11a	345707106404101	13	3–8	4,902.27	02/01/09	02/28/10	Yes	No
I11b	345707106404102	28	18–23	4,902.27	02/01/09	02/28/10	Yes	No
I12a	345707106404103	13	3–8	4,902.28	02/01/09	02/28/10	Yes	No
I13a	345706106404701	14	4–9	4,904.21	02/01/09	02/28/10	Yes	No
I13b	345706106404702	29	19–24	4,904.21	Uninstrumented	NA	NA	NA
I13c	345706106404703	49	34–39	4,904.21	02/01/09	02/28/10	12/12/06–06/12/09	06/12/09–02/28/10
I14a	345706106404704	14	4–9	4,904.06	02/01/09	02/28/10	Yes	No
I14b	345706106404705	29	19–24	4,904.06	Uninstrumented	NA	NA	NA
I15a	345713106410604	14	4–9	4,906.50	02/01/09	02/28/10	Yes	No
I15b	345713106410605	29	19–24	4,906.50	02/01/09	02/28/10	No	Yes
I16a	345713106410601	16	6–11	4,908.22	02/01/09	02/28/10	Yes	No
I16b	345713106410602	31	21–26	4,908.22	02/01/09	02/28/10	Yes	No
I16c	345713106410603	49	39–44	4,908.22	02/01/09	02/28/10	Yes	No
I17a	345713106411001	13	3–8	4,903.46	02/01/09	02/28/10	Yes	No
I17b	345713106411002	28	18–23	4,903.46	02/01/09	02/28/10	06/12/09–02/28/10	01/23/06–06/12/09
IS1	345703106404010	NA	NA	4,903.63	02/01/09	02/28/10	Yes	No
IS2	345705106405810	NA	NA	4,906.66	02/01/09	02/28/10	Yes	No
IS3	345705106410810	NA	NA	4,903.23	02/01/09	02/28/10	Yes	No

[1]Land-surface elevation for piezometers only.

[2]Measuring-point elevation for surface-water stage gages only.

Piezometers were installed using direct-push drilling technology (Lapham and others, 1997). Piezometers were constructed of 1-inch diameter, flush-threaded schedule 40 polyvinyl chloride (PVC) pipe. Each piezometer, from the bottom up, consists of a 5-ft long blank section of casing capped at the bottom (the sump), a 5-ft long screen with 0.010-inch wide screen slots, and blank casing to the land surface. Each piezometer was completed by backfilling the outside annulus surrounding the PVC with soil to a depth of about 5 ft below land surface. Bentonite pellets were then placed in the annulus from the top of the backfill to land surface. Each piezometer was developed using compressed air to pump water out of the casing and establish a good hydraulic connection between the piezometer and the aquifer.

Continuous subsurface core samples were collected at five transects (Paseo del Norte, Montaño, Barelas, Rio Bravo, and I-25) from 2004 to 2006 by using direct-push drilling. Core samples were obtained to (1) ensure that piezometer screens were placed in sand and gravel, and not clay; and (2) identify and locate any substantial changes in subsurface lithology that could potentially affect either horizontal or vertical groundwater movement. In total, 36 locations were cored within the study area. Coring locations generally corresponded to piezometer sites and included locations adjacent to the river, between the river and riverside drains on both sides of the river, and adjacent to both riverside drains. Coring depths ranged from 25 to 55 ft bls, depending on the depth of the deepest piezometer.

Cores were collected in acetate tubes; each tube was capped and labeled. Cores were described in the field at the time of collection. The core descriptions, on file with the USGS New Mexico Water Science Center, Albuquerque, N. Mex., include the depth interval that was cored, the amount of recovery from each interval, the lithology (grain size, sorting, rock type, and color), and miscellaneous remarks. The cores are stored in the New Mexico Bureau of Geology and Mineral Resources core library in Socorro, N. Mex.

Water-Level and Temperature Data

Groundwater and surface-water levels were measured in piezometers and surface-water bodies, respectively. Submersible water-pressure sensors (transducers) were installed in each piezometer and at each surface-water gage to measure and record groundwater levels on an hourly schedule; some of the transducers also were capable of recording hourly temperatures. Surface-water gages were constructed to measure and record water levels in the Rio Grande and in the riverside drains; streamflow was not computed for these gages. A total of 252 piezometers and 27 surface-water gages were installed; the number of piezometers and surface-water gages in each set of transects varied for each location (fig. 3*A–H*). Groundwater-level data are available in the USGS National Water Information System (http://dx.doi.org/10.5066/F7P55KJN).

Groundwater-level data were measured using vented and nonvented transducers (table 1). Transducers with vented cable are automatically compensated for changes in barometric pressure, but transducers with nonvented cable are not. With nonvented transducers, a calculation is required to correct the recorded water levels for changes in barometric pressure (Freeman and others, 2004). Unvented transducers record total pressure (water plus air) and convert this value to a water level. Any change in air pressure needs to be subtracted from an initial barometric pressure (pressure at the start of the water-level data set being corrected), and the result is subtracted from the recorded total water level in order to attain a corrected water level. Hourly barometric pressure values from the Albuquerque airport (National Climatologic Data Center, various dates) were used to correct all water-level data collected using nonvented transducers. Barometric water-level corrections ranged from 0.0 to about 0.5 ft.

Hourly temperature data were recorded at sites using pressure transducers that also recorded water levels. Temperature data are available in the USGS National Water Information System (http://dx.doi.org/10.5066/F7P55KJN). Vertical temperature profiles were measured at selected sites; temperature values were recorded at 5-ft intervals from the water table to the bottom of the piezometer using a calibrated temperature/water-level meter. Vertical-temperature profile data are on file with the USGS New Mexico Water Science Center, Albuquerque, N. Mex.

Slug Tests

The spatial variability of aquifer properties at each of the transect locations was estimated by conducting slug tests, a type of aquifer test. Analytical results from slug tests need to be interpreted carefully because the continuity and distribution of hydrologically distinguishable lithologies are unique to different parts of the alluvial aquifer. Type-curve matching methods are the most common analytical techniques used for slug-test analysis and provide an estimate of aquifer characteristics in different parts of the aquifer.

Slug tests were conducted by the rapid introduction of a 60-inch long weighted PVC slug, with a diameter of 0.75 inch, into a 1-inch diameter piezometer to induce a positive displacement of water in the piezometer of 1 ft or more. Water levels were recorded prior to and during the slug tests to record initial head, slug insertion, and water-level recovery to static conditions. After water levels recovered to within 5 percent of initial water levels (Butler, 1998), the slug was removed, and the subsequent water-level recovery was recorded at 1-second intervals by using pressure transducers. Slug tests were performed at 15 shallow piezometers, 31 mid-depth piezometers, and 1 deep piezometer at the Alameda, Paseo Del Norte, Montaño, Central, Barelas, Rio Bravo, Pajarito, and I-25 transects.

Hydraulic-conductivity estimates were determined by the Bouwer and Rice (1976) and Butler (1998) methods for slug-test analysis in unconfined aquifers. The Butler (1998) method is an extension of the Bouwer and Rice (1976) method to account for oscillatory responses during recovery from slug testing, observed in some highly permeable aquifers. For both methods, the recovery data are analyzed by using a family of type curves to determine the hydraulic conductivity of the aquifer near the screened intervals of the piezometers. The Bouwer and Rice (1976) method is used to estimate hydraulic conductivity through the following equation:

$$K = \frac{r_c^2 \ln\left(R_e / r_w\right)}{2L} \frac{1}{t} \ln \frac{y_0}{y_t} \quad (1)$$

where

K is hydraulic conductivity (length/time),
r_c is casing radius (length),
R_e is effective radius of influence (length),
r_w is borehole radius (length),
L is length of open interval of the well (length),
t is time (time),
y_0 is initial water level (length), and
y_t is water level at time t (time).

The Butler (1998) method for an unconfined, highly permeable aquifer is used to estimate hydraulic conductivity through the following equation:

$$K_r = \frac{t_d^*}{t^*} \frac{r_c^2 \ln\left(R_e / r_w\right)}{2 b_s C_D^*} \quad (2)$$

where

K_r is radial hydraulic conductivity (length/time);
t_d^* is dimensionless time parameter $(\frac{g}{L_e})^{1/2} t$, where g is gravitational acceleration, and L_e is effective length of water column in well, and t is time;
t^* is time (t);
r_c is casing radius (length);
R_e is effective radius of influence (length);
r_w is borehole radius (length);
b_s is screen length (length); and
C_D^* is dimensionless damping parameter.

Use of either method assumes (1) the aquifer is unconfined and infinite in areal extent; (2) the aquifer is homogeneous, isotropic, and uniform in thickness; (3) the water table is initially horizontal; (4) the well is fully or partially penetrating; (5) the water level in the well is stable; (6) the slug is introduced rapidly into the well; and (7) the screened interval is completely saturated during testing.

Assumptions regarding the extent, homogeneity, isotropy, and thickness of the aquifer were satisfied because the area of influence of the tests was relatively small. Water-table conditions, piezometer geometry, and test procedures satisfy the remaining assumptions. Slug-test results represent the hydraulic conductivity of the area immediately surrounding the well and may not be representative of the average hydraulic conductivity of the area. Complete documentation of the slug tests is in the USGS New Mexico Water Science Center aquifer-test archive, Albuquerque, N. Mex.

Horizontal Hydraulic Gradients

Horizontal hydraulic gradients used in the Darcy flux calculations were calculated using the three-point method (Heath, 1983). Daily hydraulic gradients were calculated by using the three-point method and 2009–10 daily mean water levels to compute the slope of the water table between selected sets of shallow piezometers. Daily mean water levels were not uniformly available at all transects from 2009 to 2010 (table 1), but for most piezometers, there were 13 months of data. The average of the daily values over the 13-month period is referred to as "an annual mean" in this report. For each of the paired transects, hydraulic gradients were calculated for three-piezometer combinations of adjacent, triangle-forming piezometers (piezometer triangles) between the river and the riverside drain. For example, a total of eight piezometer triangles were defined for the set of six piezometers on the west side of the Rio Grande at the I-25 transect (fig. 4). Similar piezometer triangles were defined on both sides of the Rio Grande at each transect. After the daily mean hydraulic gradient was calculated for each of the eight piezometer triangles, the daily mean hydraulic gradient for each side of the river was calculated as the average of the daily mean hydraulic gradients of the eight piezometer triangles.

Along with the horizontal hydraulic gradients, direction of groundwater flow also was calculated for each of the paired transects. Gradient directions were calculated using the coordinates of the piezometers (converted to feet from Universal Transverse Mercator Zone 13 coordinates in meters) and the depth-to-water measurements. The gradient directions were then corrected to the direction of river flow at each transect. River azimuth, or the orientation with respect to north of a line drawn along the center of the river channel, was obtained by examining digital aerial photographs in Google Earth (Google, Inc., 2011) along an approximate mid-river line through each 500-ft reach. Gradient directions presented in this report are the absolute difference from river azimuth at each transect.

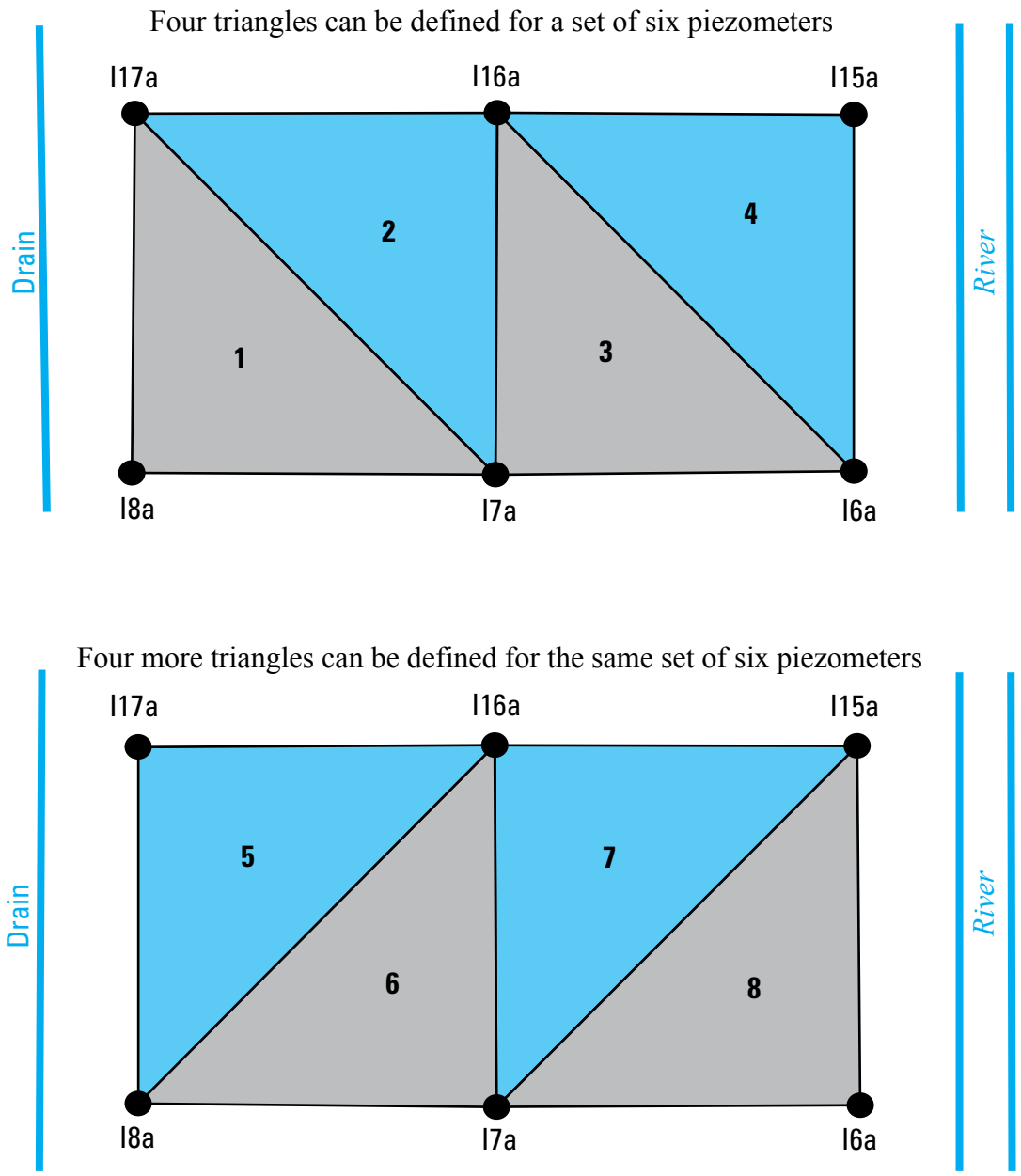

Figure 4. Piezometer triangles were defined to compute daily mean hydraulic gradients on the west side of the Rio Grande at the I-25 transect.

Darcy Flux

Temporal changes in the rate of Rio Grande leakage to the alluvial aquifer were computed using Darcy's Law. Darcy's Law defines the flow of groundwater in a homogeneous, saturated aquifer under laminar-flow conditions as proportional to the cross-sectional area and hydraulic gradient (Fetter, 1994). In equation form, Darcy's Law is:

$$Q = -KA\frac{dh}{dl} \tag{3}$$

where

Q is volumetric groundwater flow (length^3/time),
K is hydraulic conductivity (length/time),
A is cross-sectional area through which groundwater flow occurs (length^2), and
$\frac{dh}{dl}$ is hydraulic gradient (dimensionless, but is negative, by convention, in the direction of groundwater flow).

Dividing both sides by the cross-sectional area (A), and setting $q=Q/A$, the Darcy flux (also called specific flux) through a unit cross-sectional area of the aquifer can be stated as:

$$q = -K\frac{dh}{dl} \tag{4}$$

where

q is the Darcy flux of water through the aquifer (length/time).

The hydraulic-conductivity values used in the Darcy-flux calculations in this report are considered bulk values that characterize the aquifer as a homogeneous mixture of sediments and represent average conditions in the aquifer. Hydraulic-conductivity estimates were determined by analyzing the results of slug tests conducted for this study at each of the transect locations and were compared to the published reasonable range for hydraulic conductivity in undifferentiated Rio Grande alluvium (Tiedeman and others, 1998).

Suzuki-Stallman Method for Estimating Heat Flux

Specific fluxes also were computed from the temperature data collected at 10- and 20-ft depths in the alluvial aquifer using the analytical method developed by Suzuki (1960) and Stallman (1965) that was applied to horizontal flux by Moret (2007). Suzuki (1960) developed an equation and approximate analytical solution for one-dimensional (vertical) advective and conductive heat transport into rice paddy soils assuming saturated, vertical, steady-state flow in a homogenous medium with a sinusoidal daily surface temperature. Later, on the basis of Suzuki's work, Stallman (1965) developed an exact analytic solution for one-dimensional (vertical) advective and conductive heat transfer in an aquifer. The Suzuki-Stallman method relies only on temperature data, providing an independent method that can be used to check the Darcy-flux estimates generated using measured hydraulic-conductivity values and hydraulic gradients. For a more complete discussion of using heat as a groundwater tracer see Anderson (2005), Blasch and others (2007), or Constantz and others (2008).

The equation describing one-dimensional, vertical heat transport (Suzuki, 1960) is:

$$k\frac{\partial^2 T}{\partial z^2} + \rho_w c_w q_s \frac{\partial T}{\partial z} = \rho c \frac{\partial T}{\partial t} \tag{5}$$

where

k is the thermal conductivity of the saturated aquifer (sediment and water) (British Thermal Unit [International Steam Table Calorie] per time foot-degrees Fahrenheit),
T is the temperature in the aquifer (°F),
$\rho_w c_w$ is the heat capacity of the water (British Thermal Unit [International Steam Table Calorie] per cubic foot-degrees Fahrenheit),
q_s is the specific flux of water through the aquifer (length/time),
ρc is the heat capacity of the saturated aquifer (sediment and water) (British Thermal Unit [International Steam Table Calorie] per cubic foot-degrees Fahrenheit),
z is vertical distance (length), and
t is time (time).

Moret (2007) adapted the heat-transport equation (Suzuki, 1960) and analytical solution (Stallman, 1965) to use annual temperature variations in river temperature and their propagation into the adjacent aquifer to estimate rates of horizontal river leakage. For the horizontal flux, Moret (2007) used equation 5 but substituted horizontal distance x for the vertical distance z. Temperature variations in the river affect the solution to equation 5; consequently, Moret (2007) adapted Stallman's (1965) method for incorporating diurnal heating and cooling of the land surface to correct for changes in river temperature. To use the solution proposed by Stallman, it is necessary to assume that the aquifer is bounded at $x=0$ by a fully penetrating river, and all flow is uniform and horizontal in the positive x direction. Following Suzuki (1960) and Stallman (1965), Moret (2007) states that the temperature of the river, T_{river}, varies sinusoidally with a period of 1 year:

$$T_{river} = T_{avg} + T_0 \sin\left(\frac{2\pi}{\tau}t + \varphi\right) \quad (6)$$

where

T_{avg} is the average river temperature (degrees Fahrenheit),
T_0 is the magnitude of temperature oscillation in the river (degrees Fahrenheit),
τ is the period of the oscillation (time),
φ is the phase lag in temperature signal of the river (time), and
t is time (time).

If the temperature dependence of the viscosity of water is ignored, the analytical solution for advective and conductive heat transport proposed by Suzuki (1960) and further developed by Stallman (1965) (eq. 6) can be used to model the temperature oscillations in groundwater (T_{osc}) that are attributable to oscillations in river water temperature (T_{river}):

$$T_{osc} = T_0 e^{-ax} \sin\left(\frac{2\pi}{\tau}t - bx + \varphi\right) \quad (7)$$

where T_0, τ, t, x (z in eq. 5), and φ are as previously defined for equations 5 and 6,

$$a = \left[\sqrt{K_T^{\,2} + \frac{V^4}{4}} + \frac{V^2}{2}\right]^{\frac{1}{2}} - V, \text{ and} \quad (8)$$

$$b = \left[\sqrt{K_T^{\,2} + \frac{V^4}{4}} - \frac{V^2}{2}\right]^{\frac{1}{2}} \quad (9)$$

The parameter a, with units of ft^{-1}, controls the attenuation of the temperature wave. The spatial frequency parameter b, with units of radians per foot (rad/ft), controls the propagation of the wave through space. The parameters K_T and V are constants and are defined by:

$$K_T = \frac{\pi\rho c}{k\tau}, \text{ and} \quad (10)$$

$$V = \frac{\rho_w c_w q_s}{2k} \quad (11)$$

where ρc, k, τ, $\rho_w c_w$, q_s, and k are as previously defined in equations 5 and 6.

Figure 5 shows how theoretical values of a and b, calculated through use of equations 8 and 9, vary as a function of changes in the flux term (q_s) in equation 11. Type curves in figure 5 were constructed by using the average of the four values obtained by Bartolino and Niswonger (1999) for the thermal conductivity (1.25 BTU_{IT}/hr ft °F) and saturated heat capacity (48 BTU_{IT}/ft^3 °F) of the inner valley alluvial aquifer.

For parameters a and b determined from observations, the specific flux through the aquifer, q_s, can be estimated from type curves such as those in figure 5. The parameters a and b can be estimated by using temperature records from two wells

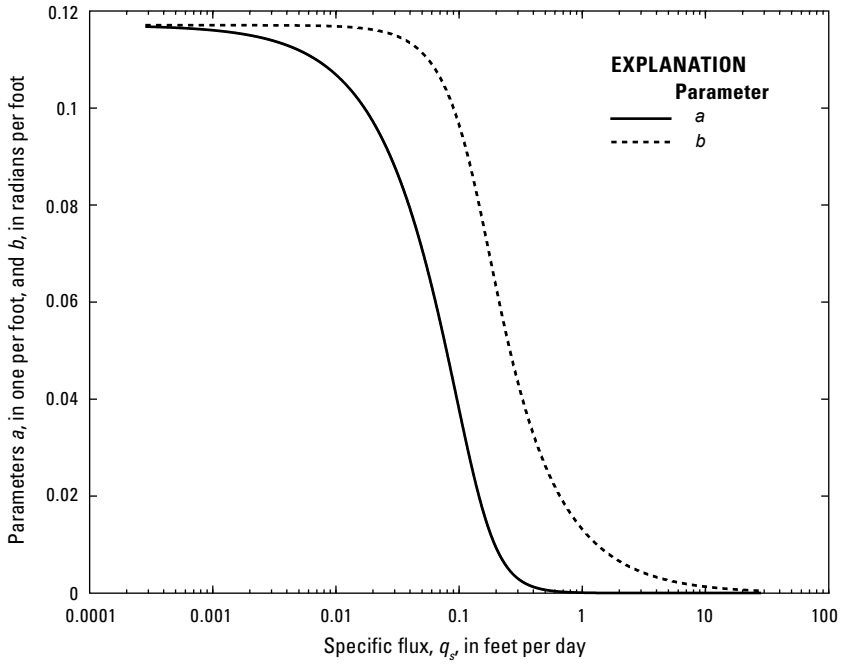

Figure 5. Type curves developed using equations 8 and 9 showing values of the parameters a and b as a function of specific flux, q_s.

at distances x_1 and x_2 from the river (Stallman, 1965; Moret, 2007). The differences between the maximum and minimum temperatures in these records, ΔTx_1 and ΔTx_2, can be used to estimate a:

$$a = \frac{-1}{x_2 - x_1} \log\left(\frac{\Delta T_{X1}}{\Delta T_{X2}}\right) \quad (12)$$

The phase lag between the two temperature records, Δt, yields b:

$$b = \frac{2\pi\Delta t}{(x_2 - x_1)\tau} \quad (13)$$

Moret (2007) found that the best way to estimate specific flux, q_s, is to plot the measured values of a and b on type curves (fig. 5). With this method, the user can determine whether a and b are physically realistic and consistent with each other and assess the sensitivity of q_s to measurement error. The Suzuki-Stallman method can only be used to estimate flux in regions of the curves where a and b vary as a function of q_s (fig. 5).

In this study, four steps were used to estimate flux from temperature data: (1) two type curves (a and b) were developed using thermal properties of the aquifer and equations 8–11 for a range of specific-flux values (fig. 5), (2) the values for a and b were calculated using equations 12 and 13 and temperatures measured in the piezometers, (3) the values for a and b calculated in the previous step were plotted on their respective type curves and matched with the corresponding flux (q_a and q_b), and (4) the q_a and q_b estimates were averaged to obtain q_{heat}.

Limitations and Assumptions of Suzuki-Stallman Method

According to Moret (2007), the Suzuki-Stallman method used in this study does not fully represent all of the factors that contribute to aquifer-temperature signals. However, the method sufficiently represents the system to produce a useful estimate of groundwater flux. Some of the limitations and assumptions with this method are described in the following sections. A complete discussion of data limitations associated with use of the Suzuki-Stallman method is found in Moret (2007).

Range of Applicability

The Suzuki-Stallman method can only be used to estimate flux in regions of the curve where a and b vary detectably as a function of specific flux (q_s). Figure 5 shows how the values of a and b vary as a function of specific flux using average thermal properties of the aquifer that were determined by Bartolino and Niswonger (1999). The exact limits of detectability depend on the accuracy of the temperature data, the magnitude of the original temperature-signal oscillation, and the distance between measuring points; for the aquifer parameters used in this study, fluxes between 10^{-3} and 1 ft/d should be detectable.

Flow Direction

The Suzuki (1960) equation was developed to measure vertical infiltration in fields and assumes that the flux is one dimensional and calculated along the flow path. However, leakage of water from the Rio Grande into the adjacent aquifer is not one dimensional. The hydraulic gradients are primarily horizontal, but vertical gradients also exist. The paired piezometer transects in this study are not oriented directly along the flow paths of river seepage, and q_{heat} was calculated between pairs of wells along each individual transect. Based on these limitations, the q_{heat} calculations likely systematically underestimate the flux.

Aquifer Heterogeneity

The Suzuki (1960) equation assumes a uniform flow field, a condition not met in a heterogeneous aquifer. If temperature signals measured at points with different flow rates are compared, then the estimated fluxes will be incorrect. Moret (2007) advises measuring the temperature at a number of depths in as many observation wells as are available to limit the effect of time-series data recorded in nonrepresentative locations.

Variable Recharge

Bartolino and Niswonger (1999) determined that the flux through the riverbed at the Paseo Del Norte site varied by roughly an order of magnitude over the course of the year, whereas the Suzuki (1960) equation assumes a constant flux. Moret (2007) modeled aquifer temperature using variable monthly recharge estimates and a constant annual flux. The Bartolino and Niswonger (1999) and Moret (2007) models agreed reasonably well, and Moret (2007) concluded that the Suzuki-Stallman method represents aquifers with annual variations in river recharge reasonably well.

Spatial Aliasing

The spatial wavelength, λ, of a temperature wave described by equation 7 is defined by:

$$\lambda = \frac{2\pi}{b} \quad (14)$$

By using figure 5, fluxes of 10^{-3} and 1 ft/d result from b values of 0.117 and 0.0132 rad/ft, respectively, and wavelengths of about 54 and 476 ft, respectively. For example, if q_s=10^{-3} ft/d, then b=0.117 (fig. 5) and λ=2π/0.117, or 54 ft;

if q_s=1 ft/d, then b=0.0132 (fig. 5), and λ=2π/0.0132, or 476 ft. When the wells used to measure temperature are separated by more than one wavelength, the apparent lag between the temperature series will be incorrect. This phenomenon is known as spatial aliasing. In this situation, b will be greatly underestimated. A measured value of b can be evaluated by plotting it with the measured a value for the same time-series pair on a plot generated by using equation 9 (for example, fig. 5). If the q_s values that correspond to a and b (q_a *and* q_b, respectively) do not agree reasonably well, then 1-year increments can be added to the measured lag.

Surface-Temperature Variations

Temperatures in shallow parts of the alluvial aquifer can be affected by the annual variation in the ground-surface temperature. The ground-surface temperature generally is an attenuated version of the atmospheric-temperature signal (Smerdon and others, 2004). Because of the exponential decay of ground-surface temperature signals with depth (Carslaw and Jaegar, 1959), groundwater temperatures measured more than approximately 5 ft below ground surface may not be substantially affected by surface warming (Silliman and Booth, 1993; Moret, 2007).

At the Paseo del Norte site, Bartolino (2003) recorded temperatures at 7 or 10, 13 or 15, 20, 26, and 33 ft below ground surface in eight piezometers installed in an east-west configuration between the east and west riverside drains. In piezometers P06 and P07 from the Bartolino (2003) dataset, Moret (2007) found no substantial difference between the temperatures recorded at depths of 7 or 10 ft and the temperatures recorded at 13 or 15 ft, indicating that the effect of atmospheric temperature is small. There was a 6.5 °F difference in the magnitudes of the temperature waves recorded at 7 and 15 ft in piezometer P08 (Bartolino, 2003). This difference, however, is greater than what would be expected if it was attributable to the atmospheric-temperature effect and is likely because of lower hydraulic conductivity of the sediments at the 7-ft depth than the deeper sediments (Moret, 2007).

Temperature Dependence of Hydraulic Conductivity

Hydraulic conductivity depends inversely on fluid viscosity and directly on fluid density, while both viscosity and density depend on temperature. The viscosity of liquid water at 32 °F is twice that of water at 77 °F (Vennard and Street, 1982). Surface-water recharge fluxes can thus vary substantially with the temperature of the water (Constantz and others, 1994). A fundamental limitation of the Suzuki-Stallman method is that it does not consider the effect of temperature on groundwater viscosity and thus hydraulic conductivity. Moret (2007) evaluated this limitation by using a two-dimensional finite-element model and concluded that if temperature time-series data appear to be sinusoidal, then the temperature dependence of hydraulic conductivity does not limit the applicability of the Suzuki-Stallman method for determining general estimates of specific flux. For additional details see Moret (2007).

Uncertainty in Thermal Properties

The thermal properties of the aquifer, k (thermal conductivity) and ρc (heat capacity), are generally not well known, but for aquifers consisting of unconsolidated sediments, the range of k values reported in the literature is small (Moret, 2007). Moret (2007) found that if site-specific measurements are not readily available, a thermal conductivity, chosen based solely on aquifer lithology, will introduce an uncertainty into the estimate of q_s of a few tens of percent. In this study, the average of the four values obtained by Bartolino and Niswonger (1999) were used for the thermal conductivity (2.16 W m^{-1} °C^{-1}). Saturated heat capacity (3.2×10^6 J m^{-3} °C^{-1}) of the inner valley alluvial aquifer was determined using values for the heat capacity of dry solids and porosity presented by Bartolino and Niswonger (1999) and the heat capacity of water (4.184×10^6 J m^{-3} °C^{-1}).

Data Error

Another possible limitation in the interpretation of temperature oscillations using the Suzuki-Stallman method is uncertainty in the estimation of best-fit sinusoids for the observed data series, which would result in uncertainty in a and b. Errors in sinusoid fitting are likely to be greatest closer to the source of the surface-water recharge (Moret, 2007).

Groundwater Hydrology

The hydrologic characteristics of groundwater movement in the study area were examined using hydraulic head measurements, water temperatures, slug-testing results, and horizontal groundwater-flux estimates. Slug-test data from 47 sites were used to determine the hydraulic conductivity of the alluvial aquifer (USGS New Mexico Water Science Center aquifer-test archive, Albuquerque). Daily mean hydraulic-head data were used to establish groundwater gradients at transect locations, and vertical water-temperature profile data were collected at selected piezometers to evaluate the depth of penetration of river recharge into the aquifer. Horizontal groundwater fluxes from the Rio Grande through the inner valley alluvial aquifer to the riverside drains were estimated using the horizontal hydraulic gradients and hydraulic-conductivity values. A seepage investigation in the riverside drains was then conducted to evaluate the accuracy of flux estimates.

Groundwater Levels and Temperatures

Hourly groundwater-level data were recorded from 252 piezometers screened at different intervals within the alluvial aquifer. Daily mean water levels are shown in figures 6*A–P*.

Groundwater-level data were used to evaluate water-level trends, measure response to increases or decreases in river stage, and calculate horizontal hydraulic gradients. In the study area, diurnal and seasonal fluctuations in water levels were common, but no substantial upward or downward long-term water-level trends were discernable from 2009 to 2010 (fig. 6*A–P*). Groundwater-level responses to stage changes in the river were measurable; water levels in piezometers closest to the river showed a more pronounced response to change in river stage than did piezometers next to or outside the drains, which are farther from the river. Vertical hydraulic gradients from nested piezometers typically were small (fig. 6*A–P*). Heads measured in the shallow and mid-depth piezometers typically were similar, however, there were exceptions, most notably at piezometers B16a, b, and c; R4a, b, and c; and R5a, b, and c, where clay-rich sediments were observed in sediment cores.

The groundwater-flow paths between the drains and the surrounding shallow aquifer are variable, and the water levels and generalized flow lines (fig. 3*A–H*) are only representative of the specific date indicated. Water levels were selected for August 15, 2009, because this represented a time when water-level data were available from most piezometers. For example, sometimes a drain will gain water from both sides of the alluvial aquifer while other times the drain might gain groundwater from the river side of the alluvial aquifer and lose water to the alluvial aquifer away from the river. Some of this variation is seasonal, and some of the variation is likely related to irrigation operations. However, water levels indicated that groundwater movement was usually away from the river toward the drains (fig. 3*A–H*). This direction of groundwater movement is reasonable because the riverside drains were designed to extend below the groundwater table, except near the downstream ends of the drains, where they empty back into the river.

While drain-water levels generally were lower than adjacent groundwater levels, there were instances where the water level in a drain was substantially higher than adjacent groundwater levels. For example, at the Montaño transects, the water level at MS3, near the downstream end of the Corrales Riverside Drain, was about 5 ft higher than the water levels at M9a and M18a on August 15, 2009 (fig. 3*C*). The depth of water in the drain at this location was about 3–4 ft, so the bottom of the drain probably was higher than the water table. These data indicate that the hydraulic interaction between the drain and groundwater at this location is minimal; this condition is likely to persist from one year to the next. At the Barelas transects, the water level at BS1 in the Albuquerque Riverside Drain was about 2.5 ft higher than the water levels in piezometers B3a and B12a on March 15, 2009 (fig. 3*E*). These water-level differences are attributable to a point of diversion structure in the drain about 900 ft downstream from B12a that obstructs flow and elevates the water level in the drain so that the water level in the drain upstream from the diversion structure was substantially higher than downstream from the diversion structure. At the Central transects, water levels in the Atrisco Lateral at CS3 are from 2 to 6 ft higher than the water levels in the adjacent piezometers C17a and C18a (fig. 3*D* and fig. 6*H*). The Atrisco Lateral is used to deliver water for irrigation and therefore is designed to have higher water levels than the surrounding groundwater. It is likely that the Atrisco Lateral is losing some water to the surrounding aquifer.

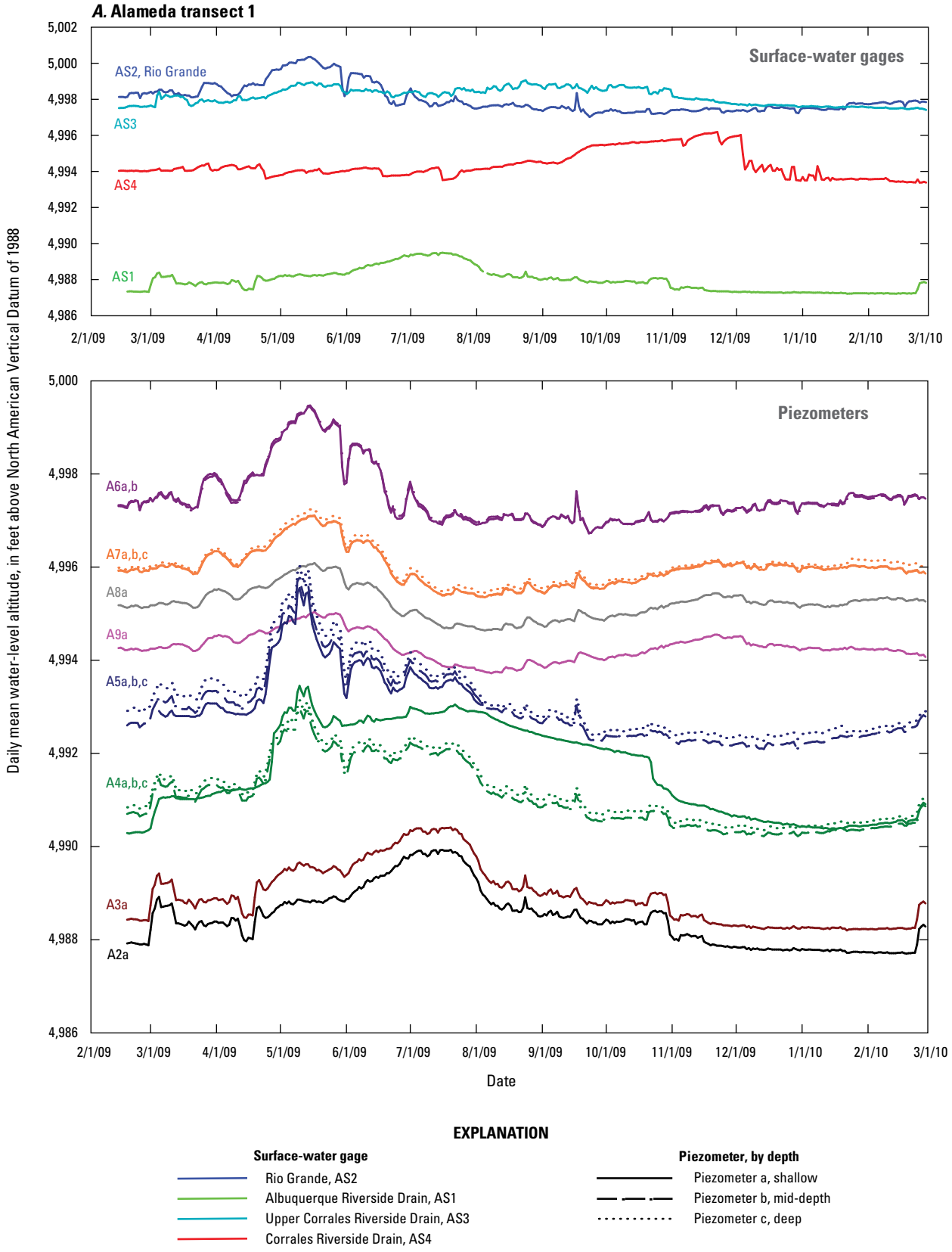

Figure 6. Daily mean water-level altitude for stage of the Rio Grande and riverside drains and for groundwater levels in piezometers at *A*, Alameda transect 1; *B*, Alameda transect 2; *C*, Paseo del Norte transect 1; *D*, Paseo del Norte transect 2; *E*, Montaño transect 1; *F*, Montaño transect 2; *G*, Central transect 1; *H*, Central transect 2; *I*, Barelas transect 1; *J*, Barelas transect 2; *K*, Rio Bravo transect 1; *L*, Rio Bravo transect 2; *M*, Pajarito transect 1; *N*, Pajarito transect 2; *O*, I-25 transect 1; and *P*, I-25 transect 2.

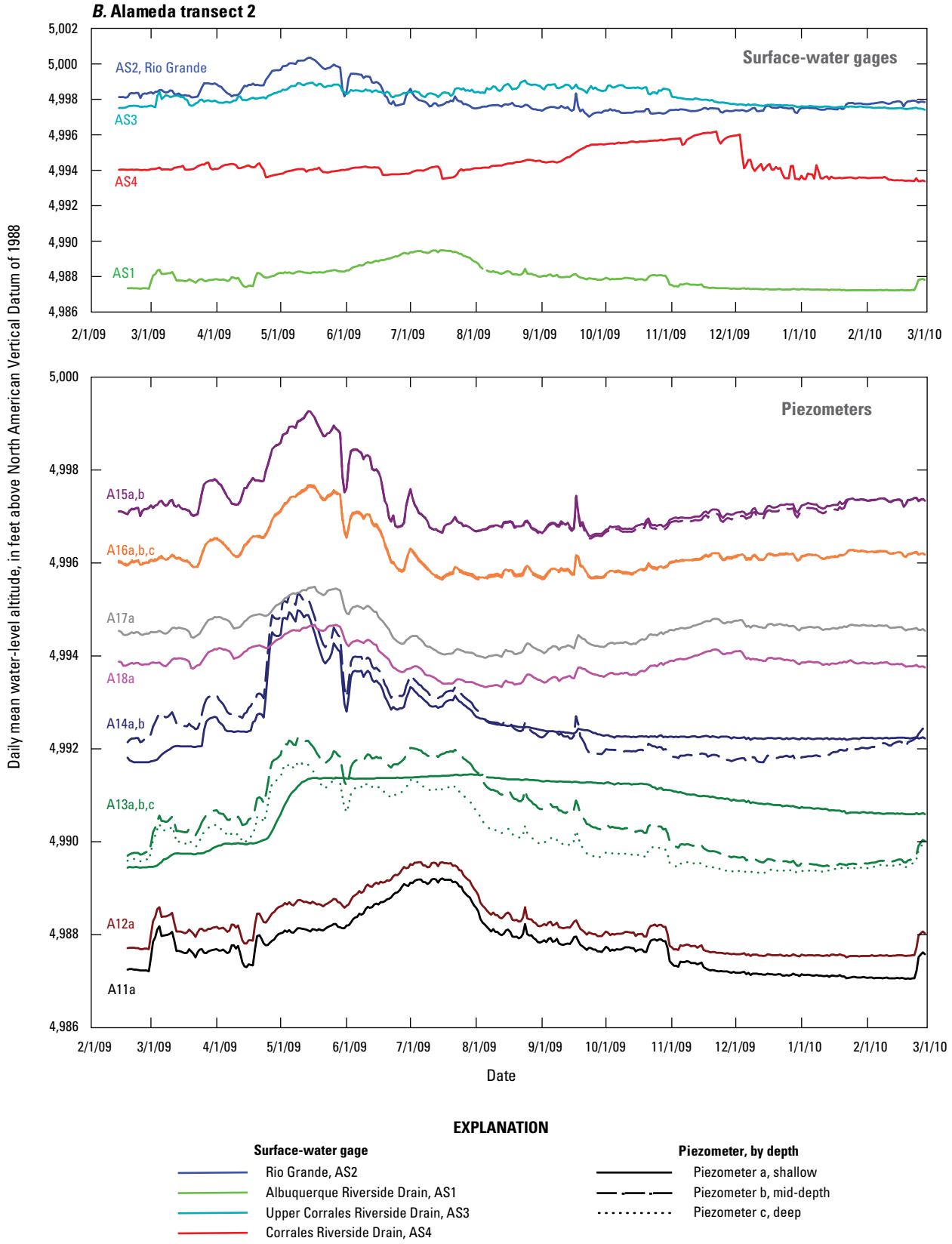

Figure 6. Daily mean water-level altitude for stage of the Rio Grande and riverside drains and for groundwater levels in piezometers at *A*, Alameda transect 1; *B*, Alameda transect 2; *C*, Paseo del Norte transect 1; *D*, Paseo del Norte transect 2; *E*, Montaño transect 1; *F*, Montaño transect 2; *G*, Central transect 1; *H*, Central transect 2; *I*, Barelas transect 1; *J*, Barelas transect 2; *K*, Rio Bravo transect 1; *L*, Rio Bravo transect 2; *M*, Pajarito transect 1; *N*, Pajarito transect 2; *O*, I-25 transect 1; and *P*, I-25 transect 2.—Continued

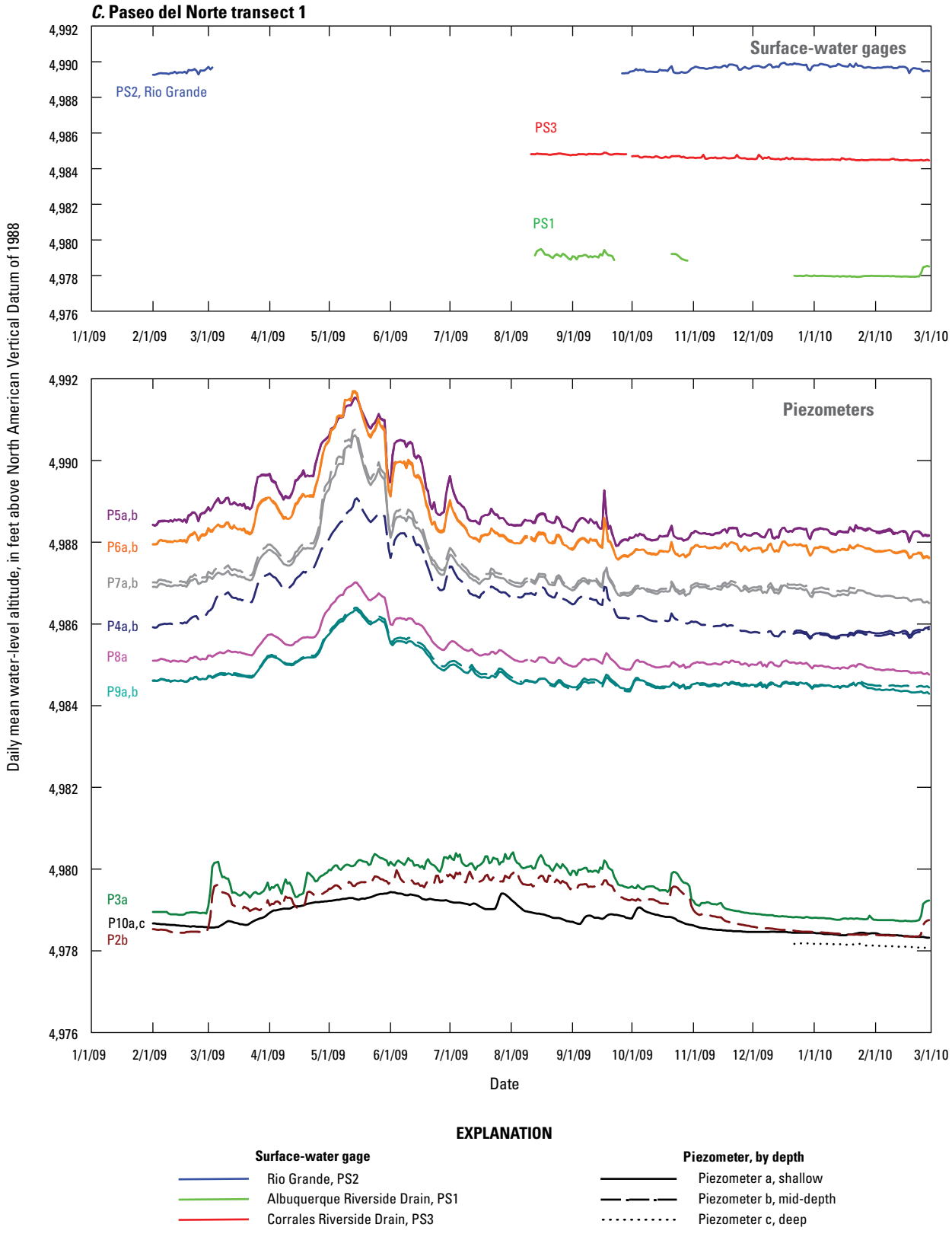

Figure 6. Daily mean water-level altitude for stage of the Rio Grande and riverside drains and for groundwater levels in piezometers at *A*, Alameda transect 1; *B*, Alameda transect 2; *C*, Paseo del Norte transect 1; *D*, Paseo del Norte transect 2; *E*, Montaño transect 1; *F*, Montaño transect 2; *G*, Central transect 1; *H*, Central transect 2; *I*, Barelas transect 1; *J*, Barelas transect 2; *K*, Rio Bravo transect 1; *L*, Rio Bravo transect 2; *M*, Pajarito transect 1; *N*, Pajarito transect 2; *O*, I-25 transect 1; and *P*, I-25 transect 2.—Continued

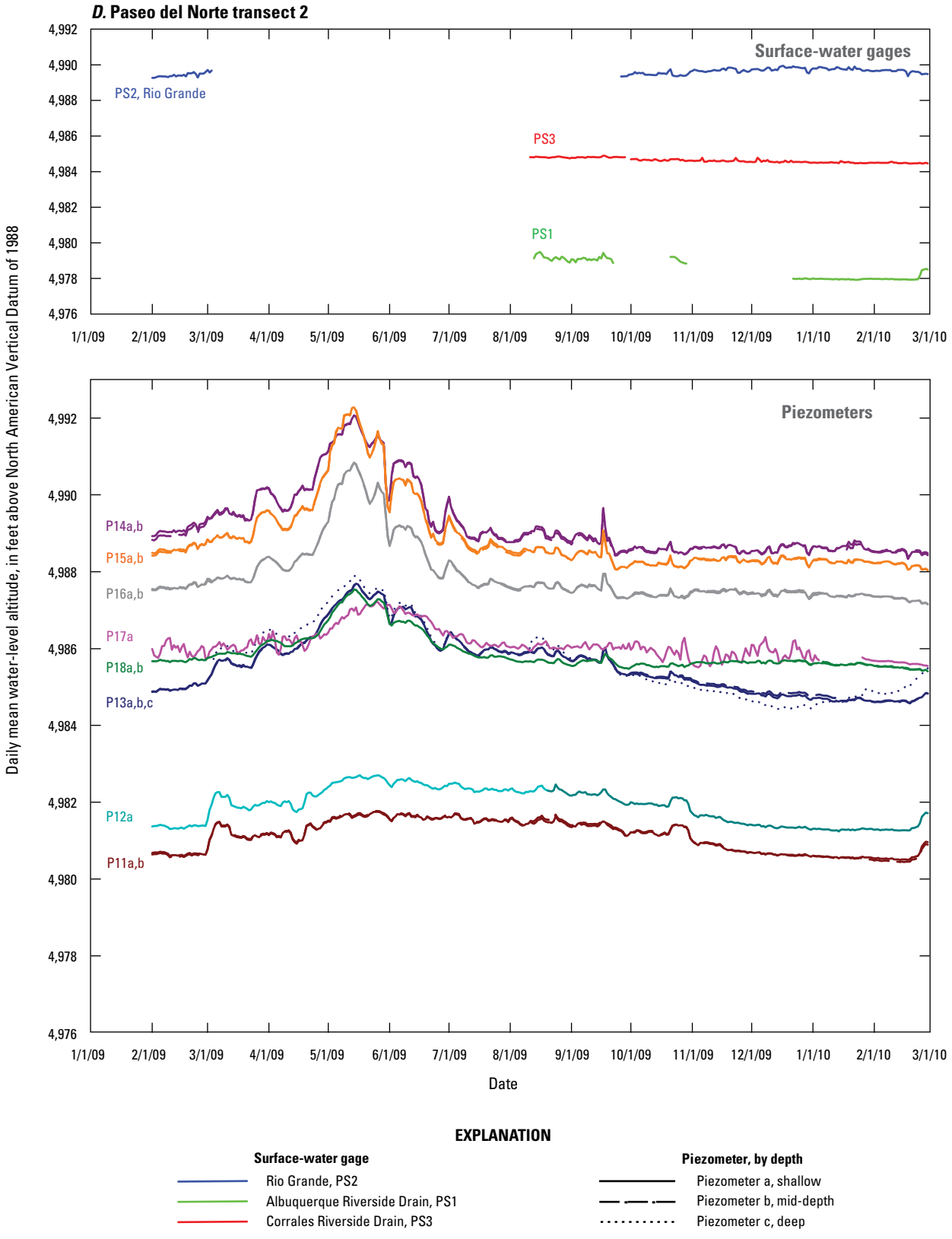

Figure 6. Daily mean water-level altitude for stage of the Rio Grande and riverside drains and for groundwater levels in piezometers at *A*, Alameda transect 1; *B*, Alameda transect 2; *C*, Paseo del Norte transect 1; *D*, Paseo del Norte transect 2; *E*, Montaño transect 1; *F*, Montaño transect 2; *G*, Central transect 1; *H*, Central transect 2; *I*, Barelas transect 1; *J*, Barelas transect 2; *K*, Rio Bravo transect 1; *L*, Rio Bravo transect 2; *M*, Pajarito transect 1; *N*, Pajarito transect 2; *O*, I-25 transect 1; and *P*, I-25 transect 2.—Continued

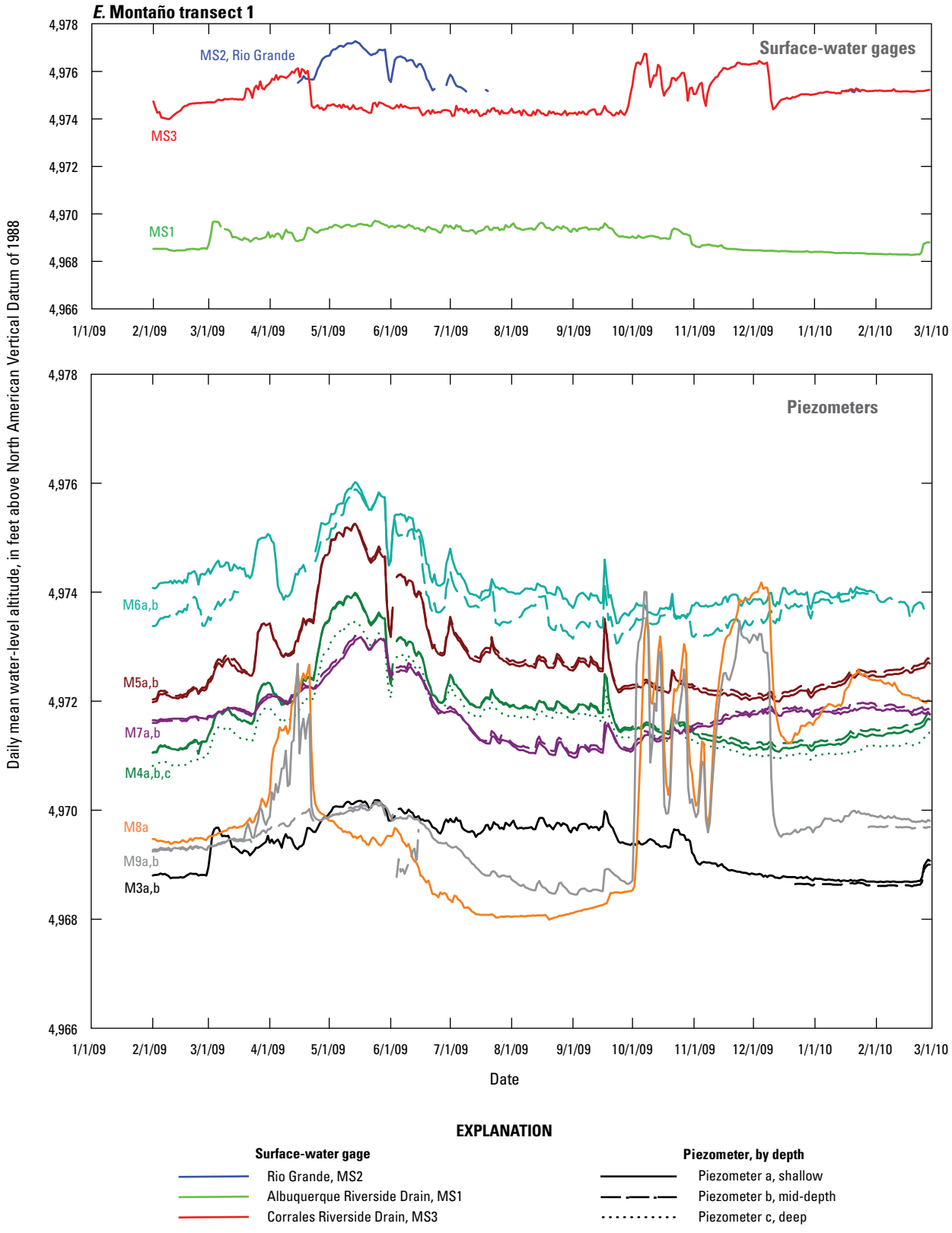

Figure 6. Daily mean water-level altitude for stage of the Rio Grande and riverside drains and for groundwater levels in piezometers at *A*, Alameda transect 1; *B*, Alameda transect 2; *C*, Paseo del Norte transect 1; *D*, Paseo del Norte transect 2; *E*, Montaño transect 1; *F*, Montaño transect 2; *G*, Central transect 1; *H*, Central transect 2; *I*, Barelas transect 1; *J*, Barelas transect 2; *K*, Rio Bravo transect 1; *L*, Rio Bravo transect 2; *M*, Pajarito transect 1; *N*, Pajarito transect 2; *O*, I-25 transect 1; and *P*, I-25 transect 2.—Continued

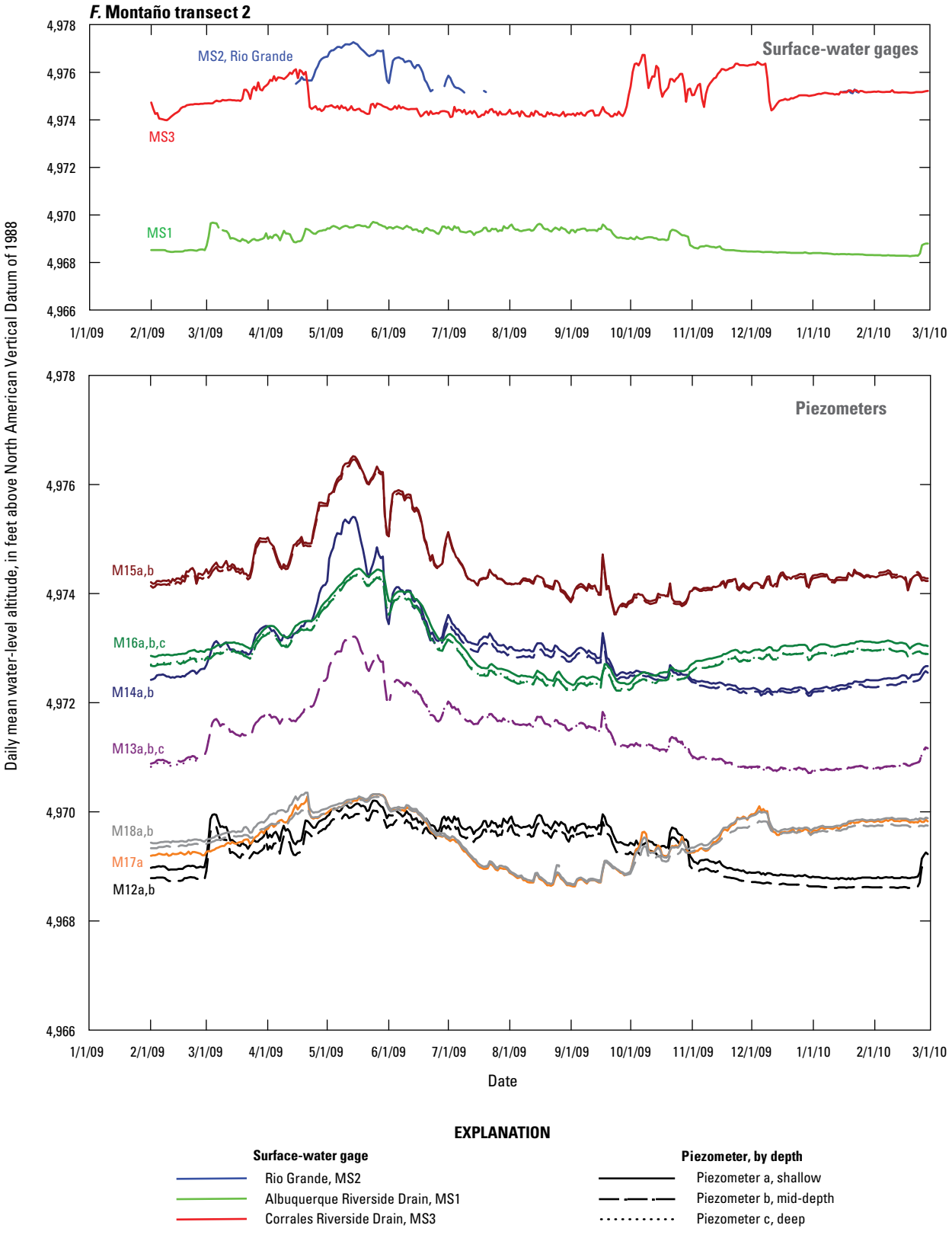

Figure 6. Daily mean water-level altitude for stage of the Rio Grande and riverside drains and for groundwater levels in piezometers at *A*, Alameda transect 1; *B*, Alameda transect 2; *C*, Paseo del Norte transect 1; *D*, Paseo del Norte transect 2; *E*, Montaño transect 1; *F*, Montaño transect 2; *G*, Central transect 1; *H*, Central transect 2; *I*, Barelas transect 1; *J*, Barelas transect 2; *K*, Rio Bravo transect 1; *L*, Rio Bravo transect 2; *M*, Pajarito transect 1; *N*, Pajarito transect 2; *O*, I-25 transect 1; and *P*, I-25 transect 2.—Continued

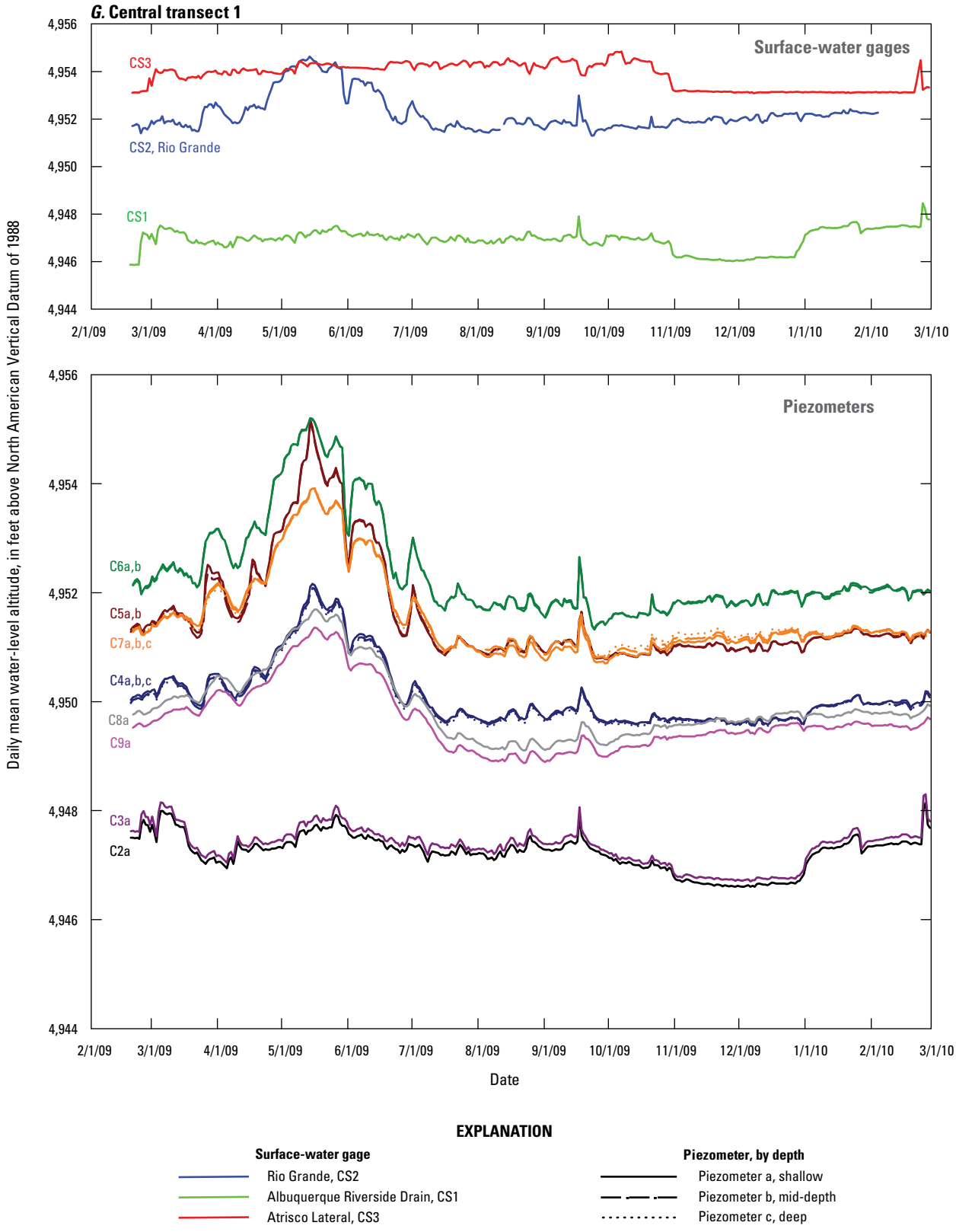

Figure 6. Daily mean water-level altitude for stage of the Rio Grande and riverside drains and for groundwater levels in piezometers at *A*, Alameda transect 1; *B*, Alameda transect 2; *C*, Paseo del Norte transect 1; *D*, Paseo del Norte transect 2; *E*, Montaño transect 1; *F*, Montaño transect 2; *G*, Central transect 1; *H*, Central transect 2; *I*, Barelas transect 1; *J*, Barelas transect 2; *K*, Rio Bravo transect 1; *L*, Rio Bravo transect 2; *M*, Pajarito transect 1; *N*, Pajarito transect 2; *O*, I-25 transect 1; and *P*, I-25 transect 2.—Continued

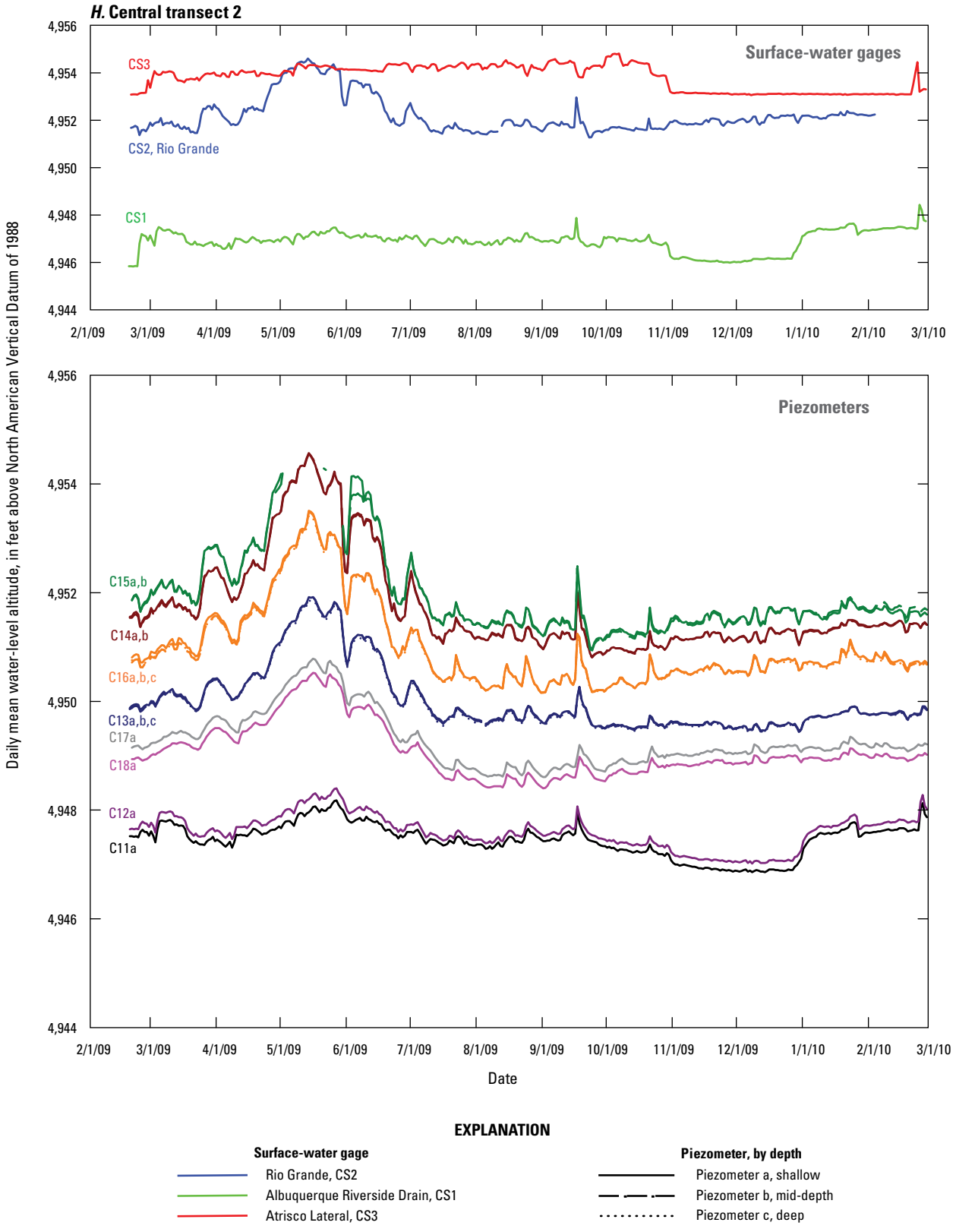

Figure 6. Daily mean water-level altitude for stage of the Rio Grande and riverside drains and for groundwater levels in piezometers at *A*, Alameda transect 1; *B*, Alameda transect 2; *C*, Paseo del Norte transect 1; *D*, Paseo del Norte transect 2; *E*, Montaño transect 1; *F*, Montaño transect 2; *G*, Central transect 1; *H*, Central transect 2; *I*, Barelas transect 1; *J*, Barelas transect 2; *K*, Rio Bravo transect 1; *L*, Rio Bravo transect 2; *M*, Pajarito transect 1; *N*, Pajarito transect 2; *O*, I-25 transect 1; and *P*, I-25 transect 2.—Continued

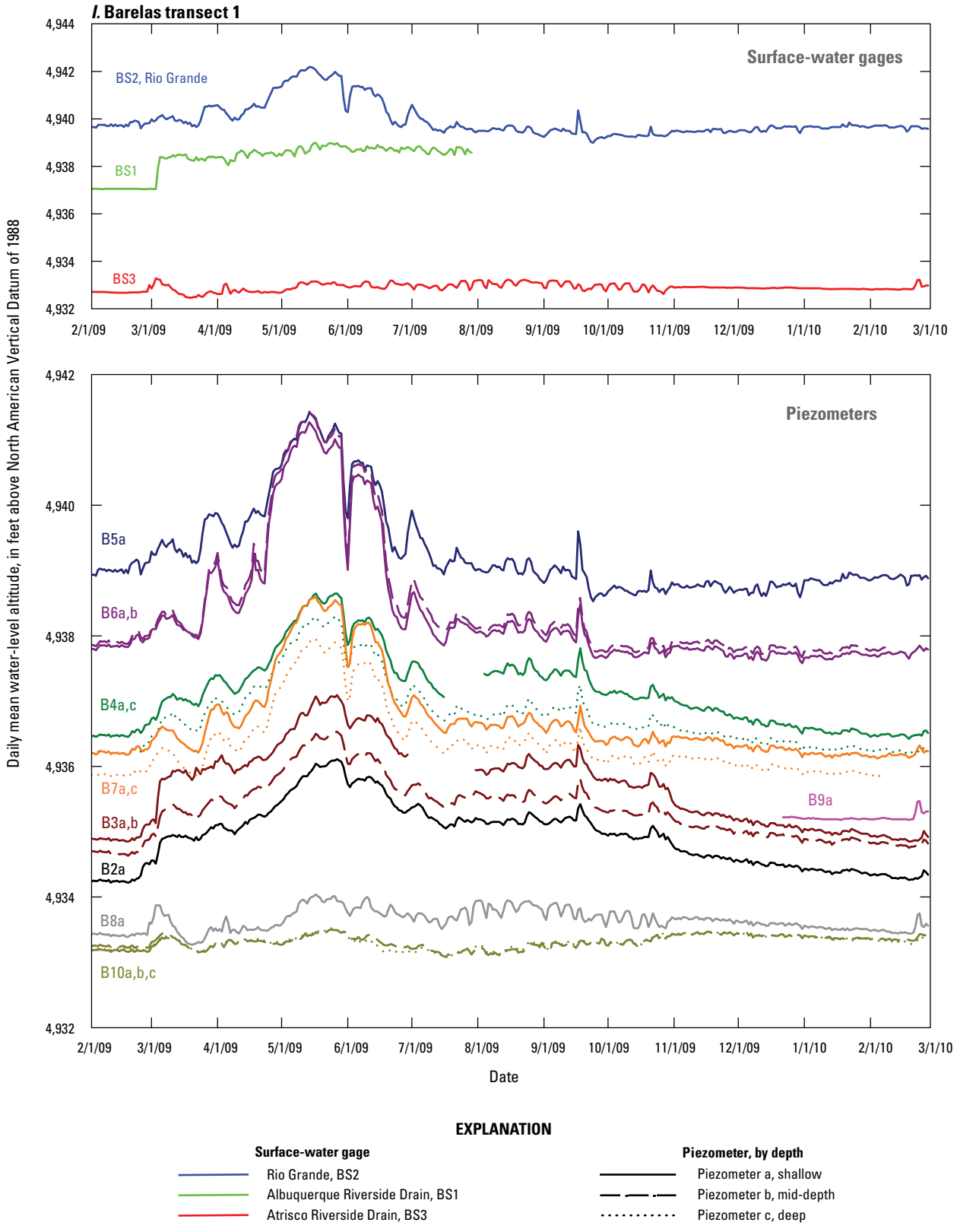

Figure 6. Daily mean water-level altitude for stage of the Rio Grande and riverside drains and for groundwater levels in piezometers at *A*, Alameda transect 1; *B*, Alameda transect 2; *C*, Paseo del Norte transect 1; *D*, Paseo del Norte transect 2; *E*, Montaño transect 1; *F*, Montaño transect 2; *G*, Central transect 1; *H*, Central transect 2; *I*, Barelas transect 1; *J*, Barelas transect 2; *K*, Rio Bravo transect 1; *L*, Rio Bravo transect 2; *M*, Pajarito transect 1; *N*, Pajarito transect 2; *O*, I-25 transect 1; and *P*, I-25 transect 2.—Continued

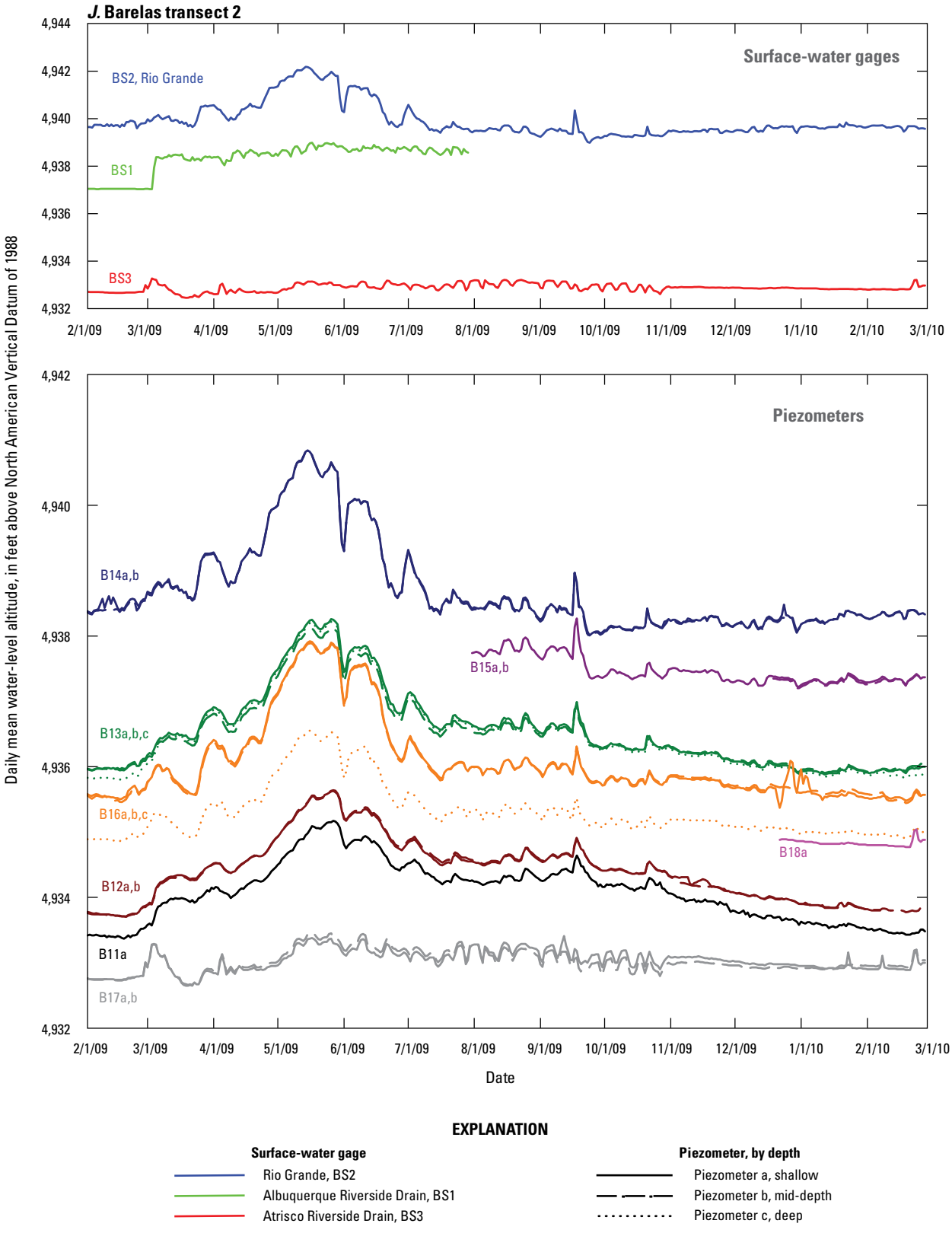

Figure 6. Daily mean water-level altitude for stage of the Rio Grande and riverside drains and for groundwater levels in piezometers at *A*, Alameda transect 1; *B*, Alameda transect 2; *C*, Paseo del Norte transect 1; *D*, Paseo del Norte transect 2; *E*, Montaño transect 1; *F*, Montaño transect 2; *G*, Central transect 1; *H*, Central transect 2; *I*, Barelas transect 1; *J*, Barelas transect 2; *K*, Rio Bravo transect 1; *L*, Rio Bravo transect 2; *M*, Pajarito transect 1; *N*, Pajarito transect 2; *O*, I-25 transect 1; and *P*, I-25 transect 2.—Continued

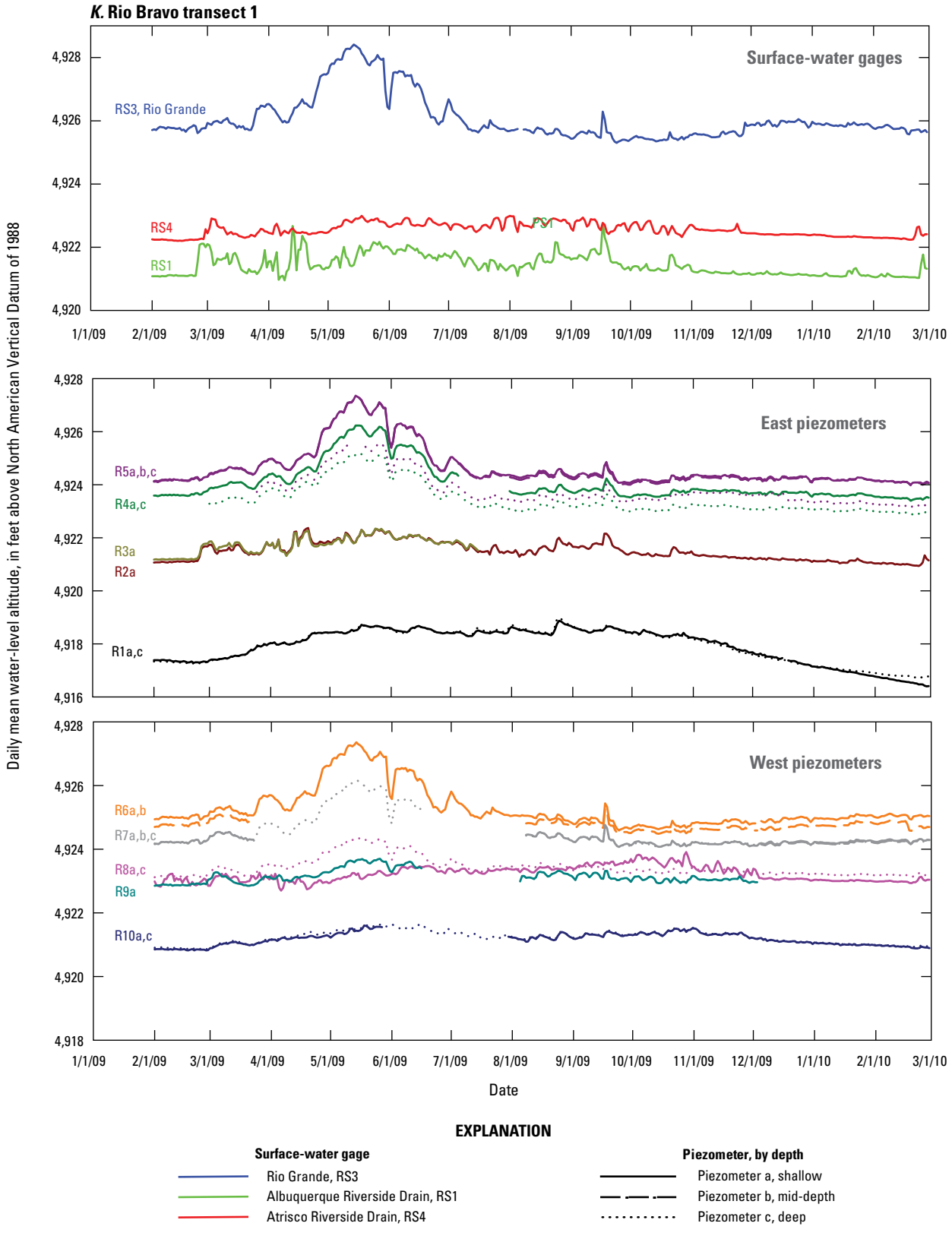

Figure 6. Daily mean water-level altitude for stage of the Rio Grande and riverside drains and for groundwater levels in piezometers at *A*, Alameda transect 1; *B*, Alameda transect 2; *C*, Paseo del Norte transect 1; *D*, Paseo del Norte transect 2; *E*, Montaño transect 1; *F*, Montaño transect 2; *G*, Central transect 1; *H*, Central transect 2; *I*, Barelas transect 1; *J*, Barelas transect 2; *K*, Rio Bravo transect 1; *L*, Rio Bravo transect 2; *M*, Pajarito transect 1; *N*, Pajarito transect 2; *O*, I-25 transect 1; and *P*, I-25 transect 2.—Continued

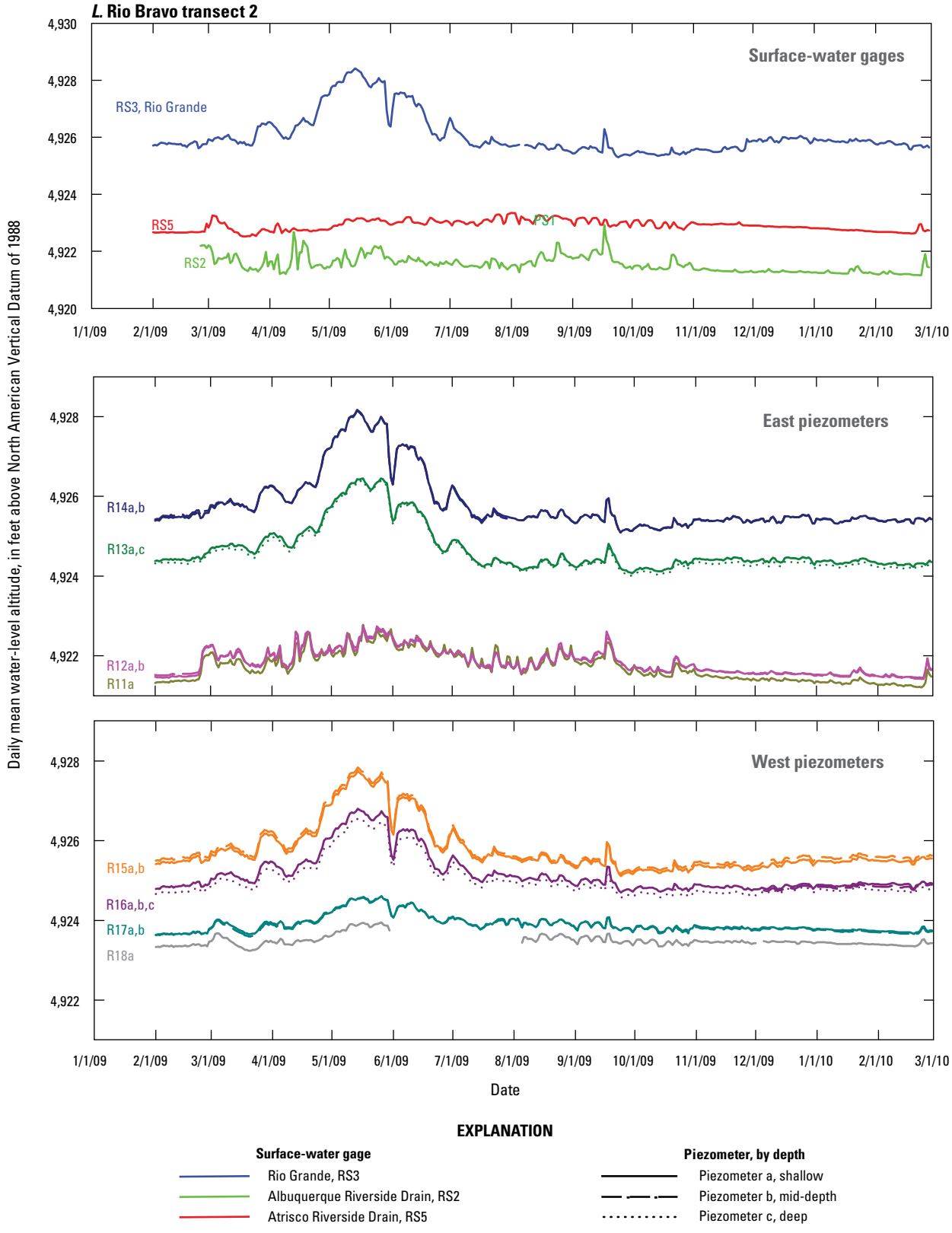

Figure 6. Daily mean water-level altitude for stage of the Rio Grande and riverside drains and for groundwater levels in piezometers at *A*, Alameda transect 1; *B*, Alameda transect 2; *C*, Paseo del Norte transect 1; *D*, Paseo del Norte transect 2; *E*, Montaño transect 1; *F*, Montaño transect 2; *G*, Central transect 1; *H*, Central transect 2; *I*, Barelas transect 1; *J*, Barelas transect 2; *K*, Rio Bravo transect 1; *L*, Rio Bravo transect 2; *M*, Pajarito transect 1; *N*, Pajarito transect 2; *O*, I-25 transect 1; and *P*, I-25 transect 2.—Continued

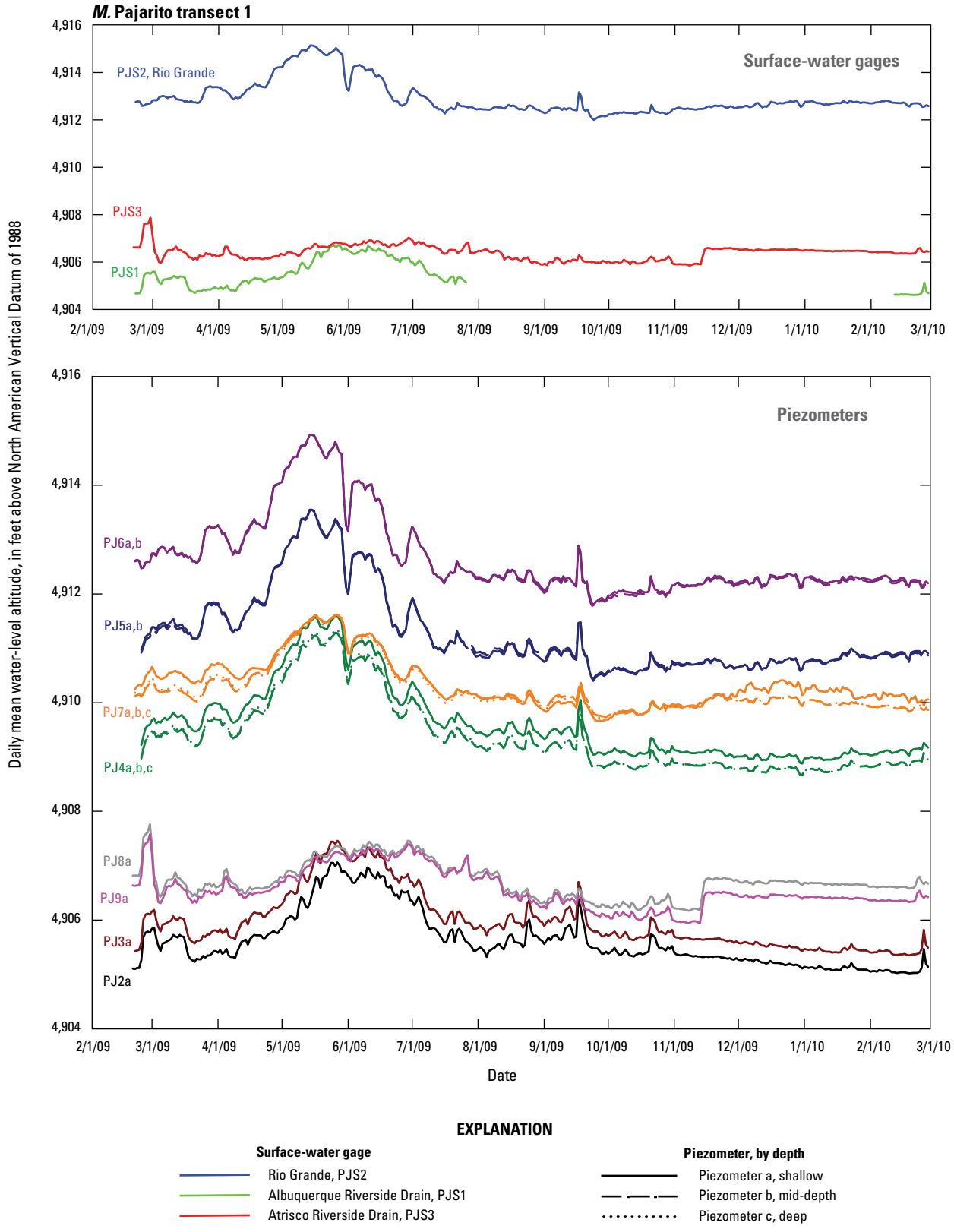

Figure 6. Daily mean water-level altitude for stage of the Rio Grande and riverside drains and for groundwater levels in piezometers at *A*, Alameda transect 1; *B*, Alameda transect 2; *C*, Paseo del Norte transect 1; *D*, Paseo del Norte transect 2; *E*, Montaño transect 1; *F*, Montaño transect 2; *G*, Central transect 1; *H*, Central transect 2; *I*, Barelas transect 1; *J*, Barelas transect 2; *K*, Rio Bravo transect 1; *L*, Rio Bravo transect 2; *M*, Pajarito transect 1; *N*, Pajarito transect 2; *O*, I-25 transect 1; and *P*, I-25 transect 2.—Continued

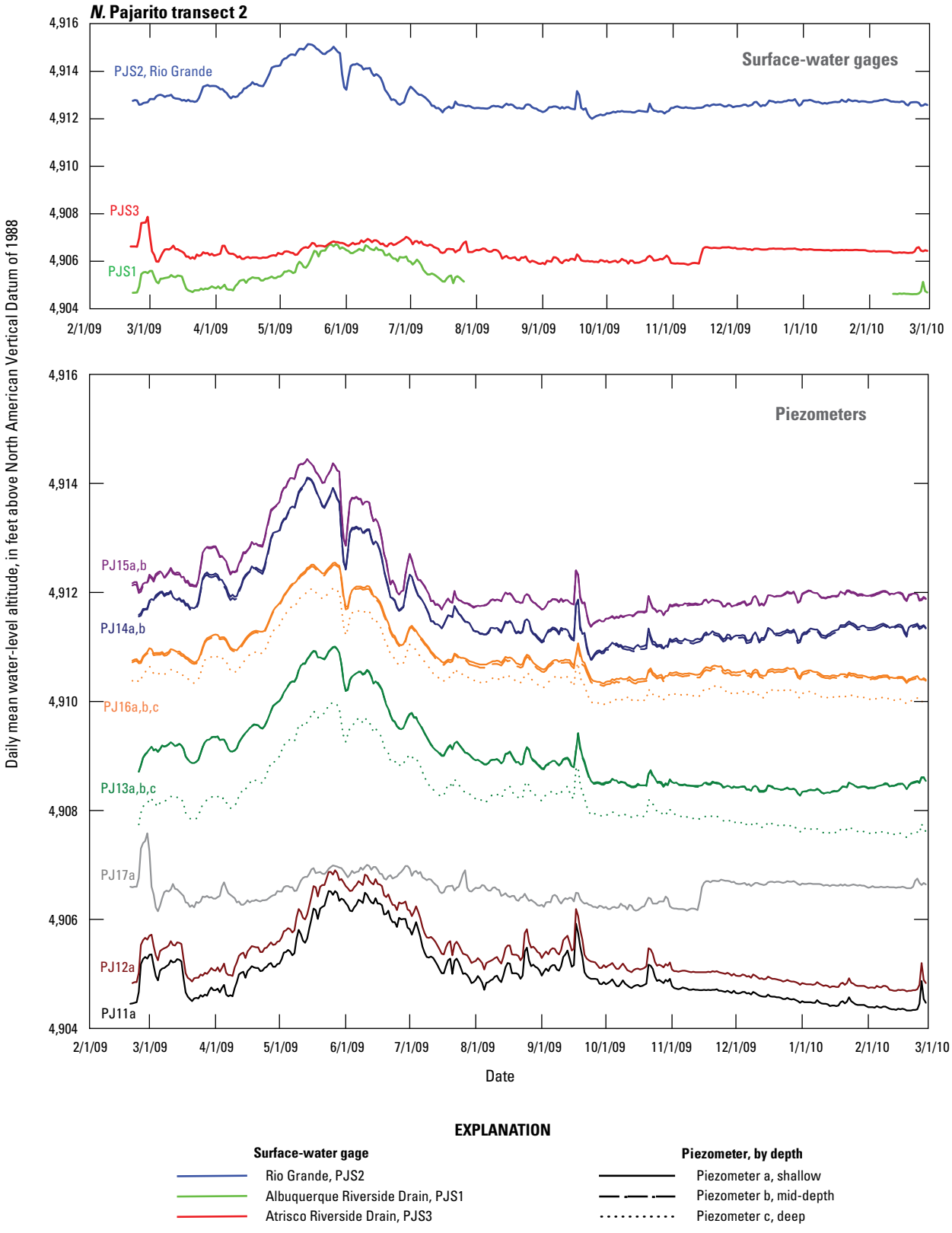

Figure 6. Daily mean water-level altitude for stage of the Rio Grande and riverside drains and for groundwater levels in piezometers at *A*, Alameda transect 1; *B*, Alameda transect 2; *C*, Paseo del Norte transect 1; *D*, Paseo del Norte transect 2; *E*, Montaño transect 1; *F*, Montaño transect 2; *G*, Central transect 1; *H*, Central transect 2; *I*, Barelas transect 1; *J*, Barelas transect 2; *K*, Rio Bravo transect 1; *L*, Rio Bravo transect 2; *M*, Pajarito transect 1; *N*, Pajarito transect 2; *O*, I-25 transect 1; and *P*, I-25 transect 2.—Continued

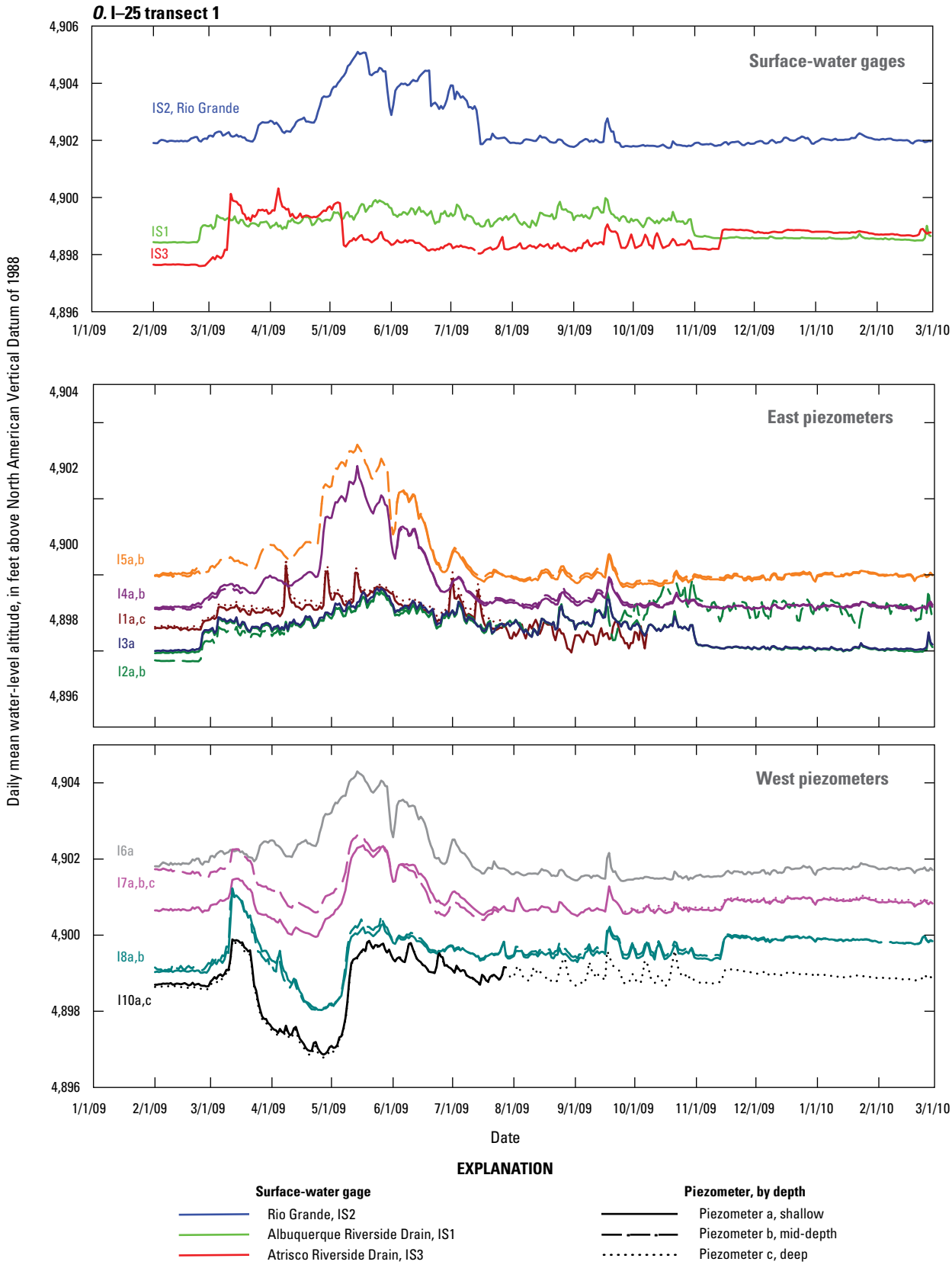

Figure 6. Daily mean water-level altitude for stage of the Rio Grande and riverside drains and for groundwater levels in piezometers at *A*, Alameda transect 1; *B*, Alameda transect 2; *C*, Paseo del Norte transect 1; *D*, Paseo del Norte transect 2; *E*, Montaño transect 1; *F*, Montaño transect 2; *G*, Central transect 1; *H*, Central transect 2; *I*, Barelas transect 1; *J*, Barelas transect 2; *K*, Rio Bravo transect 1; *L*, Rio Bravo transect 2; *M*, Pajarito transect 1; *N*, Pajarito transect 2; *O*, I-25 transect 1; and *P*, I-25 transect 2.—Continued

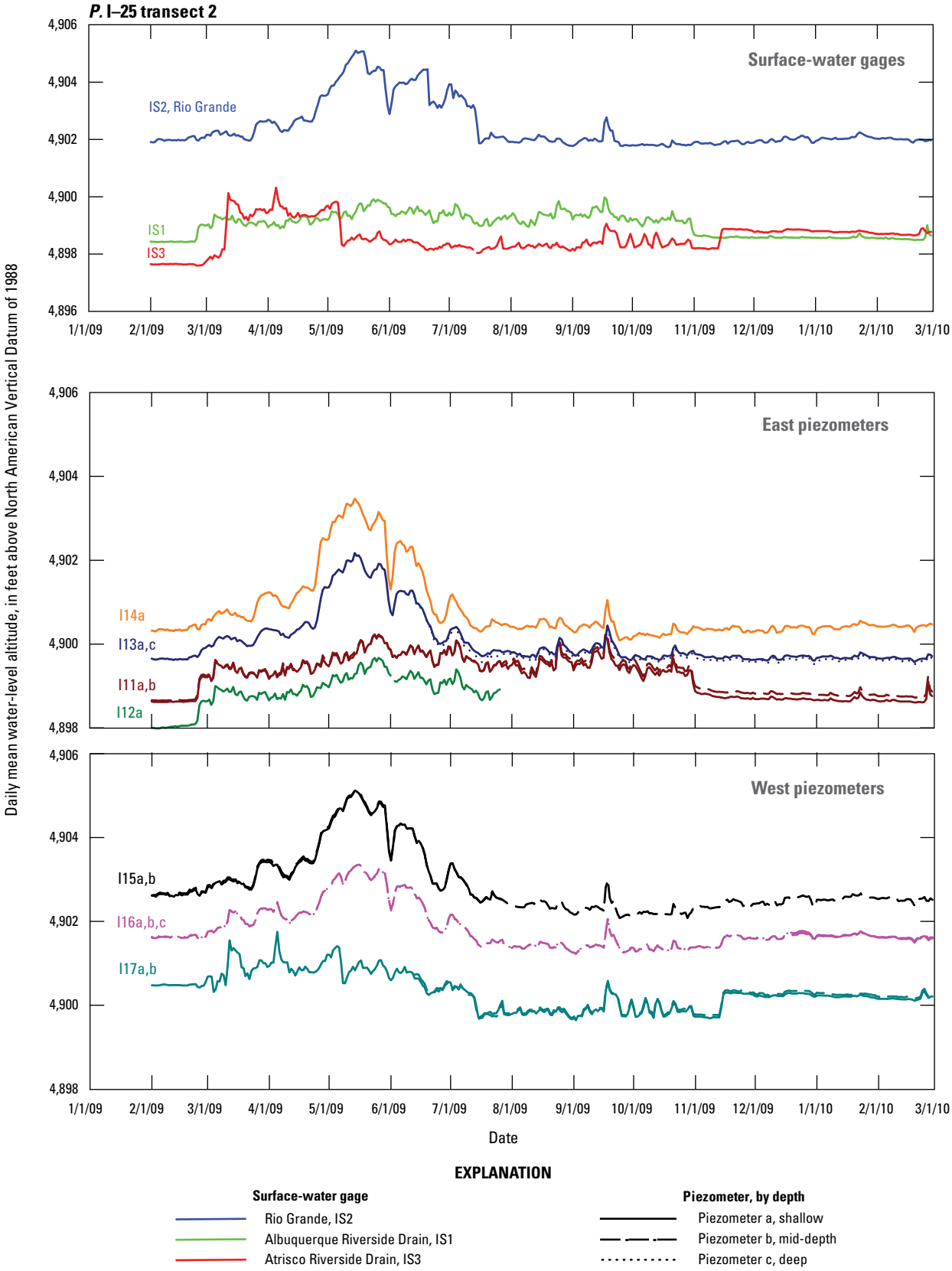

Figure 6. Daily mean water-level altitude for stage of the Rio Grande and riverside drains and for groundwater levels in piezometers at *A*, Alameda transect 1; *B*, Alameda transect 2; *C*, Paseo del Norte transect 1; *D*, Paseo del Norte transect 2; *E*, Montaño transect 1; *F*, Montaño transect 2; *G*, Central transect 1; *H*, Central transect 2; *I*, Barelas transect 1; *J*, Barelas transect 2; *K*, Rio Bravo transect 1; *L*, Rio Bravo transect 2; *M*, Pajarito transect 1; *N*, Pajarito transect 2; *O*, I-25 transect 1; and *P*, I-25 transect 2.—Continued

Hourly groundwater temperatures were recorded at depths of 10 and 20 ft bls in selected piezometer nests. Daily mean water temperature for all measurement points are shown in figure 7*A–P*. Large seasonal ranges in surface-water temperature are apparent; surface-water temperatures ranged from 29 °F in the winter to 81 °F in the summer. Surface-water temperatures in the drains typically were similar to temperatures measured in the Rio Grande, but the magnitudes of temperature fluctuations in the river were somewhat greater than in the drains. Maximum and minimum water temperatures in piezometers generally indicate a decrease in amplitude and an increase in time lag of the temperature signal with increasing depth and distance from the river. High-frequency temperature fluctuations of a few degrees in shallow piezometers installed adjacent to the river rapidly dissipated with depth and distance from the river. For example, the high-frequency temperature fluctuations that are evident in piezometer P5a, next to the river, are not evident in piezometers P4a and P3a (fig. 7*C*), which are farther away from the river (fig. 3*B*). The high-frequency fluctuations were not recorded in mid-depth piezometers or shallow piezometers located more than a few hundred feet from the river. Dampening of lower-frequency temperature signals can result from local-scale heterogeneities. For example, short-term (daily to weekly) temperature variations recorded in piezometer nests M14a and C6a, shallow piezometers adjacent to the river, are substantially attenuated 400–500 ft to the west in piezometer nests M13 and C7 (figs. 3*C* and 3*D* and figs. 7*F* and 7*G*, respectively).

Monthly vertical temperature profiles were collected during the months of October 2008 through November 2009 (with the exception of November 2008 and September 2009) in the deepest piezometer at selected piezometer nests (fig. 8). Temperature-profile data were collected to evaluate the depth of the alluvial aquifer that is influenced by leakage from the river. Temperatures were recorded at 5-ft intervals from about 0.5 ft below the water surface to the bottom of each piezometer. Although piezometers were constructed with a screened interval of 5 ft near the bottom of the piezometer, the temperature of water in blank (nonscreened) casing was assumed to be the same as the temperature of water outside the casing. Groundwater-temperature profiles in figure 8 form envelopes that bracket the warmest temperatures from August to October and coolest temperatures from February to April. Groundwater temperatures recorded between October 2008 and November 2009 were most variable at depths less than 30 ft and generally ranged from 40 to 70 °F.

Temperature envelopes in figure 8 generally can be qualitatively classified as fan- or tulip-shaped reflecting the direction and velocity of groundwater flow (Stonestrom and Constantz, 2003). At piezometers A7, A8, M7, C3, C4, C8, R3, R8, PJ8, I3, I4, and I5, the fan-shape of the temperature envelope shows that the seasonal temperature extinction depth (the depth at which seasonal temperature variations are not observed) ranges from 20 to 30 ft bls. Piezometers with fan-shaped temperature envelopes are indicated with an "F" in the lower right corner of the temperature profile in figure 8. Temperature fluctuations near the water table in these fan-shaped envelopes generally are 20 °F or less for the period between October 2008 and November 2009. The compressed nature of fan-shaped temperature envelopes is indicative of areas where (1) vertical groundwater flow is limited, (2) horizontal advective transport of heat is relatively uniform, or (3) groundwater is upwelling to discharge points. At the remaining piezometer nests, temperature fluctuations near the water table generally are greater than 30 °F for the period between October 2008 and November 2009. These temperature envelopes generally are more tulip-like in shape with seasonal temperature-extinction depths below the depths of observation and broad changes in temperature throughout the depths of observation. Temperature inflections with depth in tulip-shaped temperature envelopes show sharp changes in heat fluxes associated with heterogeneous groundwater-flow patterns (Constantz and others, 2003). Tulip-shaped envelopes in figure 8 (indicated by a "T" in the lower right corner) show inflections between 10 and 30 ft bls that suggest heat fluxes from the Rio Grande are greatly reduced below about 30 ft bls. Exceptions occur on the east side of the Rio Grande between Paseo del Norte and Barelas where geological heterogeneities and/or regional pumping may induce groundwater flux from the river to greater depths. Local-scale heterogeneities result in large ranges of groundwater flux and may reduce flux rates where clay- or silt-rich low-permeability sediments are present. Temperature-profile curves presented by Bartolino and Niswonger (1999, fig. 2) indicate that heat flux from the Rio Grande penetrated to depths ranging from 9 to 15 meters (about 29 to 49 ft) bls.

The relative importance of horizontal or vertical temperature fluxes can be visually evaluated by using temperature profiles in figure 8. To distinguish between horizontal and vertical flow from the river, Reiter (2001) presented temperature profiles in the Albuquerque area that alluded to the importance of cool horizontal flow; vertical flow alone could not cool water deep in the aquifer to temperatures below those observed at the shallowest depths. Reiter's (2001) conclusions can be applied to temperature profiles at piezometer nest I6 (fig. 8), for example, where a negative temperature gradient to a depth of about 20 ft bls in January 2009 is shown. At 20 ft bls, the temperature is from 4 to 5 °F cooler than is observed at the shallower depths, indicating that cool horizontal flow is needed to reduce groundwater temperatures below those observed near the water table. Similarly, the importance of horizontal flux from the Rio Grande can be qualitatively noted in temperature profiles from piezometer nests A4, A6, P3, P4, P5, P6, M3, M4, C7, B4, B6, B7, B8, R4, R5, R6, R7, R8, PJ4, PJ5, PJ7, I6, and I7 (fig. 8). These piezometers are indicated with boldface font labels in figure 8.

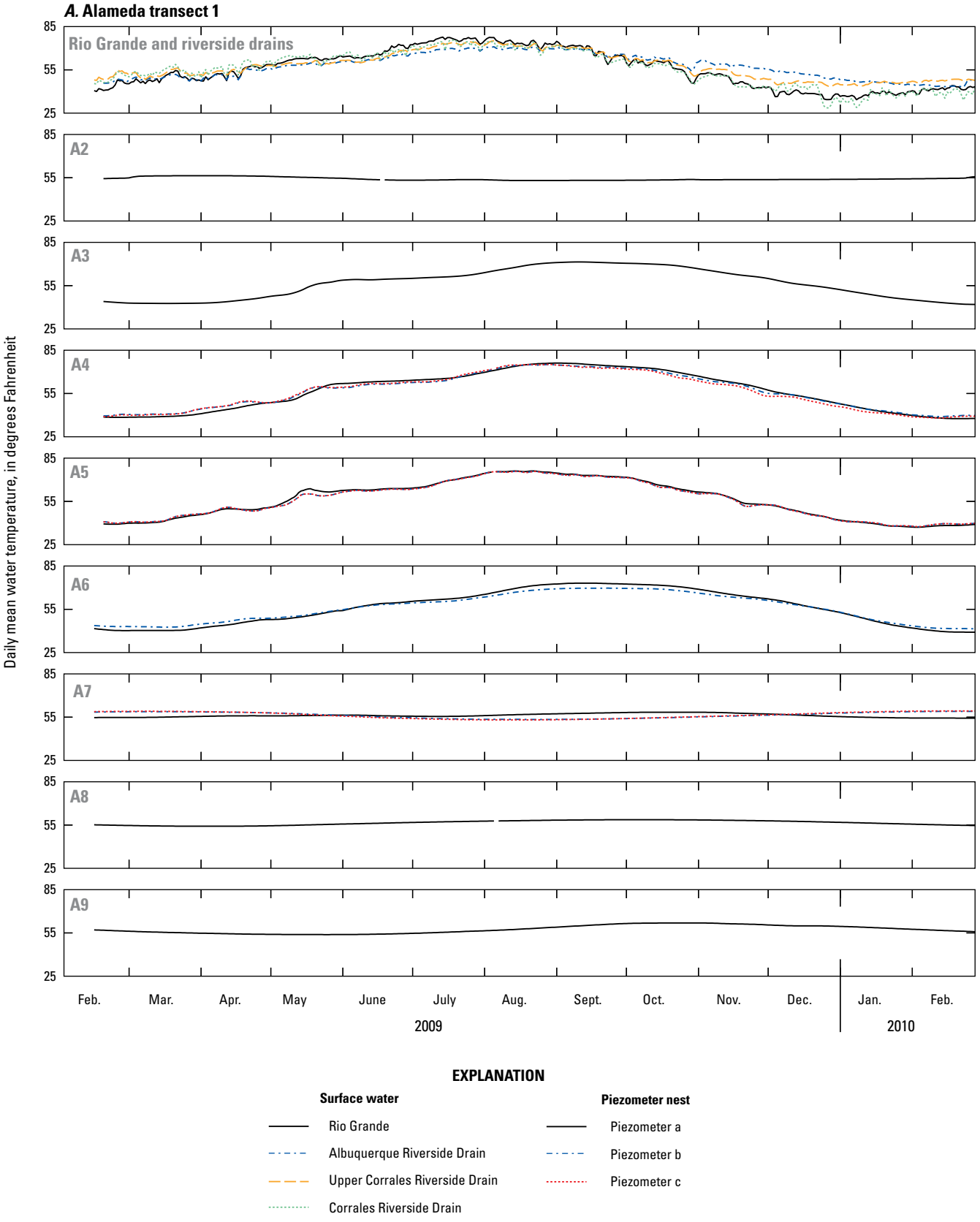

Figure 7. Water temperatures in the Rio Grande and riverside drains and daily mean groundwater temperatures in piezometers at *A*, Alameda transect 1; *B*, Alameda transect 2; *C*, Paseo del Norte transect 1; *D*, Paseo del Norte transect 2; *E*, Montaño transect 1; *F*, Montaño transect 2; *G*, Central transect 1; *H*, Central transect 2; *I*, Barelas transect 1; *J*, Barelas transect 2; *K*, Rio Bravo transect 1; *L*, Rio Bravo transect 2; *M*, Pajarito transect 1; *N*, Pajarito transect 2; *O*, I-25 transect 1; and *P*, I-25 transect 2.

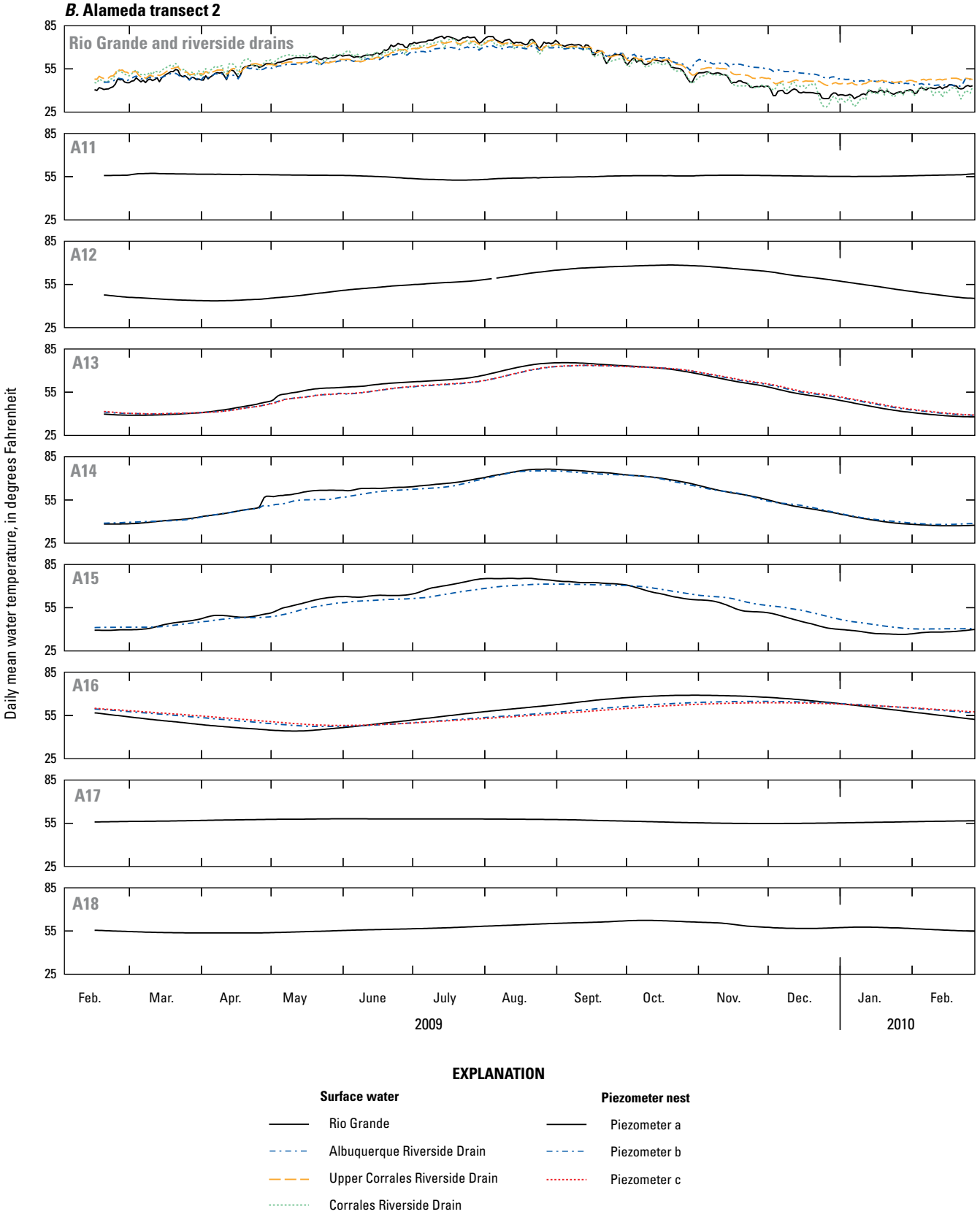

Figure 7. Water temperatures in the Rio Grande and riverside drains and daily mean groundwater temperatures in piezometers at *A*, Alameda transect 1; *B*, Alameda transect 2; *C*, Paseo del Norte transect 1; *D*, Paseo del Norte transect 2; *E*, Montaño transect 1; *F*, Montaño transect 2; *G*, Central transect 1; *H*, Central transect 2; *I*, Barelas transect 1; *J*, Barelas transect 2; *K*, Rio Bravo transect 1; *L*, Rio Bravo transect 2; *M*, Pajarito transect 1; *N*, Pajarito transect 2; *O*, I-25 transect 1; and *P*, I-25 transect 2.—Continued

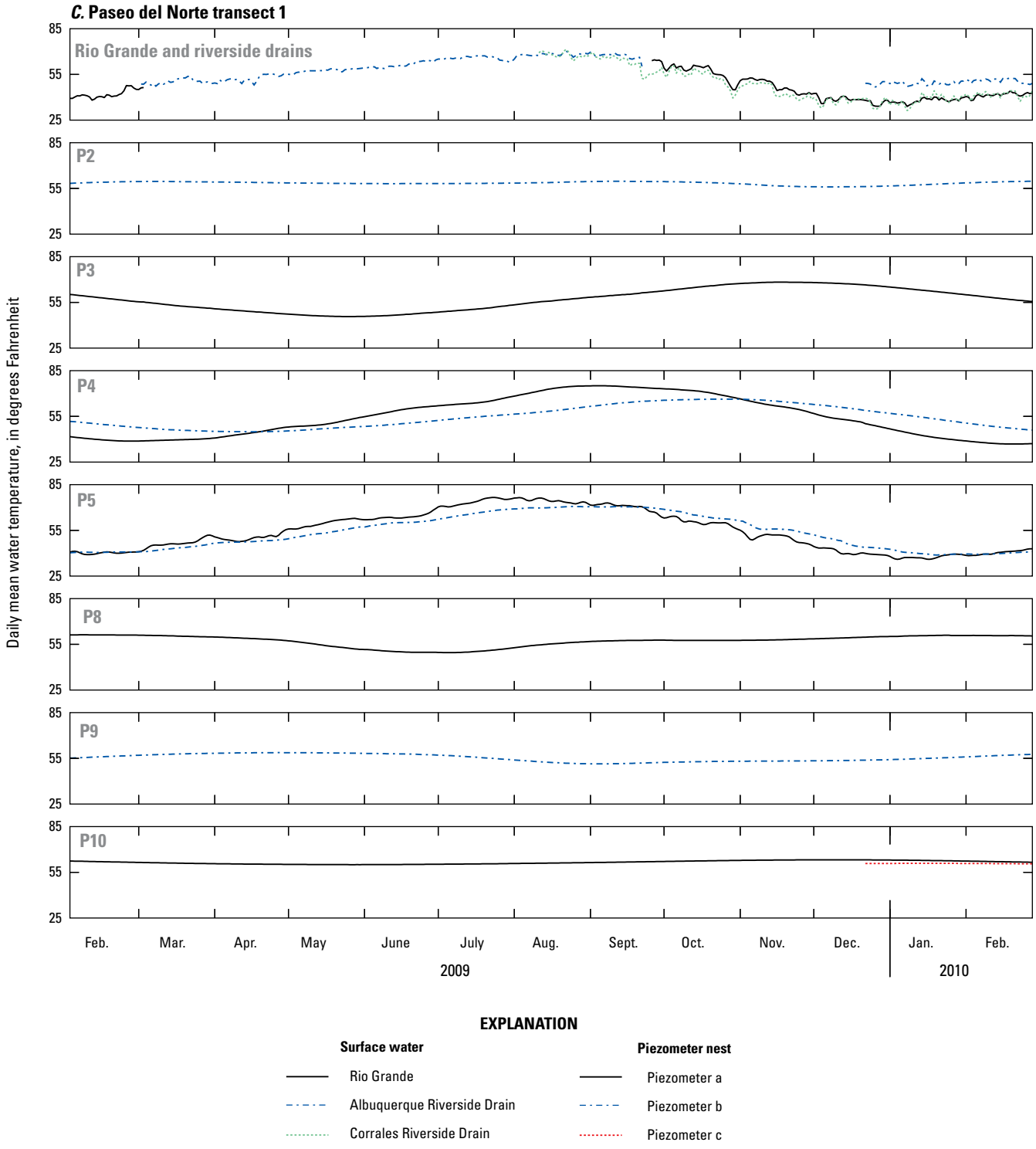

Figure 7. Water temperatures in the Rio Grande and riverside drains and daily mean groundwater temperatures in piezometers at *A*, Alameda transect 1; *B*, Alameda transect 2; *C*, Paseo del Norte transect 1; *D*, Paseo del Norte transect 2; *E*, Montaño transect 1; *F*, Montaño transect 2; *G*, Central transect 1; *H*, Central transect 2; *I*, Barelas transect 1; *J*, Barelas transect 2; *K*, Rio Bravo transect 1; *L*, Rio Bravo transect 2; *M*, Pajarito transect 1; *N*, Pajarito transect 2; *O*, I-25 transect 1; and *P*, I-25 transect 2.—Continued

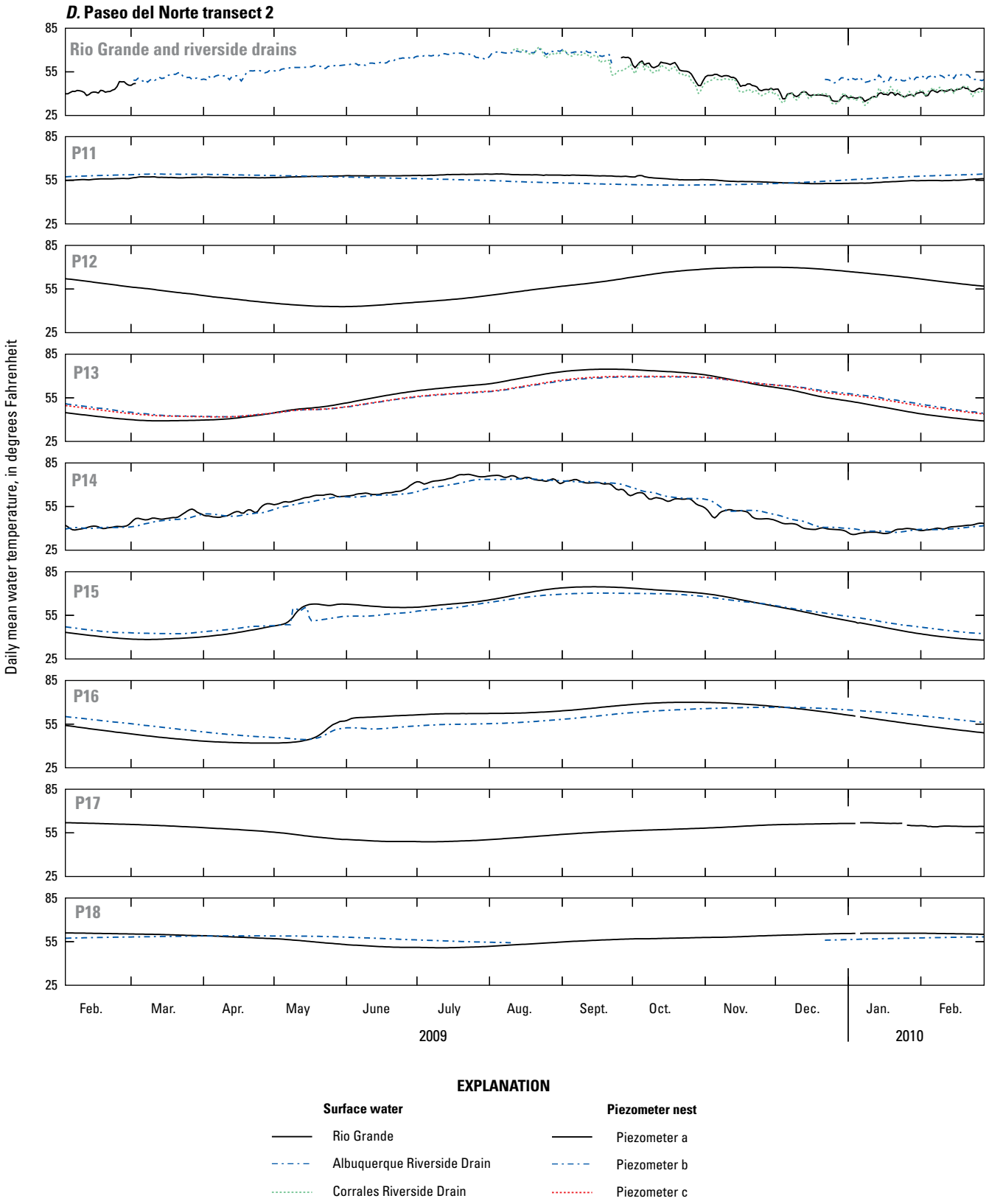

Figure 7. Water temperatures in the Rio Grande and riverside drains and daily mean groundwater temperatures in piezometers at *A*, Alameda transect 1; *B*, Alameda transect 2; *C*, Paseo del Norte transect 1; *D*, Paseo del Norte transect 2; *E*, Montaño transect 1; *F*, Montaño transect 2; *G*, Central transect 1; *H*, Central transect 2; *I*, Barelas transect 1; *J*, Barelas transect 2; *K*, Rio Bravo transect 1; *L*, Rio Bravo transect 2; *M*, Pajarito transect 1; *N*, Pajarito transect 2; *O*, I-25 transect 1; and *P*, I-25 transect 2.—Continued

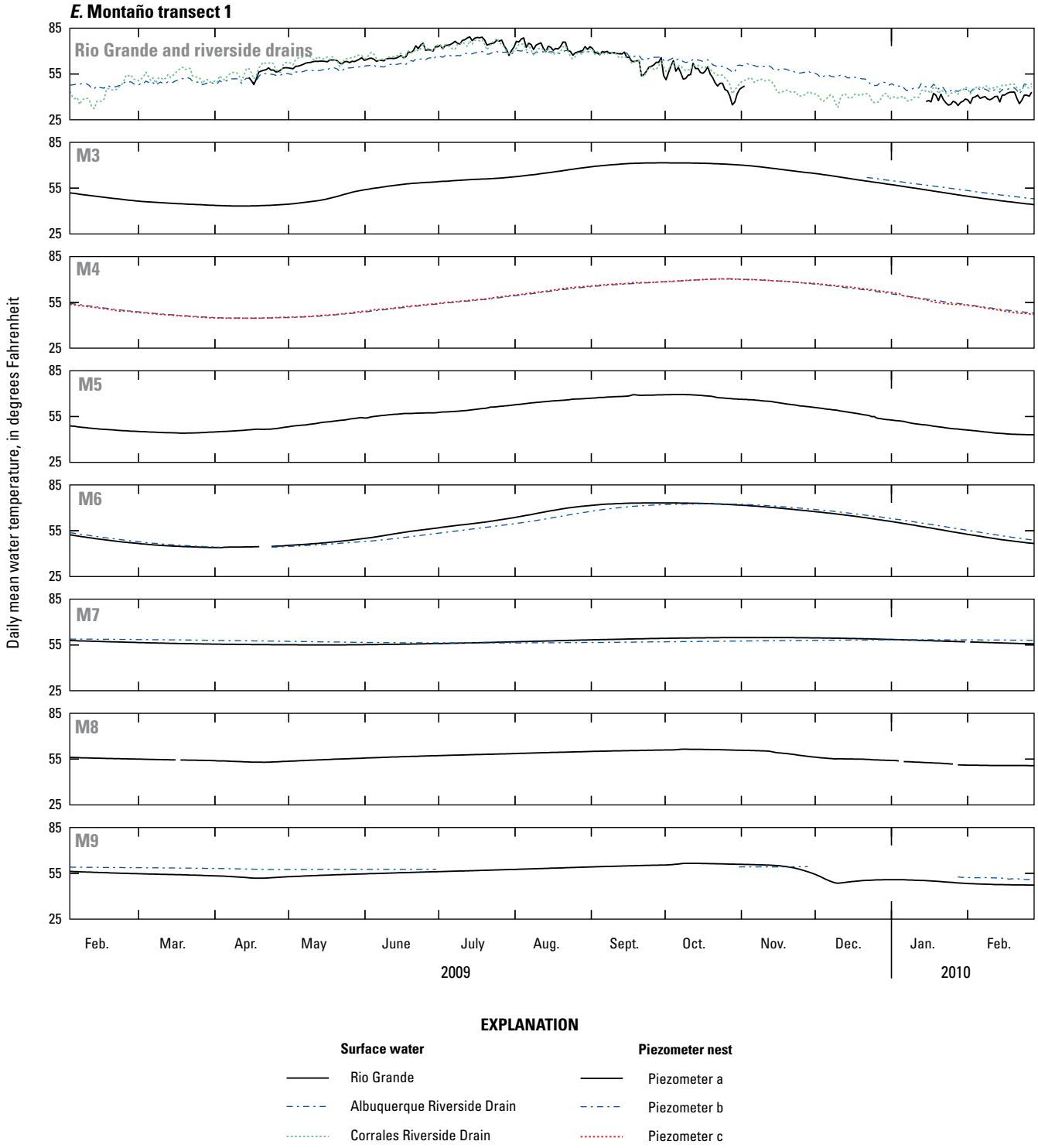

Figure 7. Water temperatures in the Rio Grande and riverside drains and daily mean groundwater temperatures in piezometers at *A*, Alameda transect 1; *B*, Alameda transect 2; *C*, Paseo del Norte transect 1; *D*, Paseo del Norte transect 2; *E*, Montaño transect 1; *F*, Montaño transect 2; *G*, Central transect 1; *H*, Central transect 2; *I*, Barelas transect 1; *J*, Barelas transect 2; *K*, Rio Bravo transect 1; *L*, Rio Bravo transect 2; *M*, Pajarito transect 1; *N*, Pajarito transect 2; *O*, I-25 transect 1; and *P*, I-25 transect 2.—Continued

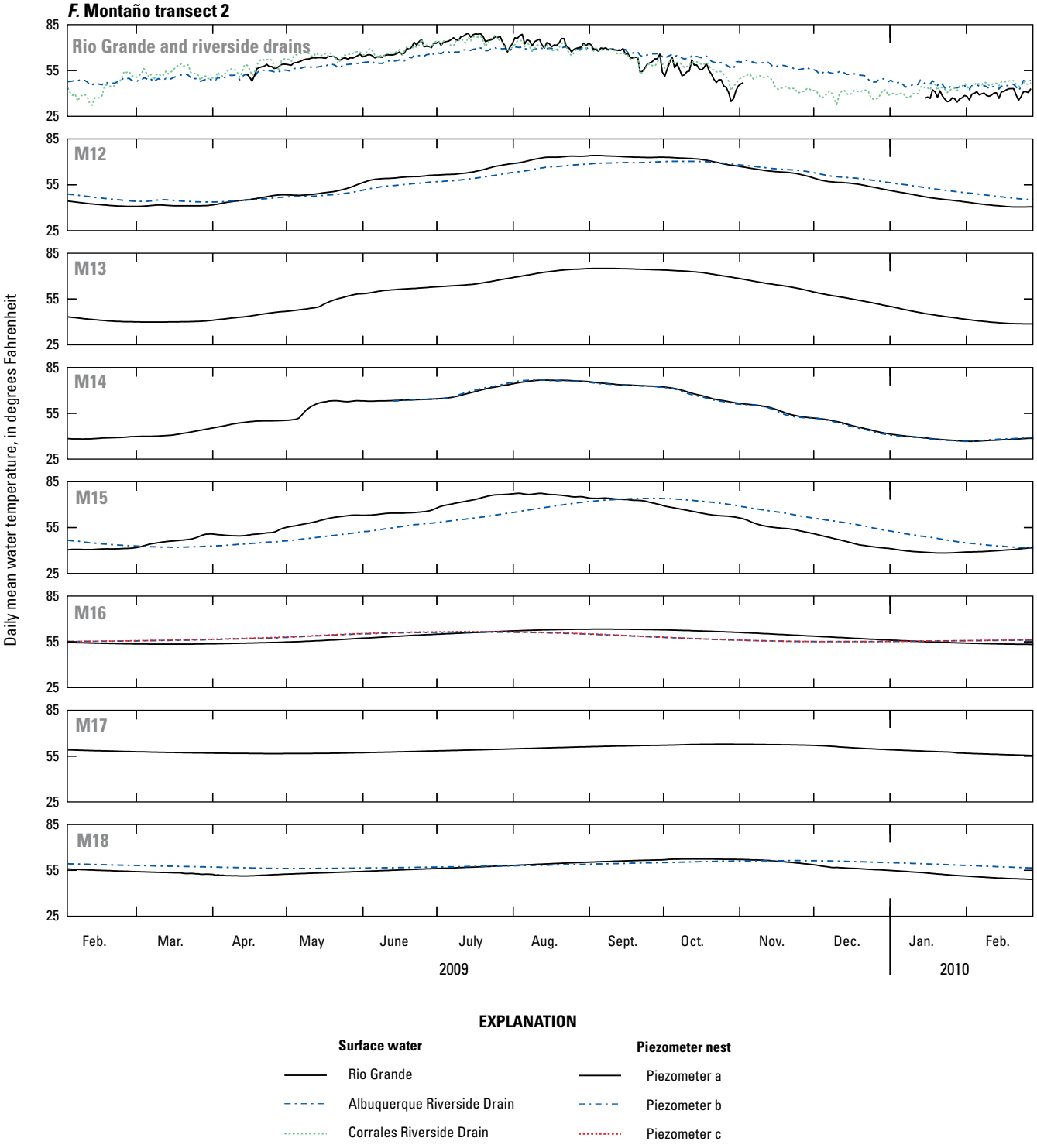

Figure 7. Water temperatures in the Rio Grande and riverside drains and daily mean groundwater temperatures in piezometers at *A*, Alameda transect 1; *B*, Alameda transect 2; *C*, Paseo del Norte transect 1; *D*, Paseo del Norte transect 2; *E*, Montaño transect 1; *F*, Montaño transect 2; *G*, Central transect 1; *H*, Central transect 2; *I*, Barelas transect 1; *J*, Barelas transect 2; *K*, Rio Bravo transect 1; *L*, Rio Bravo transect 2; *M*, Pajarito transect 1; *N*, Pajarito transect 2; *O*, I-25 transect 1; and *P*, I-25 transect 2.—Continued

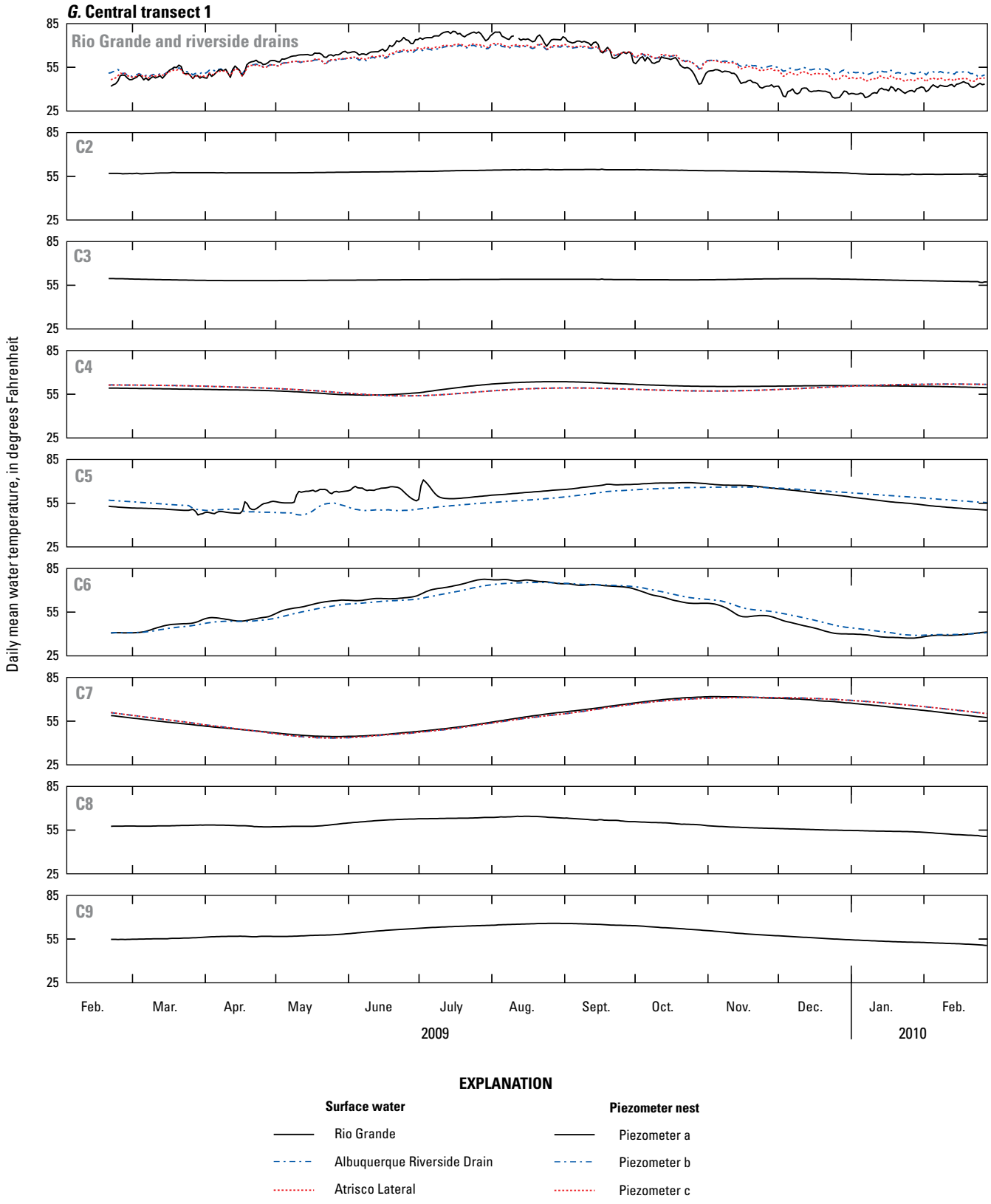

Figure 7. Water temperatures in the Rio Grande and riverside drains and daily mean groundwater temperatures in piezometers at *A*, Alameda transect 1; *B*, Alameda transect 2; *C*, Paseo del Norte transect 1; *D*, Paseo del Norte transect 2; *E*, Montaño transect 1; *F*, Montaño transect 2; *G*, Central transect 1; *H*, Central transect 2; *I*, Barelas transect 1; *J*, Barelas transect 2; *K*, Rio Bravo transect 1; *L*, Rio Bravo transect 2; *M*, Pajarito transect 1; *N*, Pajarito transect 2; *O*, I-25 transect 1; and *P*, I-25 transect 2.—Continued

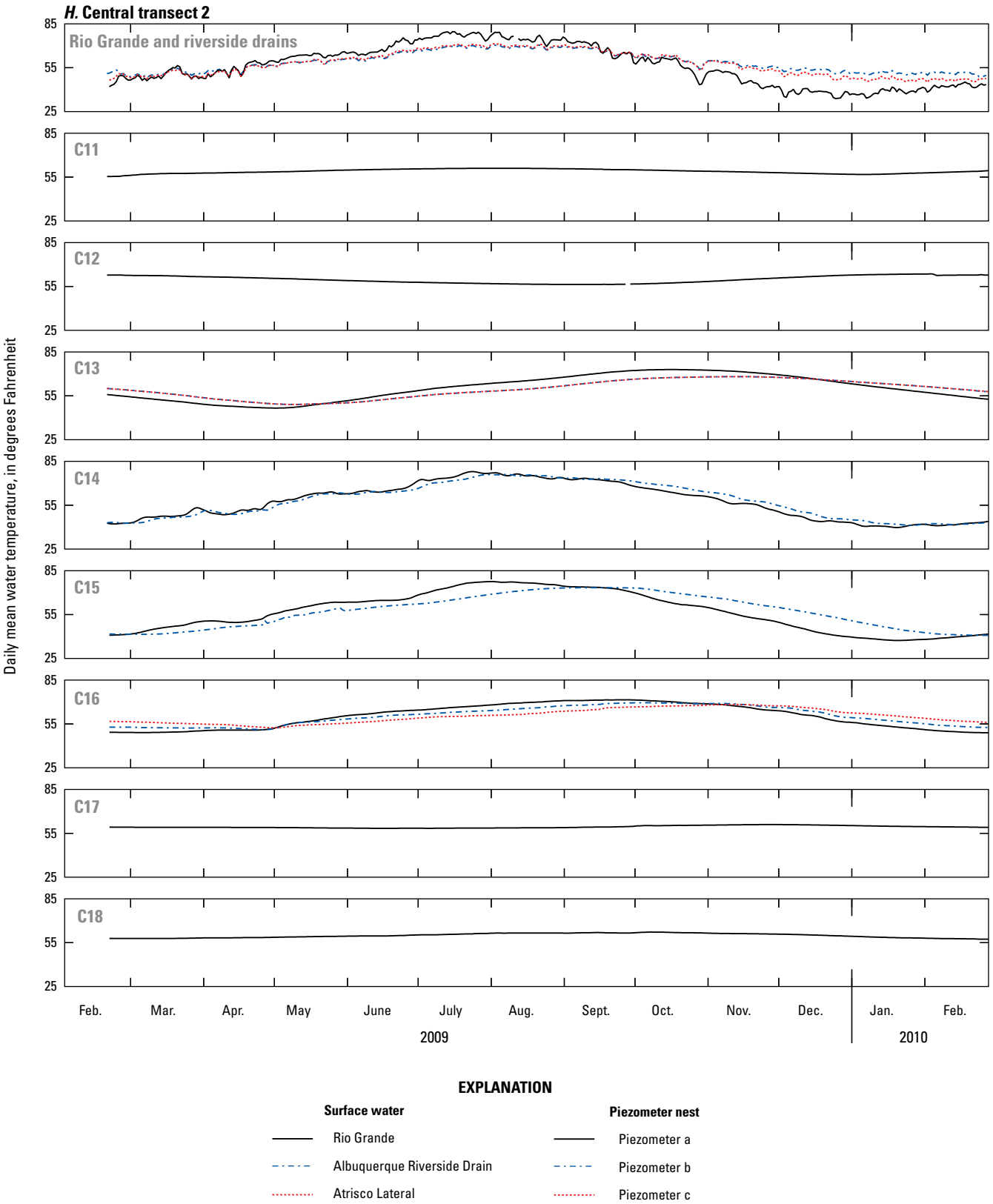

Figure 7. Water temperatures in the Rio Grande and riverside drains and daily mean groundwater temperatures in piezometers at *A*, Alameda transect 1; *B*, Alameda transect 2; *C*, Paseo del Norte transect 1; *D*, Paseo del Norte transect 2; *E*, Montaño transect 1; *F*, Montaño transect 2; *G*, Central transect 1; *H*, Central transect 2; *I*, Barelas transect 1; *J*, Barelas transect 2; *K*, Rio Bravo transect 1; *L*, Rio Bravo transect 2; *M*, Pajarito transect 1; *N*, Pajarito transect 2; *O*, I-25 transect 1; and *P*, I-25 transect 2.—Continued

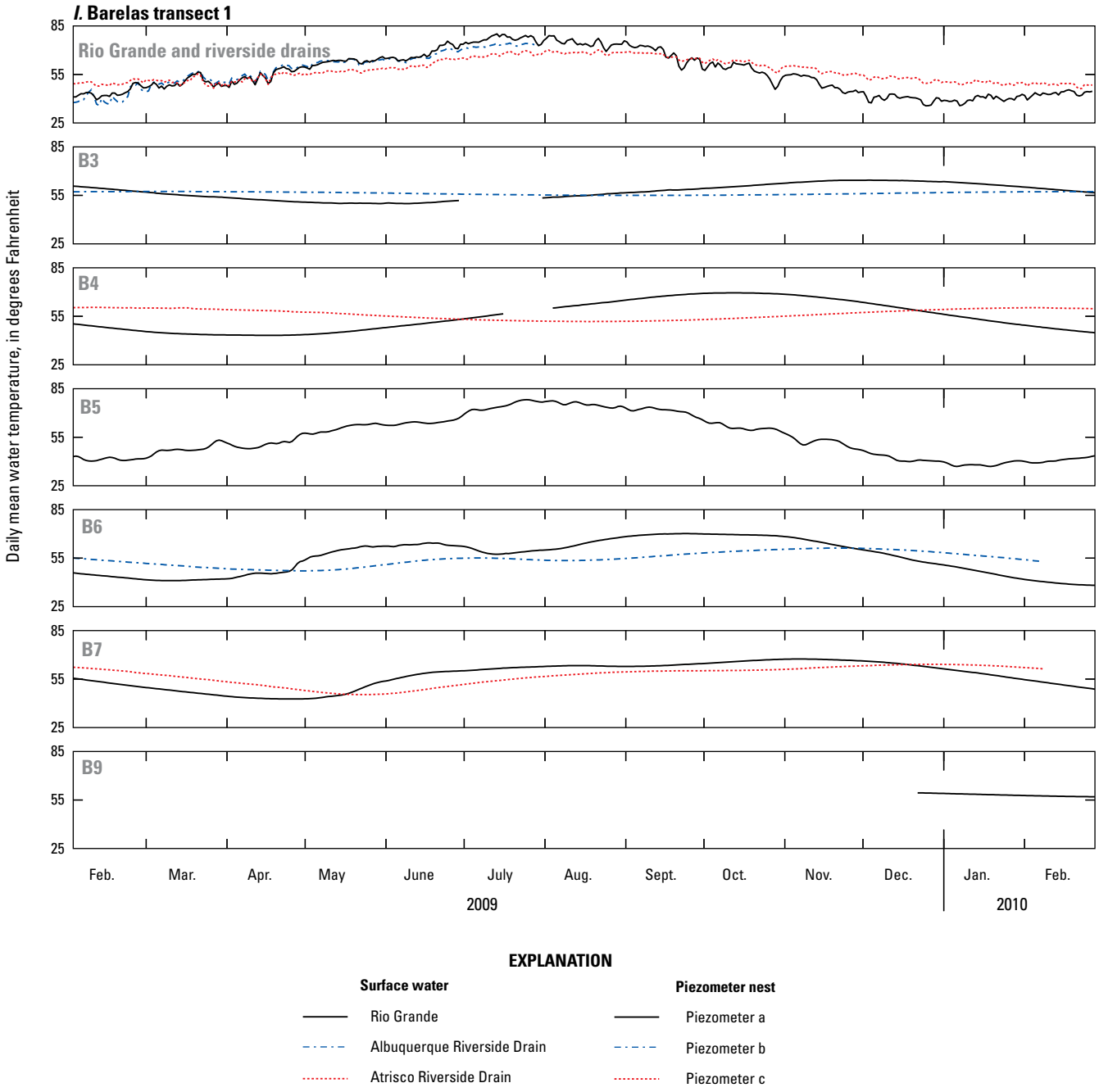

Figure 7. Water temperatures in the Rio Grande and riverside drains and daily mean groundwater temperatures in piezometers at *A*, Alameda transect 1; *B*, Alameda transect 2; *C*, Paseo del Norte transect 1; *D*, Paseo del Norte transect 2; *E*, Montaño transect 1; *F*, Montaño transect 2; *G*, Central transect 1; *H*, Central transect 2; *I*, Barelas transect 1; *J*, Barelas transect 2; *K*, Rio Bravo transect 1; *L*, Rio Bravo transect 2; *M*, Pajarito transect 1; *N*, Pajarito transect 2; *O*, I-25 transect 1; and *P*, I-25 transect 2.—Continued

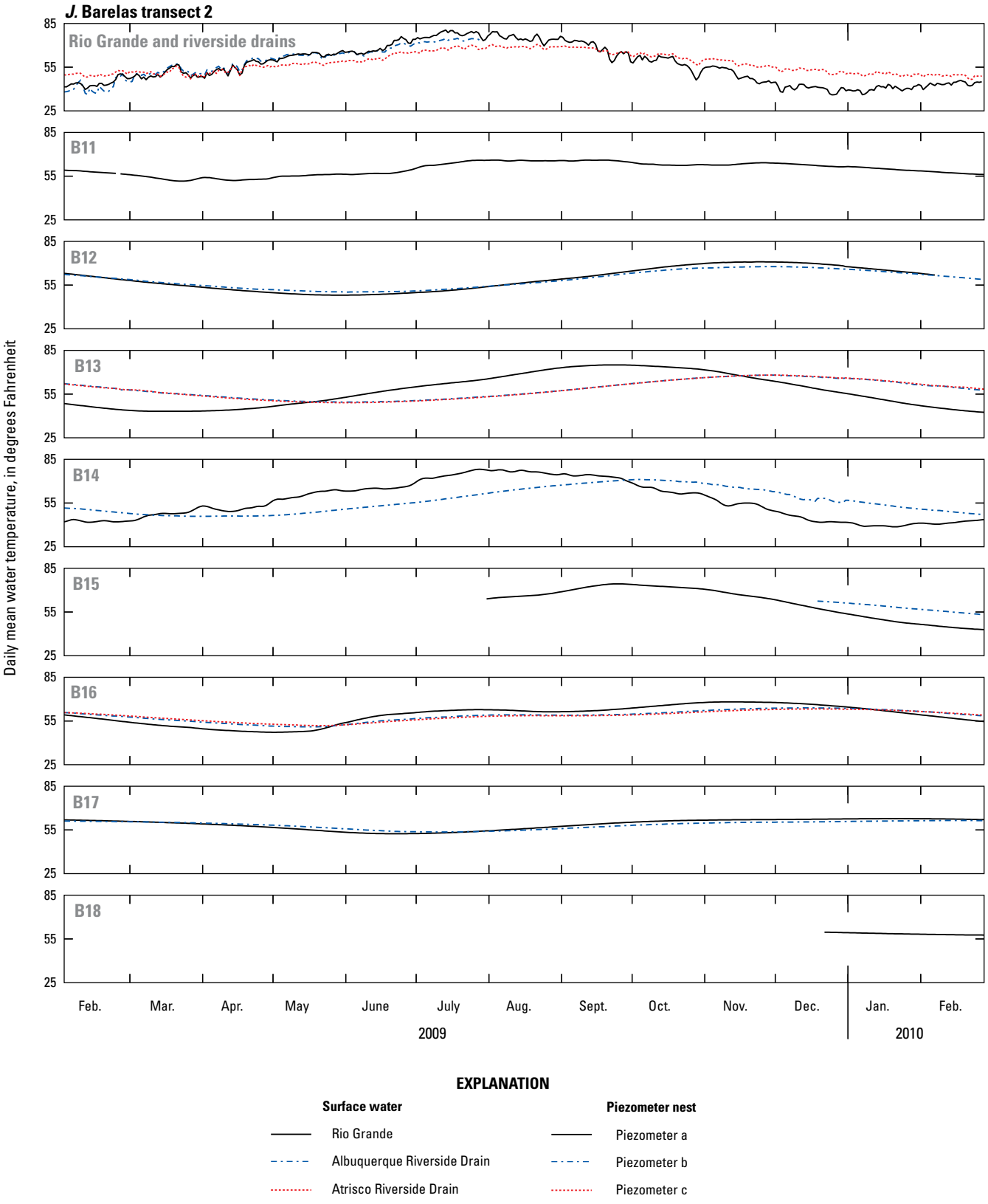

Figure 7. Water temperatures in the Rio Grande and riverside drains and daily mean groundwater temperatures in piezometers at *A*, Alameda transect 1; *B*, Alameda transect 2; *C*, Paseo del Norte transect 1; *D*, Paseo del Norte transect 2; *E*, Montaño transect 1; *F*, Montaño transect 2; *G*, Central transect 1; *H*, Central transect 2; *I*, Barelas transect 1; *J*, Barelas transect 2; *K*, Rio Bravo transect 1; *L*, Rio Bravo transect 2; *M*, Pajarito transect 1; *N*, Pajarito transect 2; *O*, I-25 transect 1; and *P*, I-25 transect 2.—Continued

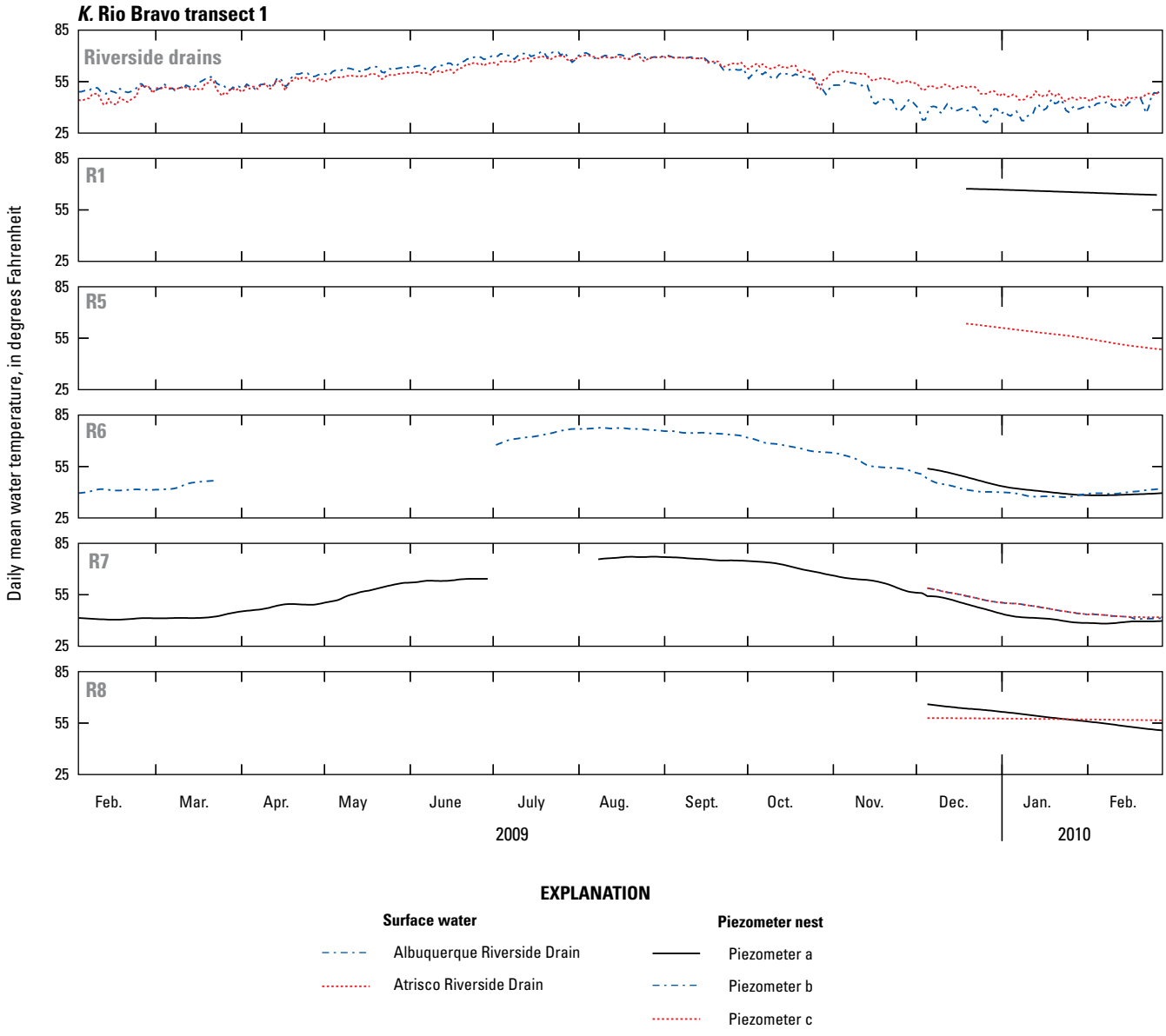

Figure 7. Water temperatures in the Rio Grande and riverside drains and daily mean groundwater temperatures in piezometers at *A*, Alameda transect 1; *B*, Alameda transect 2; *C*, Paseo del Norte transect 1; *D*, Paseo del Norte transect 2; *E*, Montaño transect 1; *F*, Montaño transect 2; *G*, Central transect 1; *H*, Central transect 2; *I*, Barelas transect 1; *J*, Barelas transect 2; *K*, Rio Bravo transect 1; *L*, Rio Bravo transect 2; *M*, Pajarito transect 1; *N*, Pajarito transect 2; *O*, I-25 transect 1; and *P*, I-25 transect 2.—Continued

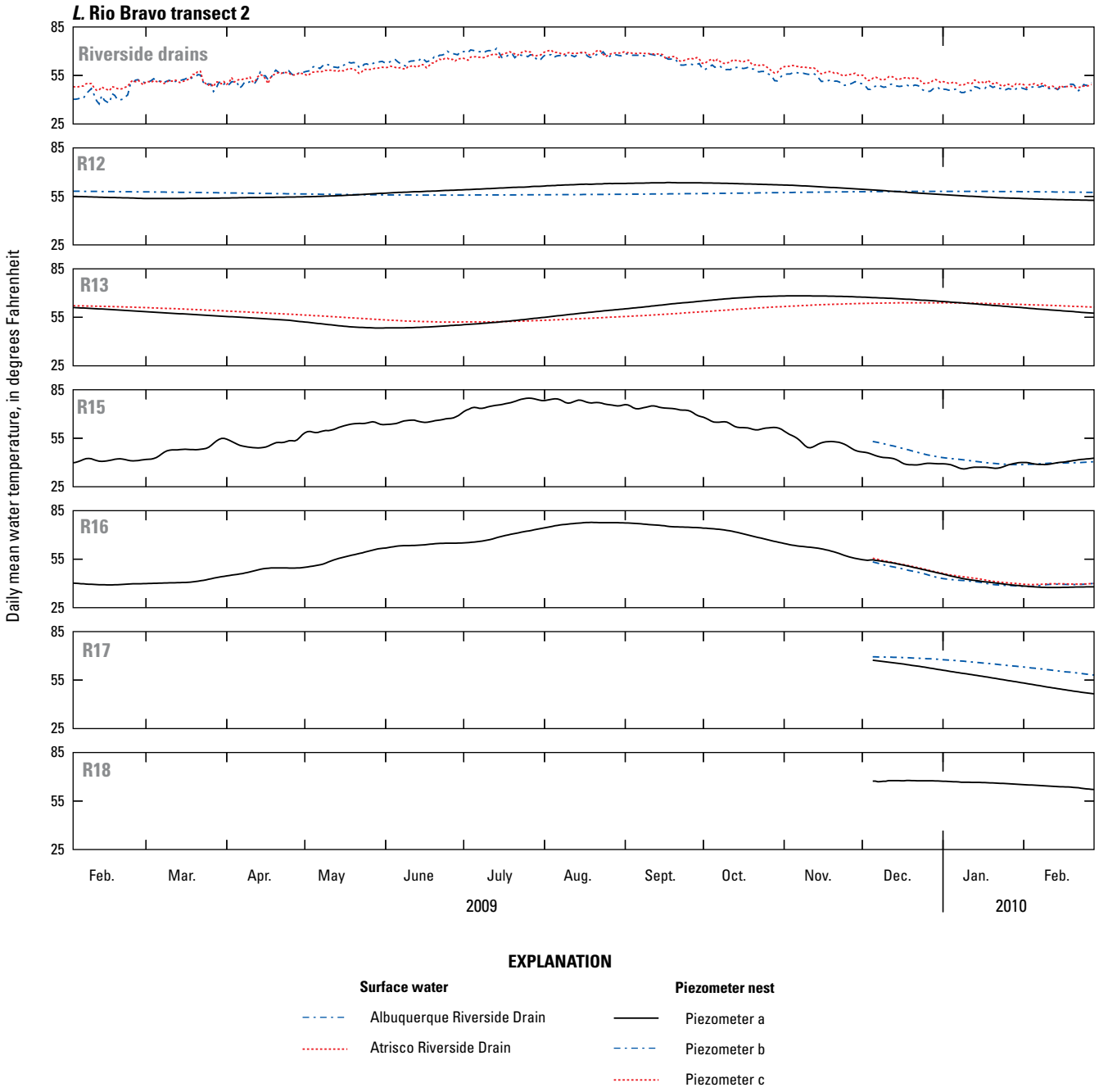

Figure 7. Water temperatures in the Rio Grande and riverside drains and daily mean groundwater temperatures in piezometers at *A*, Alameda transect 1; *B*, Alameda transect 2; *C*, Paseo del Norte transect 1; *D*, Paseo del Norte transect 2; *E*, Montaño transect 1; *F*, Montaño transect 2; *G*, Central transect 1; *H*, Central transect 2; *I*, Barelas transect 1; *J*, Barelas transect 2; *K*, Rio Bravo transect 1; *L*, Rio Bravo transect 2; *M*, Pajarito transect 1; *N*, Pajarito transect 2; *O*, I-25 transect 1; and *P*, I-25 transect 2.—Continued

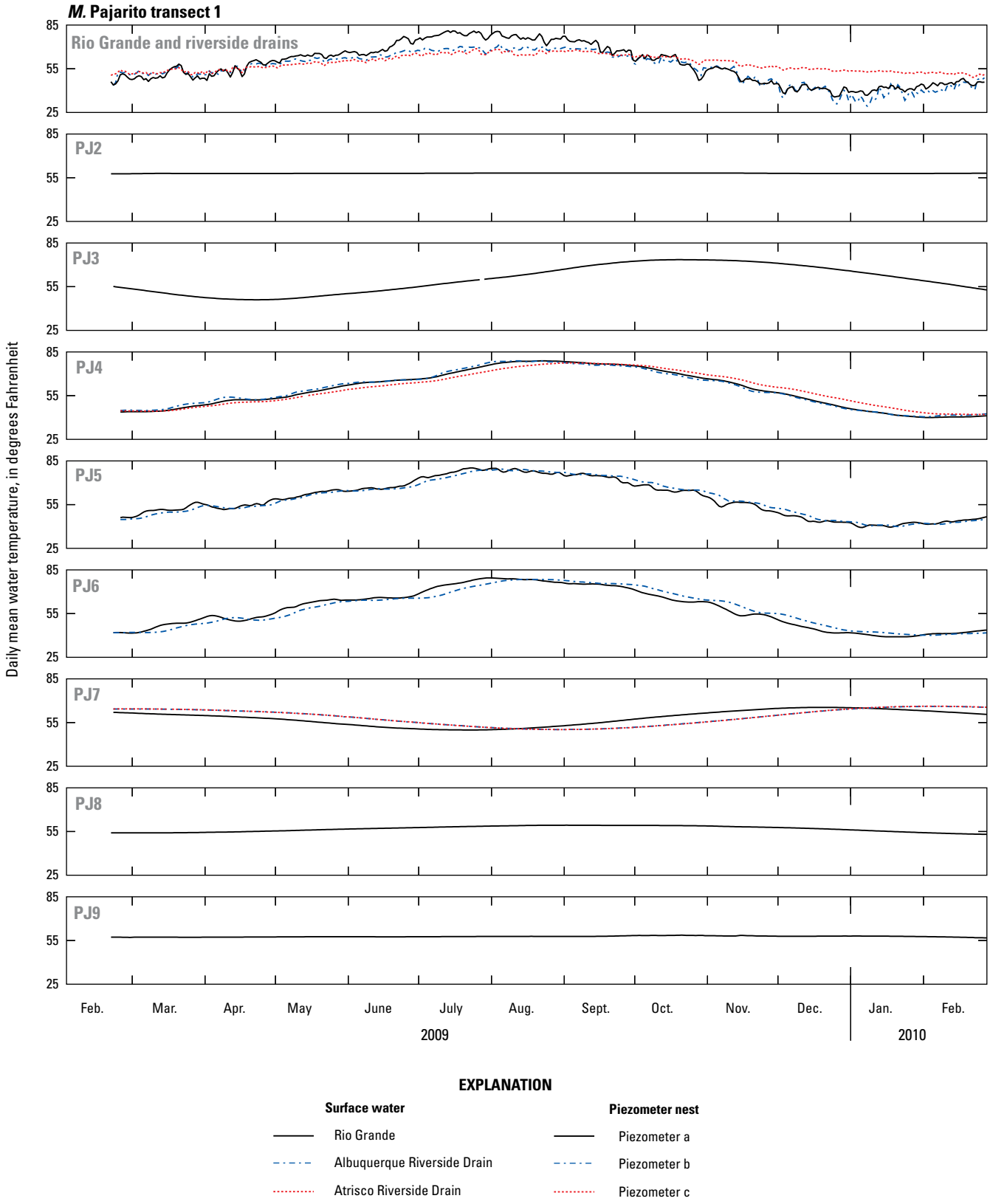

Figure 7. Water temperatures in the Rio Grande and riverside drains and daily mean groundwater temperatures in piezometers at *A*, Alameda transect 1; *B*, Alameda transect 2; *C*, Paseo del Norte transect 1; *D*, Paseo del Norte transect 2; *E*, Montaño transect 1; *F*, Montaño transect 2; *G*, Central transect 1; *H*, Central transect 2; *I*, Barelas transect 1; *J*, Barelas transect 2; *K*, Rio Bravo transect 1; *L*, Rio Bravo transect 2; *M*, Pajarito transect 1; *N*, Pajarito transect 2; *O*, I-25 transect 1; and *P*, I-25 transect 2.—Continued

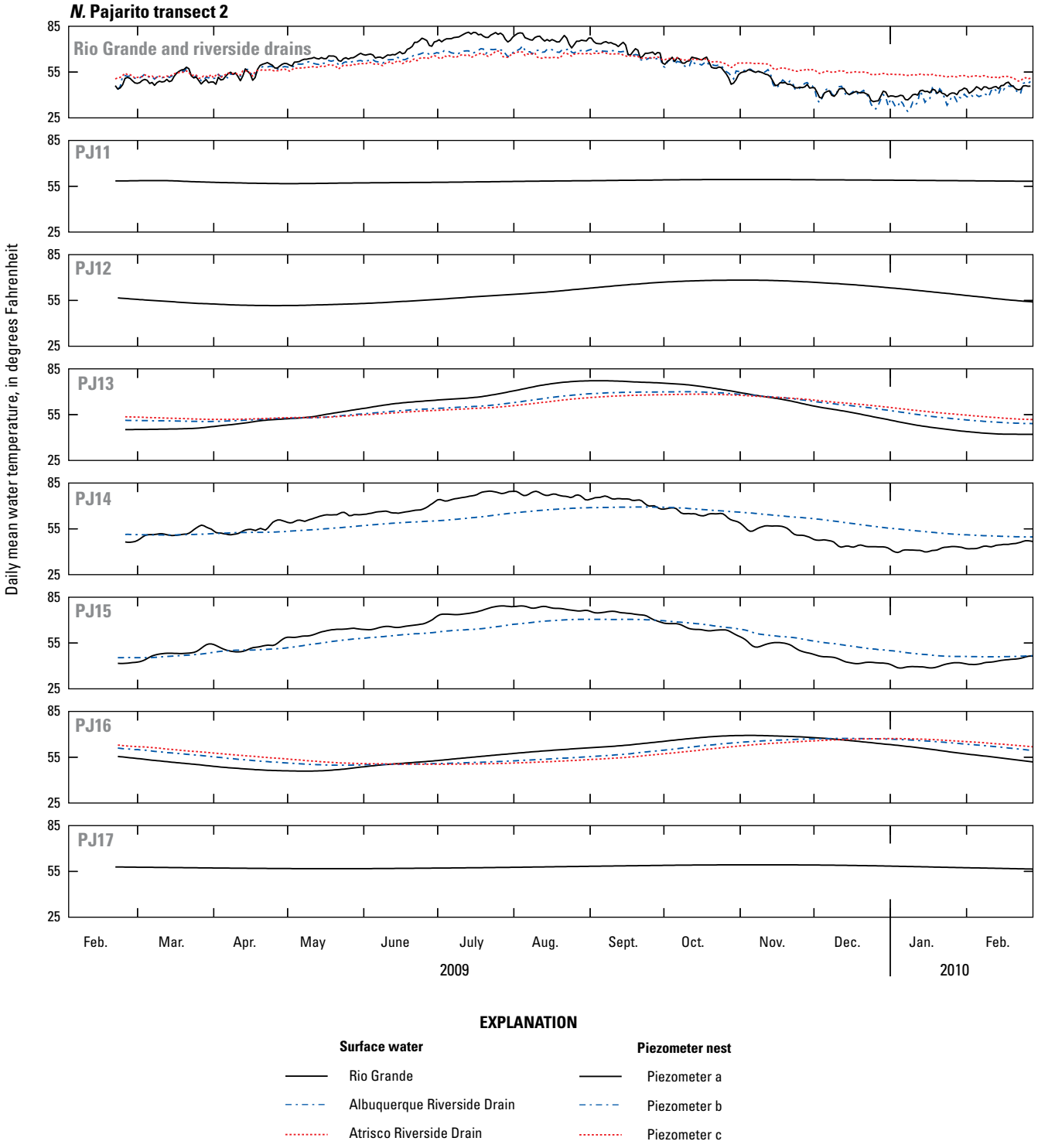

Figure 7. Water temperatures in the Rio Grande and riverside drains and daily mean groundwater temperatures in piezometers at *A*, Alameda transect 1; *B*, Alameda transect 2; *C*, Paseo del Norte transect 1; *D*, Paseo del Norte transect 2; *E*, Montaño transect 1; *F*, Montaño transect 2; *G*, Central transect 1; *H*, Central transect 2; *I*, Barelas transect 1; *J*, Barelas transect 2; *K*, Rio Bravo transect 1; *L*, Rio Bravo transect 2; *M*, Pajarito transect 1; *N*, Pajarito transect 2; *O*, I-25 transect 1; and *P*, I-25 transect 2.—Continued

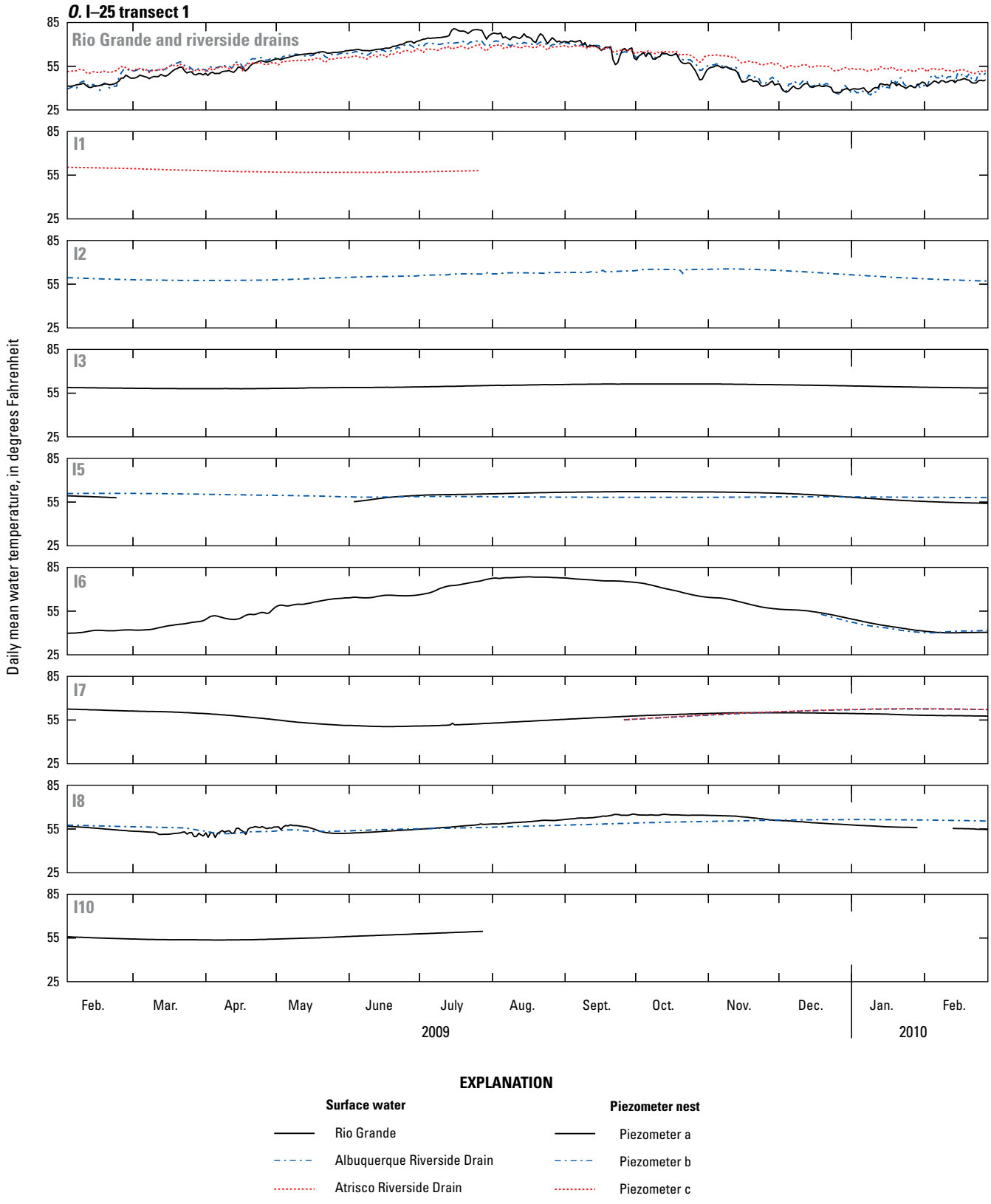

Figure 7. Water temperatures in the Rio Grande and riverside drains and daily mean groundwater temperatures in piezometers at *A*, Alameda transect 1; *B*, Alameda transect 2; *C*, Paseo del Norte transect 1; *D*, Paseo del Norte transect 2; *E*, Montaño transect 1; *F*, Montaño transect 2; *G*, Central transect 1; *H*, Central transect 2; *I*, Barelas transect 1; *J*, Barelas transect 2; *K*, Rio Bravo transect 1; *L*, Rio Bravo transect 2; *M*, Pajarito transect 1; *N*, Pajarito transect 2; *O*, I-25 transect 1; and *P*, I-25 transect 2.—Continued

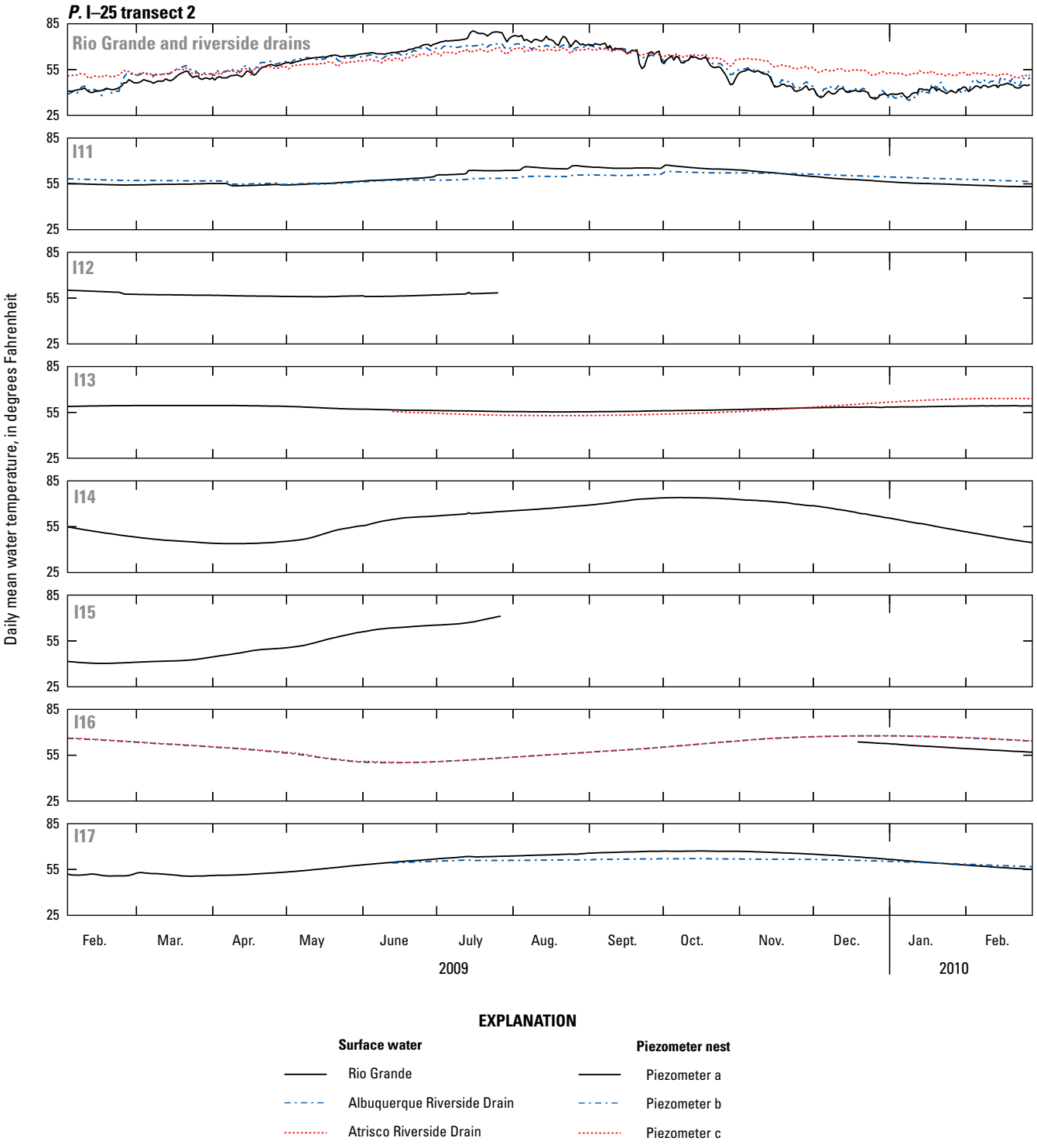

Figure 7. Water temperatures in the Rio Grande and riverside drains and daily mean groundwater temperatures in piezometers at *A*, Alameda transect 1; *B*, Alameda transect 2; *C*, Paseo del Norte transect 1; *D*, Paseo del Norte transect 2; *E*, Montaño transect 1; *F*, Montaño transect 2; *G*, Central transect 1; *H*, Central transect 2; *I*, Barelas transect 1; *J*, Barelas transect 2; *K*, Rio Bravo transect 1; *L*, Rio Bravo transect 2; *M*, Pajarito transect 1; *N*, Pajarito transect 2; *O*, I-25 transect 1; and *P*, I-25 transect 2.—Continued

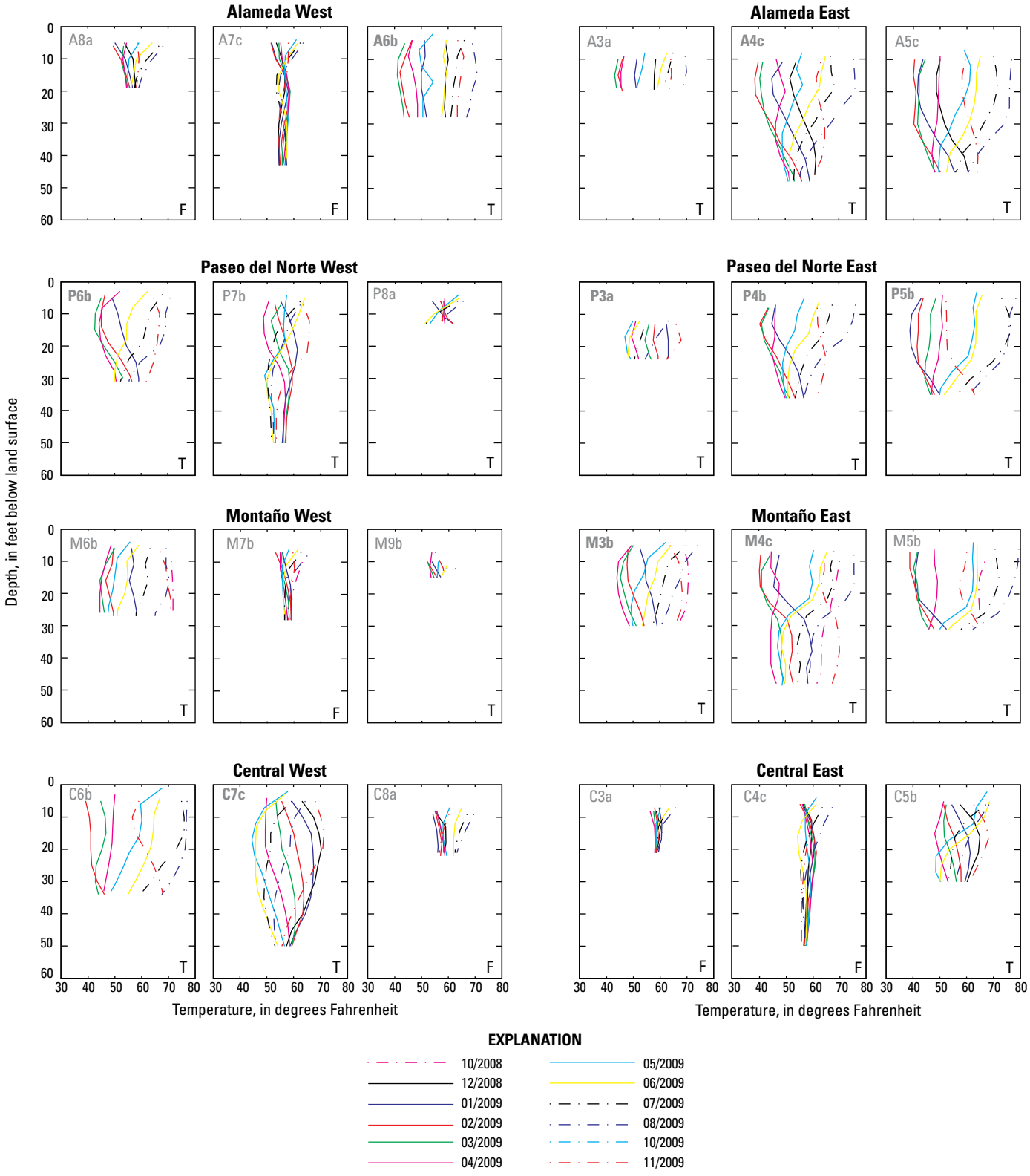

Figure 8. Monthly vertical temperature profiles in piezometers, 2008–9.

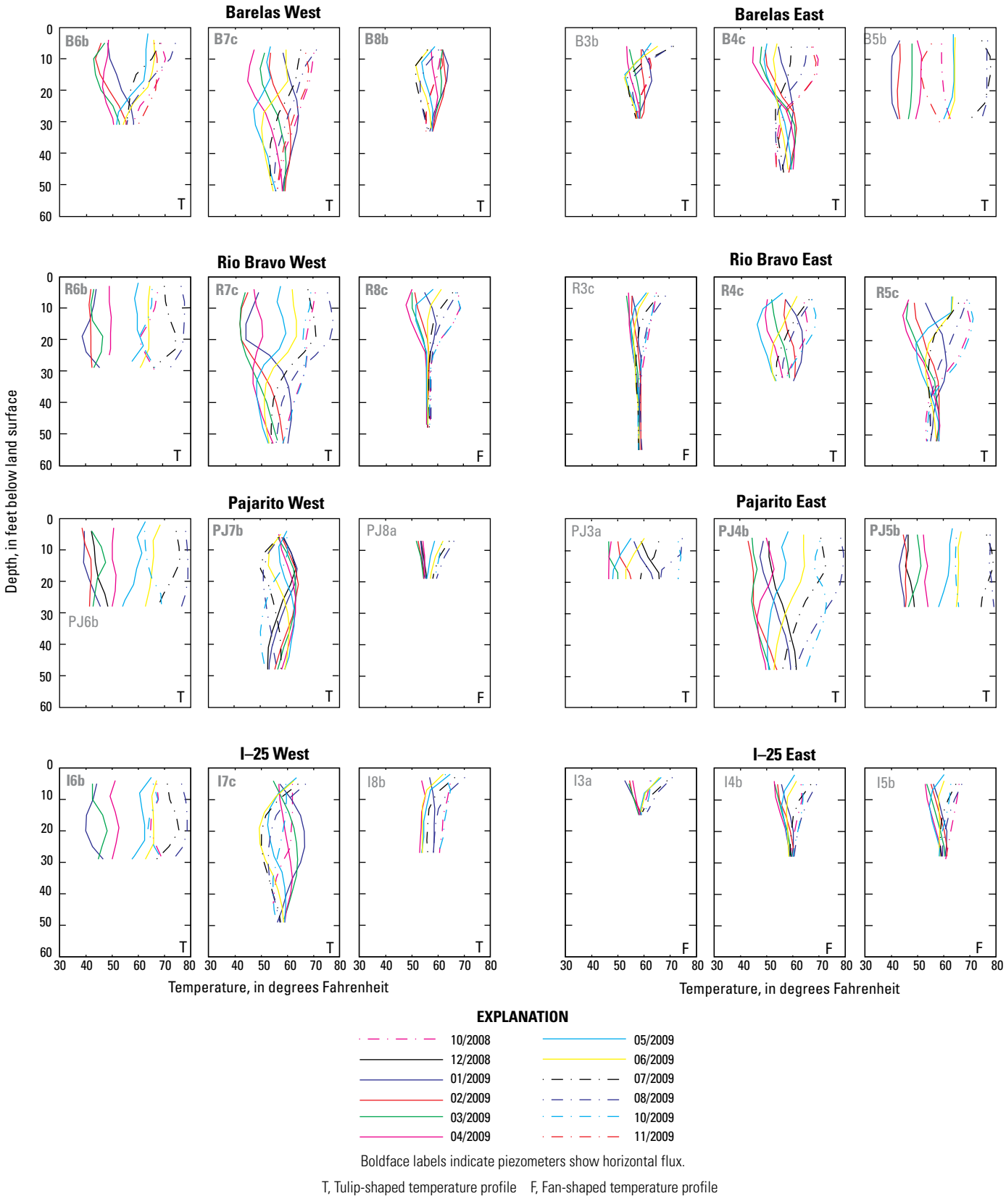

Figure 8. Monthly vertical temperature profiles in piezometers, 2008–9.—Continued

On both sides of the river, temperature profiles indicate that the seasonal temperature-extinction depth is below the depth of observation. The shape of the temperature envelope at piezometer nest A4, M4, R7, PJ4, and PJ7 indicates that heat from the Rio Grande is transported to depths greater than 50 ft bls, and that horizontal flux from the Rio Grande must be substantial to account for a range of 10 °F at that depth. The curvature of the M4 profiles indicates that multiple zones of horizontal flow exist at depths from 10 to 20 ft and 45 ft bls. These zones may be separated by less permeable material in the interval from 30 to 40 ft bls. The compressed nature of the temperature profiles at Montaño West (M7 and M9), Central East (C3 and C4), and I-25 East (I3, I4, and I5) provides a sharp contrast to the variability in temperature profiles on the east side of the Rio Grande at Montaño. Compressed profiles generally indicate the presence of a discharge zone or low rates of groundwater flux (Reiter, 2001; Anderson, 2005).

Horizontal Hydraulic Gradients

Water-level data from shallow piezometers indicated that the annual mean magnitude of horizontal-hydraulic gradients in the Rio Grande inner valley alluvial aquifer ranged from 0.0024 (I-25 East) to 0.0144 (Pajarito East) (table 2). Generally, horizontal gradients on the east side of the river were more variable and greater than those on the west side of the river. Horizontal gradients were not constant at any of the transects, and there were noticeable variations that could be attributed to seasonal fluctuations in water levels in the river or drains and irrigation operations. Barelas and Rio Bravo transects are the only locations where the difference in gradient is less than 40 percent from one side of the river to the other. Horizontal gradients on the east side of the river decreased in a downstream direction through the study area. An exception occurred at the Pajarito transect, where the east-side gradient was equal to or greater than gradients at the northern locations. Horizontal gradients on the west side of the river were generally greater at the four downstream locations than the four upstream locations. Geologic heterogeneities in the aquifer sediments likely contribute to the spatial variability in the horizontal-hydraulic gradients. Groundwater pumping contributing to a cone of depression (fig. 2) also could affect the gradients on the east side of the river.

Table 2. Annual mean magnitude of groundwater horizontal hydraulic gradient and direction of groundwater flow at piezometer transects, Rio Grande inner valley alluvial aquifer, Albuquerque, New Mexico, 2009–10. Range of values is given in parentheses next to gradient and direction averages. Groundwater-flow direction is relative to the downstream direction of the Rio Grande channel at each transect where zero degrees is parallel to the channel and 90 degrees is perpendicular to and away from the channel.

[Site locations shown in figures 3*A*–*H*; ft/ft, foot per foot]

		West		East	
Transect location	Azimuth of Rio Grande at transect	Annual mean horizontal hydraulic gradient (range) (ft/ft)	Annual mean downstream direction relative to Rio Grande (range) (degrees)[1]	Annual mean horizontal hydraulic gradient (range) (ft/ft)	Annual mean downstream direction relative to Rio Grande (range) (degrees)[1]
Alameda	214	0.0045 (0.004–0.006)	76 (72–80)	0.0137 (0.010–0.024)	87 (79–92)
Paseo Del Norte	191	0.0053 (0.004–0.010)	81 (73–95)	0.0109 (0.009–0.012)	57 (47–93)
Montaño	216	0.0033 (0.003–0.006)	64 (32–86)	0.0103 (0.008–0.015)	95 (91–101)
Central	112	0.0040 (0.003–0.006)	88 (81–94)	0.0062 (0.005–0.011)	78 (75–80)
Barelas	175	0.0078 (0.007–0.009)	73 (70–78)	0.0087 (0.007–0.011)	83 (78–87)
Rio Bravo	181	0.0070 (0.005–0.008)	81 (78–83)	0.0048 (0.004–0.007)	70 (61–82)
Pajarito	203	0.0072 (0.006–0.009)	77 (71–83)	0.0144 (0.012–0.019)	100 (97–101)
I-25	163	0.0050 (0.003–0.009)	60 (41–70)	0.0024 (0.002–0.004)	69 (58–85)

[1]Orientation relative to downstream direction of Rio Grande.

The annual mean direction of horizontal groundwater flow ranged from 57 to 100 degrees relative to the downstream direction of the Rio Grande (groundwater flow at a direction of 90 degrees would be orthogonal to the river) (table 2). At most of the transects, there are noticeable differences in gradient directions between the east and west sides of the Rio Grande (table 2). There is more variability in the average direction of horizontal groundwater flow on the east side of the river than on the west side. Flow is more orthogonal to and away from the river than parallel to the river at most transect locations, which may be the result of a combination of factors such as the close proximity of the piezometers to the river, short distances between the river and drains, aquifer geology, and groundwater pumping by the City of Albuquerque.

Hydraulic Conductivity

During slug tests, the water-level responses in 17 piezometers were nonoscillatory and were analyzed using the Bouwer and Rice (1976) slug-test analysis method. The water-level responses at 30 piezometers exhibited oscillatory behavior and were analyzed using the Butler (1998) slug-test analysis method (table 3). Results from 47 slug tests performed in the alluvial aquifer for this study indicate the spatial variability of hydraulic properties in the inner valley alluvial aquifer is limited (fig. 9). Median hydraulic-conductivity values were evaluated for each pair of transects and ranged from 30 ft/d (Montaño) to 120 ft/d (Central) (fig. 9). The median hydraulic-conductivity value for all transects was 50 ft/d. Slug-test results from piezometers on the east side of the river were not substantially different from those on the west side.

Table 3. Summary of slug-test results from piezometers in the Rio Grande inner valley alluvial aquifer, Albuquerque, New Mexico.

[K, hydraulic conductivity; ft/d, foot per day; ft, foot; bls, below land surface; A. Alameda; b, mid-depth piezometer; n.d., no data; P, Paseo del Norte; a, shallow piezometer; M, Montaño; C, Central; B, Barelas; R, Rio Bravo; c, deep piezometer; PJ, Pajarito; I, I-25]

Site identifier	Other identifier (figs. 3*A*–*H*)	Test date	Slug test K (ft/d)	Method of analysis	Piezometer depth (ft)	Screened interval (ft)	Lithology of screen interval	Water level (ft bls)
351204106381602	A4b	3/27/2010	40	Butler (1998)	29	19–24	n.d.	8.69
351205106381602	A5b	3/27/2010	70	Butler (1998)	29	19–24	n.d.	10.29
351208106382702	A6b	3/27/2010	140	Butler (1998)	29	19–24	n.d.	3.27
351209106383002	A7b	3/27/2010	50	Butler (1998)	29	19–24	n.d.	4.56
351054106390101	P4a	2/2/2009	50	Bouwer and Rice (1976)	16	6–11	silty sand	6.81
351054106390102	P4b	2/2/2009	40	Butler (1998)	35	25–30	silty sand	7.47
351054106390401	P5a	2/2/2009	40	Bouwer and Rice (1976)	16	6–11	silty sand	4.95
351054106390402	P5b	2/2/2009	40	Butler (1998)	35	25–30	silty sand	5.08
351055106391101	P6a	1/30/2009	70	Butler (1998)	16	6–11	n.d.	4.03
351055106391102	P6b	1/30/2009	20	Butler (1998)	31	21–26	n.d.	4.10
351054106391301	P7a	1/30/2009	60	Bouwer and Rice (1976)	16	6–11	sand	6.17
351054106391302	P7b	1/30/2009	70	Butler (1998)	31	21–26	sand	6.08
350842106403101	M4a	1/28/2009	30	Bouwer and Rice (1976)	15	5–10	sand	7.70
350842106403102	M4b	1/28/2009	160	Butler (1998)	30	20–25	silty sand	7.80
350842106403201	M5a	1/28/2009	20	Bouwer and Rice (1976)	15	5–10	n.d.	5.79
350842106403202	M5b	1/28/2009	60	Butler (1998)	32	22–27	clayey sand	6.40
350848106404703	M6a	1/28/2009	30	Bouwer and Rice (1976)	13	3–8	n.d.	7.35
350848106404704	M6b	1/28/2009	10	Bouwer and Rice (1976)	28	18–23	n.d.	5.42

Table 3. Summary of slug-test results from piezometers in the Rio Grande inner valley alluvial aquifer, Albuquerque, New Mexico.—Continued

[K, hydraulic conductivity; ft/d, foot per day; ft, foot; bls, below land surface; A. Alameda; b, mid-depth piezometer; n.d., no data; P, Paseo del Norte; a, shallow piezometer; M, Montaño; C, Central; B, Barelas; R, Rio Bravo; c, deep piezometer; PJ, Pajarito; I, I-25]

Site identifier	Other identifier (figs. 3*A*–*H*)	Test date	Slug test K (ft/d)	Method of analysis	Piezometer depth (ft)	Screened interval (ft)	Lithology of screen interval	Water level (ft bls)
350848106404702	M7b	1/28/2009	10	Bouwer and Rice (1976)	30	20–25	sand	6.71
350531106405802	C4b	3/26/2010	100	Butler (1998)	31	21–26	n.d.	5.05
350529106410402	C5b	3/26/2010	240	Butler (1998)	31	21–26	n.d.	5.33
350524106410402	C6b	3/26/2010	90	Butler (1998)	31	21–26	n.d.	3.62
350522106410502	C7b	3/26/2010	140	Butler (1998)	31	21–26	n.d.	3.62
350402106392601	B4a	1/30/2009	20	Bouwer and Rice (1976)	16	6–11	sand	5.27
350402106392602	B4b	1/30/2009	10	Bouwer and Rice (1976)	31	21–26	silty sand	5.79
350402106392902	B5b	1/30/2009	60	Butler (1998)	30	20–25	silty sand	3.98
350400106393701	B6a	1/30/2009	60	Butler (1998)	17	7–12	n.d.	4.53
350400106393702	B6b	1/30/2009	90	Butler (1998)	32	22–27	silty sand	4.84
350359106393901	B7a	1/30/2009	60	Butler (1998)	17	7–12	silty sand	6.42
350359106393902	B7b	1/30/2009	50	Butler (1998)	32	22–27	silty sand	6.46
350143106402401	R6a	1/29/2009	50	Bouwer and Rice (1976)	15	5–10	silty sand	2.81
350143106402402	R6b	1/29/2009	50	Butler (1998)	34	24–29	silty sand	3.05
350143106402503	R7a	1/29/2009	30	Bouwer and Rice (1976)	15	5–10	silty sand	3.35
350143106402501	R7b	1/29/2009	20	Bouwer and Rice (1976)	35	25–30	silty sand	4.31
350144106401101	R13a	2/6/2009	10	Butler (1998)	15	5–10	silty sand	3.98
350144106401102	R13b	2/6/2009	90	Butler (1998)	30	20–25	silty sand	4.02
350144106401103	R13c	2/6/2009	40	Butler (1998)	56	46–51	sand gravel	4.19
345904106410902	PJ4b	3/26/2010	4	Bouwer and Rice (1976)	29	19–24	n.d.	4.54
345904106411002	PJ5b	3/26/2010	90	Butler (1998)	29	19–24	n.d.	5.70
345905106411502	PJ6b	3/26/2010	60	Butler (1998)	29	19–24	n.d.	2.93
345906106412002	PJ7b	3/26/2010	3	Bouwer and Rice (1976)	29	19–24	n.d.	5.39
345701106404501	I4a	1/29/2009	30	Bouwer and Rice (1976)	14	4–9	silty sand	3.81
345701106404502	I4b	1/29/2009	60	Butler (1998)	29	19–24	sand	4.52
345701106404601	I5a	1/29/2009	5	Bouwer and Rice (1976)	14	4–9	n.d.	4.18
345701106404602	I5b	1/29/2009	80	Butler (1998)	29	19–24	n.d.	4.76
345707106410102	I6b	1/29/2009	100	Butler (1998)	29	19–24	silty sand	4.38
345706106410202	I7b	1/29/2009	40	Butler (1998)	29	19–24	silty sand	4.41

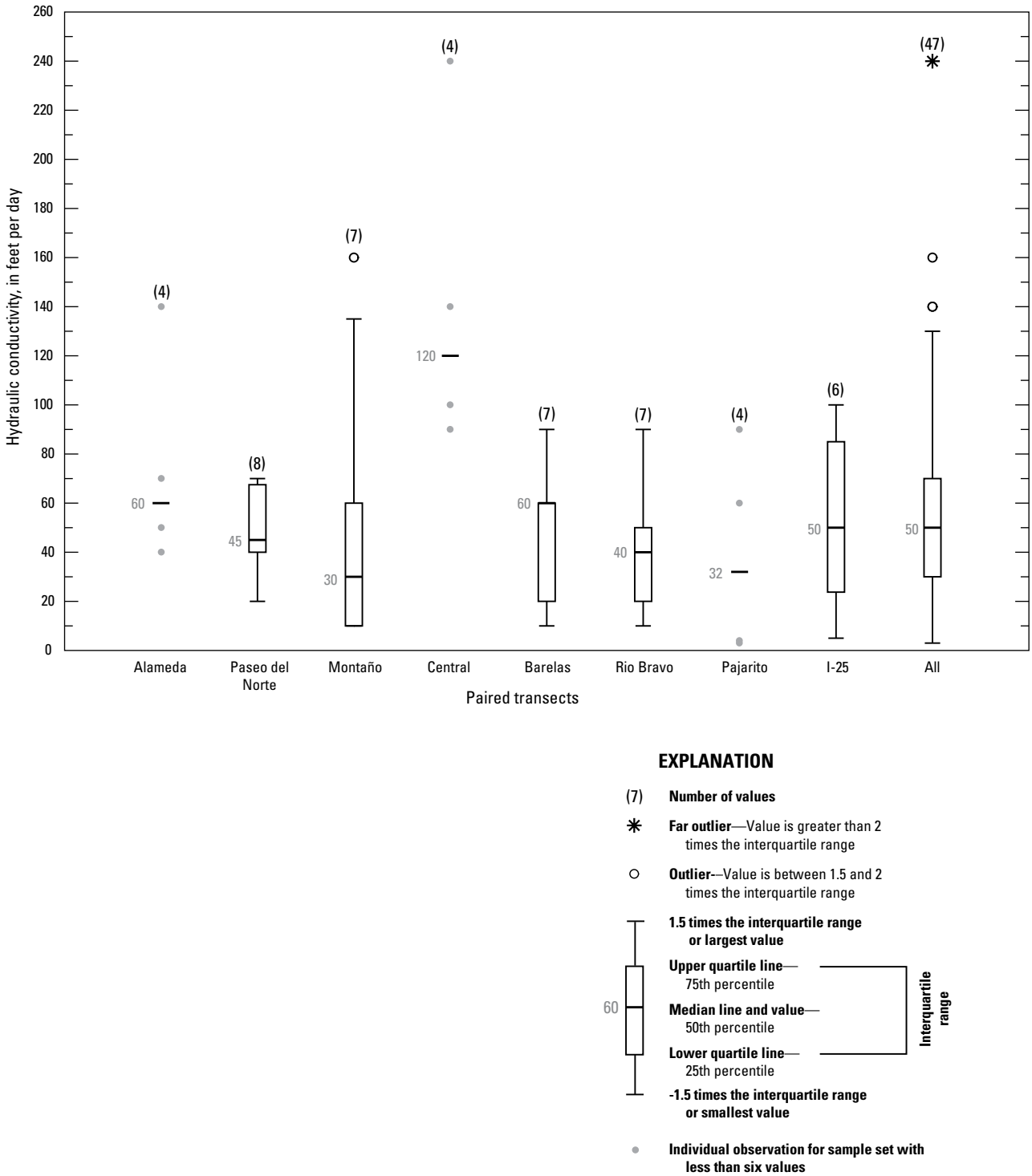

Figure 9. Hydraulic conductivities estimated from slug tests conducted at selected locations in the Rio Grande inner valley alluvial aquifer, Albuquerque, New Mexico.

Slug tests performed for this study hydraulically stressed only a limited portion of the aquifer surrounding each piezometer; however, the range of estimated hydraulic conductivities used in previous investigations (10 to 150 ft/d [Kernodle and others, 1995; Tiedeman and others, 1998; McAda, 2001]) was similar to the range of median hydraulic-conductivity values estimated in this study. Lithologic variability, attributable to complexly interfingered gravels, sands, silts, and clays in the alluvial aquifer, was noted in cores over distances of a few tens of feet or less (Rankin and others, 2013). Because coring was performed, in part, so the screened interval of each piezometer was placed in sandy material to ensure communication with the aquifer, the slug-test results provide a measurement of the heterogeneity of sandy zone hydraulic conductivities within the alluvial aquifer but do not provide an overall measurement of the heterogeneity of hydraulic conductivity in the aquifer. The range of literature-cited hydraulic conductivity values determined from regional-scale modeling (Sanford and others, 2003), aquifer tests (McAda, 2001), and well-to-well heat-transport modeling (Moret, 2007) provide a basis for comparison to the range of hydraulic conductivities in the current study (see following section "Darcy Flux").

Estimation of Horizontal Groundwater Flux from the Rio Grande

Horizontal groundwater flux from the Rio Grande to the inner valley alluvial aquifer east and west of the river was estimated by using results from calculations of horizontal-hydraulic gradients (determined from analysis of water-level data), analysis of slug-test data, and heat-transport modeling. In the following report sections, the portion of transects 1 and 2 that are east of the river are referred to as the "east transects" and the portion of transects 1 and 2 that are west of the river are referred to as the "west transects."

Darcy Flux

Darcy flux (q_{slug} on fig. 10) through the inner valley alluvial aquifer at each of the eight transect locations was calculated using daily mean hydraulic gradients (calculated using shallow piezometer hydraulic-head data) and the median hydraulic conductivity for each transect from slug-test results (fig. 9). These q_{slug} flux values were compared to $q_{Tiedeman}$ flux values (fig. 10), which were calculated by using a plausible range of hydraulic conductivity for the inner valley alluvial aquifer reported by Tiedeman and others (1998). The periods for which q_{slug} and $q_{Tiedeman}$ fluxes were calculated varied from transect to transect, depending on the availability of water-level data, from February 2009 through January 2010 (fig. 10).

Darcy-flux values calculated using the shallow piezometer data represent average fluxes through the upper 30 ft of the aquifer, or to the approximate base of the screened interval of mid-depth piezometers. Bartolino (2003) indicated that vertical gradients in the Rio Grande inner valley alluvial aquifer can be minor to these depths. These results are generally corroborated by the hydrographs of shallow and mid-depth piezometers (fig. 6*A–P*) and temperature profiles (fig. 8).

Daily mean groundwater fluxes (q_{slug}) through the inner valley alluvial aquifer calculated by using median hydraulic conductivities from slug tests (fig. 9) and daily mean hydraulic gradients ranged from about 0.01 ft/d (Montaño West) to between 1.0 and 2.0 ft/d (Central East) (fig. 10). The range in q_{slug} fluxes through the Albuquerque area primarily depended on variations in hydraulic gradients (table 2) and slug-test hydraulic-conductivity values (fig. 9 and table 3), in accordance with Darcy's Law (eqs. 3 and 4). With the exception of the Central bridge location, results indicated a general decrease in q_{slug} fluxes downstream from Alameda to I-25 on the east side of the river, corresponding to a decrease in the magnitude of computed gradients. At Central, however, the median slug-test hydraulic conductivity was 120 ft/d (fig. 9), resulting in a q_{slug} flux which was roughly three times that of the q_{slug} flux at Montaño where the median slug-test hydraulic conductivity was 30 ft/d (fig. 9). Hydrologically significant clay layers (Bartolino and Sterling, 2000) likely reduced the rate of q_{slug} flux through the inner valley alluvial aquifer in downstream parts of the study area.

The range of daily mean q_{slug} fluxes at the Paseo del Norte and Rio Bravo transects generally were similar on both sides of the river (fig. 10). At most transects, however, the q_{slug} fluxes were higher on the east side of the Rio Grande than on the west side (fig. 10). In these cases, the differing values of q_{slug} flux can be attributed to lesser gradients on the west side of the river than on the east side. All locations showed an increase in q_{slug} flux corresponding to periods of high flow in the Rio Grande, although q_{slug} fluxes were more responsive to changes in river flow in transects on the east side of the Rio Grande.

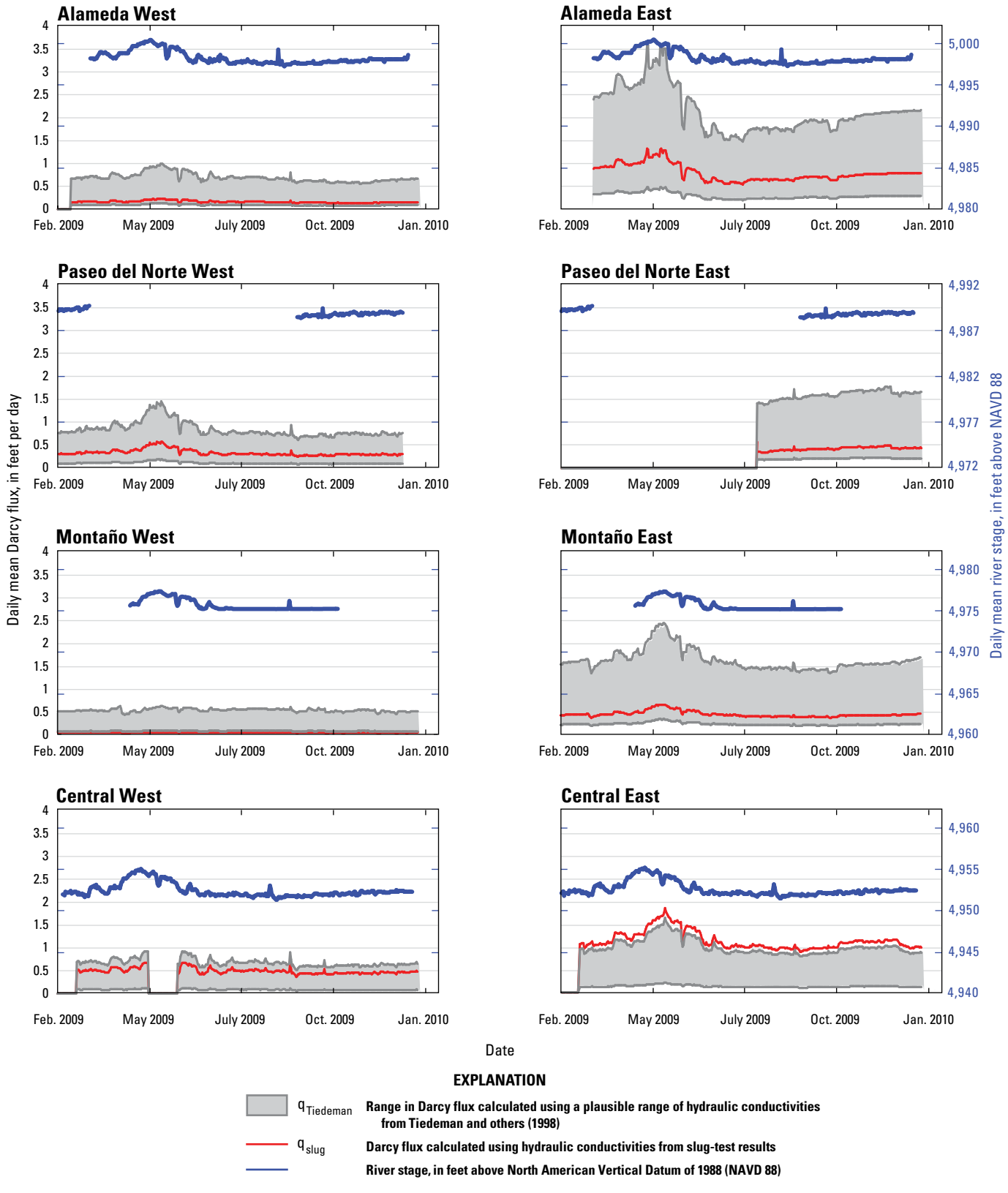

Figure 10. Daily mean Darcy flux calculated from daily mean hydraulic gradients and slug-test derived hydraulic conductivities, daily mean Darcy flux calculated from daily mean hydraulic gradients and a plausible range of hydraulic conductivities (Tiedeman and others, 1998), and daily mean Rio Grande stage for the Alameda, Paseo del Norte, Montaño, and Central transects and the Barelas, Rio Bravo, Pajarito, and I-25 transects, Rio Grande inner valley alluvial aquifer, 2009–10.

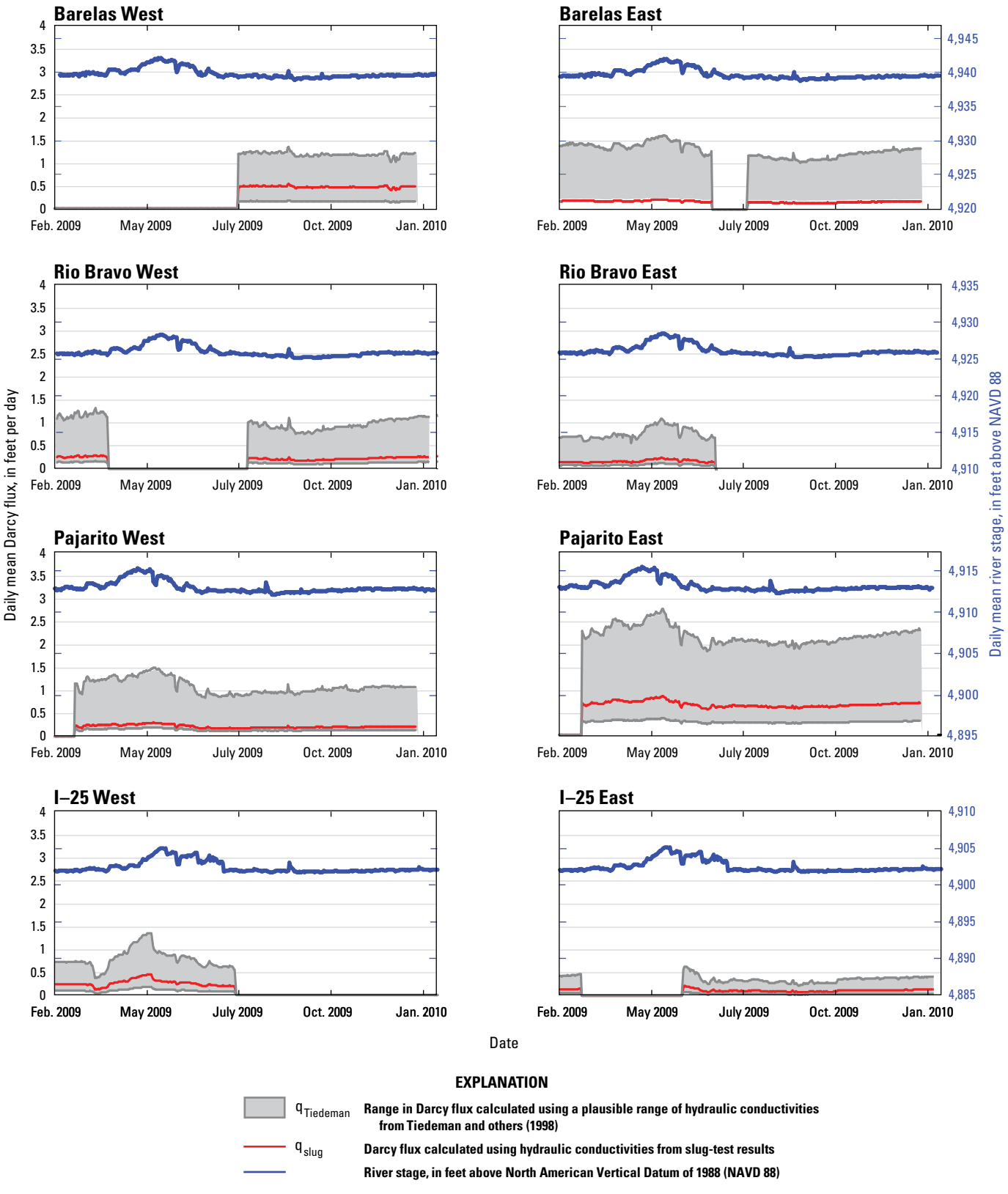

Figure 10. Daily mean Darcy flux calculated from daily mean hydraulic gradients and slug-test derived hydraulic conductivities, daily mean Darcy flux calculated from daily mean hydraulic gradients and a plausible range of hydraulic conductivities (Tiedeman and others, 1998), and daily mean Rio Grande stage for the Alameda, Paseo del Norte, Montaño, and Central transects and the Barelas, Rio Bravo, Pajarito, and I-25 transects, Rio Grande inner valley alluvial aquifer, 2009–10.—Continued

The daily mean $q_{Tiedeman}$ fluxes (fig. 10) through the alluvial aquifer were calculated using a plausible range of hydraulic conductivities (20 to 150 ft/d) compiled by Tiedeman and others (1998) and the daily mean hydraulic gradients calculated in this study (fig. 10). Daily mean q_{slug} flux values (fig. 10) generally plot near the lower end of the daily mean $q_{Tiedeman\ flux}$ range because the q_{slug} flux was constrained by site-scale hydraulic conductivities, ranging from 30 to 120 ft/d (fig. 9). The difference between q_{slug} flux values relative to the range of $q_{Tiedeman}$ flux values was likely the result of differences in bulk aquifer properties measured at different scales. Inverse modeling, also at basin scale, by Tiedeman and others (1998), resulted in a slightly larger range of hydraulic conductivities (73 to 209 ft/d) than those estimated from slug-test data. Simulated hydraulic gradients produced when Tiedeman and others (1998) used a hydraulic conductivity of 73 ft/d best match the hydraulic gradients calculated for this study. Other simulations at a basin scale have used hydraulic conductivities of 24 ft/d (Sanford and others, 2003) and 45 ft/d (McAda and Barroll, 2002). The refinement of scale offered by the present study indicates that the magnitude of computed flux in the alluvial aquifer based solely on hydraulic-conductivity estimates from slug tests generally is consistent with that computed in large-scale models.

Heat-Flux Modeling

Results of calculations of horizontal groundwater flux in the alluvial aquifer using the Suzuki-Stallman method of heat-transport modeling are listed in table 4. Application of the Suzuki-Stallman method yields one set of q_a and q_b specific-flux values for each temperature time-series pair analyzed. A temperature time-series pair consists of concurrent daily mean water-temperature data from two piezometers or from a surface-water gage and a piezometer. Because the water temperatures were observed to have a wavelength of about a year, q_a and q_b specific-flux values are considered to represent the annual flux. Some variance in the annual q_a and q_b specific fluxes probably resulted from analyzing temperature datasets with differing time spans (table 4). Only one temperature time-series pair was available for analysis at the Rio Bravo East and Rio Bravo West paired transects; three temperature time-series pairs were available for analysis from the Paseo Del Norte West paired transect. Values of *a* (the attenuation of the temperature wave) calculated from temperatures collected at 10 ft and 20 ft bls ranged from 7.0×10^{-5} to 1.7×10^{-2} and 2.0×10^{-4} to 4.8×10^{-2} ft^{-1}, respectively. Similarly, values of *b* (the spatial frequency) calculated from daily mean temperatures collected at both the 10- and 20-ft depths ranged from 0.01 to 1.05 rad/ft for both depths.

Values of *a* and *b* were transformed to specific-flux values of q_a and q_b by using type curves in figure 5; q_a and q_b were then averaged to obtain the q_{heat} specific flux (table 4). At 10 ft bls, the specific-flux values of q_a and q_b, collectively, ranged from 0.05 to 1.88 ft/d. At 20 ft bls, values of q_a and q_b, collectively, ranged from 0.04 to 1.67 ft/d. The standard deviation from the mean of all specific-flux (q_{heat}) values calculated with the Suzuki-Stallman method was 0.17, which indicates a relatively small range of q_a and q_b and lends confidence to the results in table 4. Of some concern is the fact that the estimates of q_b were systematically less than the estimates of q_a. Moret (2007) suggests this may indicate that temperature-signal phases were slightly distorted by the effects of temperature on water viscosity (cold water moves more slowly through the aquifer than warm water so the timing of the arrival of temperature peaks and troughs at various locations in the aquifer would be slightly different than predicted by Stallman's [1965] equations).

The one-dimensional Suzuki-Stallman method assumes that groundwater flow in the alluvial aquifer was oriented orthogonal to the Rio Grande channel for all temperature time-series pairs used in this study. Gradient orientations (table 2), however, indicate groundwater flow was not orthogonal to the channel, so the assumption of orthogonality likely introduced some error into the analytical results for paired transects summarized in figure 11. This error can be accounted for by adjusting the distance between measuring points in equations 12 and 13.

In addition, all of the temperature time-series pairs used in this study were spatially aliased. The values of *a* and *b* were determined by iteratively adding 1-year increments to measured time lags until modeled sinusoidal curves matched observed data. In general, observed and modeled data fit well. Results of temperature time-series pair analyses (table 4) were rejected if temperature time-series curves were not sinusoidal or if the specific flux values of q_a and q_b disagreed by more than 50 percent.

Specific-flux values of q_a and q_b determined for each temperature time-series pair were averaged to get a mean Suzuki-Stallman q_{heat} flux (table 4). Box plots of q_{heat} flux show the greatest median annual value at Alameda East (0.50 ft/d) and, excluding the single value for Rio Bravo West, the lowest median annual value at Alameda West (0.25 ft/d) (fig. 11). Overall, q_{heat} fluxes on the east side of the river are greater than fluxes on the west side of the river and generally decrease in a downstream direction (fig. 11). The larger sample sizes, which capture more variability, from both sides of the Barelas, Alameda, Central, and Pajarito paired transects, indicate that local-scale geologic heterogeneities may produce a range of Suzuki-Stallman q_{heat} fluxes. The ranges of heterogeneity observed at the Barelas, Alameda, Central, and Pajarito transects are likely present at all paired transect locations, but the ranges are not as well characterized because sample sizes were smaller at the other four transect locations.

Table 4. Annual flux between individual time-series pairs and depths in the Rio Grande inner valley alluvial aquifer, Albuquerque, New Mexico, 2009–10. Transducers were set about 10 feet below land surface in shallow ("a") wells and were set at about 20 feet in mid-depth ("b") wells.

[Site locations shown in figures 3*A–H*; a temperature time-series pair consists of concurrent daily mean water-temperature data from two piezometers or from a surface-water gage and a piezometer; a, temperature wave attenuation parameter (eq. 12); ft, foot; q_a, flux determined using value of a and curve a on figure 5; ft/d, foot per day; b, spatial frequency parameter (eq. 13); rad/ft, radians per foot; q_b, flux determined using value of b and curve b on figure 5; q_{heat}, average of q_a and q_b; —, not reported]

Transect location	Temperature time-series pair	Time series location (relative to river)	Year	a (1/ft)	q_a (ft/d)	b (rad/ft)	q_b (ft/d)	q_{heat} (ft/d)
Alameda	AS2/A5a	east	2009	6.1E-4	0.51	0.03	0.46	0.49
Alameda	AS2/A5b	east	2009	6.6E-4	0.50	0.03	0.46	0.48
Alameda	AS2/A4a	east	2009	4.9E-4	0.55	0.02	0.59	0.57
Alameda	AS2/A4b	east	2009	7.5E-4	0.48	0.02	0.59	0.54
Alameda	AS2/A3a	east	2009	7.5E-4	0.48	0.02	0.56	0.52
Alameda	A5a/A4a	east	2009	7.0E-5	1.06	0.09	0.12	0.59
Alameda	A5a/A3a	east	2009	8.0E-4	0.47	0.04	0.34	0.41
Alameda	A5b/A4b	east	2009	7.2E-4	0.49	0.03	0.43	0.46
Alameda	A4a/A3a	east	2009	6.4E-4	0.51	0.02	0.53	0.52
Alameda	AS2/A14a	east	2009	4.3E-4	0.58	0.02	0.61	0.60
Alameda	AS2/A14b	east	2009	5.9E-4	0.52	0.02	0.61	0.57
Alameda	AS2/A13a	east	2009	4.5E-4	0.57	0.02	0.57	0.57
Alameda	AS2/A13b	east	2009	6.5E-4	0.50	0.02	0.53	0.52
Alameda	AS2/A12a	east	2009	9.4E-4	0.45	0.03	0.50	0.47
Alameda	A14a/A13a	east	2009	4.5E-4	0.57	0.07	0.18	0.37
Alameda	A14b/A13b	east	2009	7.7E-4	0.48	0.07	0.18	0.33
Alameda	A14a/A12a	east	2009	1.9E-3	0.35	0.03	0.44	0.40
Alameda	A13a/A12a	east	2009	2.1E-3	0.34	0.04	0.35	0.35
Alameda	AS2/A6a	west	2009	2.6E-3	0.32	0.06	0.21	0.26
Alameda	AS2/A6b	west	2009	4.3E-3	0.26	0.06	0.21	0.23
Alameda	AS2/A7a	west	2009	6.3E-3	0.23	0.05	0.24	0.24
Alameda	AS2/A7b	west	2009	5.4E-3	0.24	0.05	0.24	0.24
Alameda	AS2/A8a	west	2009	3.6E-3	0.28	0.04	0.29	0.29
Alameda	A6a/A8a	west	2009	3.8E-3	0.28	0.05	0.24	0.26
Alameda	A6a/A7a	west	2009	7.6E-3	0.22	0.05	0.25	0.24
Alameda	A6b/A7b	west	2009	5.7E-3	0.24	0.05	0.25	0.24
Alameda	A7a/A8a	west	2009	—	—	—	—	—
Alameda	AS2/A15a	west	2009	2.0E-3	0.35	0.11	0.05	0.20
Alameda	AS2/A15b	west	2009	6.2E-3	0.23	0.11	0.04	0.14
Alameda	AS2/A16a	west	2009	2.0E-3	0.35	0.05	0.25	0.30
Alameda	AS2/A16b	west	2009	3.2E-3	0.29	0.05	0.25	0.27
Alameda	AS2/A17a	west	2009	4.0E-3	0.27	0.06	0.23	0.25
Alameda	A15a/A16a	west	2009	1.9E-3	0.35	0.04	0.36	0.36
Alameda	A15b/A16b	west	2009	1.9E-3	0.35	0.04	0.36	0.36
Alameda	A15a/A17a	west	2009	3.6E-3	0.28	0.06	0.21	0.25
Alameda	A16a/A17a	west	2009	5.7E-3	0.24	0.06	0.20	0.22
Alameda	AS2/A17a	west	2009	4.0E-3	0.27	0.06	0.23	0.25

Table 4. Annual flux between individual time-series pairs and depths in the Rio Grande inner valley alluvial aquifer, Albuquerque, New Mexico, 2009–10. Transducers were set about 10 feet below land surface in shallow ("a") wells and were set at about 20 feet in mid-depth ("b") wells.—Continued

[Site locations shown in figures 3*A–H*; a temperature time-series pair consists of concurrent daily mean water-temperature data from two piezometers or from a surface-water gage and a piezometer; a, temperature wave attenuation parameter (eq. 12); ft, foot; q_a, flux determined using value of a and curve a on figure 5; ft/d, foot per day; b, spatial frequency parameter (eq. 13); rad/ft, radians per foot; q_b, flux determined using value of b and curve b on figure 5; q_{heat}, average of q_a and q_b; —, not reported]

Transect location	Temperature time-series pair	Time series location (relative to river)	Year	a (1/ft)	q_a (ft/d)	b (rad/ft)	q_b (ft/d)	q_{heat} (ft/d)
Alameda	A15a/A16a	west	2009	1.9E-3	0.35	0.04	0.36	0.36
Alameda	A15b/A16b	west	2009	1.9E-3	0.35	0.04	0.36	0.36
Alameda	A15a/A17a	west	2009	3.6E-3	0.28	0.06	0.21	0.25
Alameda	A16a/A17a	west	2009	5.7E-3	0.24	0.06	0.20	0.22
Paseo Del Norte	P5a/P4a	east	2009	4.9E-4	0.55	0.03	0.44	0.50
Paseo Del Norte	P5b/P4b	east	2009	1.0E-3	0.43	0.03	0.43	0.43
Paseo Del Norte	P5a/P3a	east	2009	6.7E-4	0.50	0.03	0.42	0.46
Paseo Del Norte	P4a/P3a	east	2009	7.4E-4	0.48	0.03	0.41	0.45
Paseo Del Norte	P14a/P13a	east	2009	4.1E-4	0.59	0.02	0.61	0.60
Paseo Del Norte	P14b/P13b	east	2009	8.2E-4	0.46	0.03	0.37	0.42
Paseo Del Norte	P14a/P12a	east	2009	5.0E-4	0.55	0.02	0.53	0.54
Paseo Del Norte	P13a/P12a	east	2009	5.6E-4	0.53	0.03	0.48	0.51
Paseo Del Norte	P15a/P16a	west	2009	1.6E-3	0.37	0.04	0.30	0.34
Paseo Del Norte	P15a/P17a	west	2009	8.2E-4	0.47	0.03	0.45	0.46
Paseo Del Norte	P16a/P17a	west	2009	6.8E-4	0.50	0.03	0.45	0.48
Montaño	M5b/M4b	east	2009	—	—	—	—	—
Montaño	M14b/M12b	east	2009	1.2E-3	0.41	0.04	0.29	0.35
Montaño	M13a/M12a	east	2009	4.7E-4	0.56	0.03	0.43	0.50
Montaño	M7a/M8a	west	2009	—	—	—	—	—
Montaño	M6a/M7a	west	2009	3.2E-3	0.29	0.04	0.32	0.31
Montaño	M6a/M8a	west	2009	6.1E-4	0.51	0.03	0.47	0.49
Montaño	M6b/M7b	west	2009	5.1E-3	0.25	0.05	0.24	0.24
Montaño	M15a/M16a	west	2009	3.8E-3	0.28	0.05	0.25	0.26
Montaño	M15a/M17a	west	2009	8.9E-4	0.45	0.03	0.42	0.44
Montaño	M16a/M17a	west	2009	—	—	—	—	—
Montaño	M15b/M16b	west	2009	4.0E-3	0.27	0.05	0.25	0.26
Montaño	M15b/M17b	west	2009	1.4E-3	0.39	0.04	0.37	0.38
Montaño	M16b/M17b	west	2009	5.4E-4	0.54	0.02	0.55	0.54

Table 4. Annual flux between individual time-series pairs and depths in the Rio Grande inner valley alluvial aquifer, Albuquerque, New Mexico, 2009–10. Transducers were set about 10 feet below land surface in shallow ("a") wells and were set at about 20 feet in mid-depth ("b") wells.—Continued

[Site locations shown in figures 3*A–H*; a temperature time-series pair consists of concurrent daily mean water-temperature data from two piezometers or from a surface-water gage and a piezometer; a, temperature wave attenuation parameter (eq. 12); ft, foot; q_a, flux determined using value of a and curve a on figure 5; ft/d, foot per day; b, spatial frequency parameter (eq. 13); rad/ft, radians per foot; q_b, flux determined using value of b and curve b on figure 5; q_{heat}, average of q_a and q_b; —, not reported]

Transect location	Temperature time-series pair	Time series location (relative to river)	Year	a (1/ft)	q_a (ft/d)	b (rad/ft)	q_b (ft/d)	q_{heat} (ft/d)
Central	CS2/C5a	east	2009	2.2E-3	0.33	0.05	0.27	0.30
Central	CS2/C5b	east	2009	2.9E-3	0.30	0.05	0.27	0.29
Central	CS2/C4a	east	2009	—	—	—	—	—
Central	CS2/C4b	east	2009	—	—	—	—	—
Central	CS2/C3a	east	2009	—	—	—	—	—
Central	CS2/C14a	east	2009	2.7E-3	0.31	0.01	1.67	0.99
Central	CS2/C14b	east	2009	7.9E-4	0.47	0.01	1.58	1.03
Central	CS2/C13a	east	2009	9.4E-4	0.45	0.04	0.33	0.39
Central	CS2/C13b	east	2009	1.9E-3	0.35	0.04	0.33	0.34
Central	C5a/C4a	east	2009	—	—	—	—	—
Central	C5b/C4b	east	2009	—	—	—	—	—
Central	C5a/C3a	east	2009	—	—	—	—	—
Central	C4a/C3a	east	2009	—	—	—	—	—
Central	C14a/C13a	east	2009	1.3E-3	0.40	0.03	0.47	0.43
Central	C14b/C13b	east	2009	2.1E-3	0.34	0.05	0.26	0.30
Central	CS2/C6a	west	2009	2.7E-3	0.31	0.01	1.88	1.10
Central	CS2/C6b	west	2009	2.7E-3	0.31	0.01	1.67	0.99
Central	CS2/C7a	west	2009	1.2E-3	0.41	0.04	0.35	0.38
Central	CS2/C7b	west	2009	1.1E-3	0.42	0.04	0.35	0.39
Central	CS2/C8a	west	2009	2.2E-3	0.33	0.04	0.29	0.31
Central	CS2/C15a	west	2009	2.8E-3	0.31	0.01	1.59	0.95
Central	CS2/C15b	west	2009	3.1E-3	0.30	0.01	1.10	0.70
Central	CS2/C16a	west	2009	2.3E-3	0.33	0.04	0.30	0.31
Central	CS2/C16b	west	2009	2.9E-3	0.30	0.04	0.29	0.30
Central	CS2/C17a	west	2009	3.8E-3	0.28	0.05	0.27	0.27
Central	C6a/C7a	west	2009	2.0E-3	0.34	0.04	0.30	0.32
Central	C6b/C7b	west	2009	1.4E-3	0.39	0.04	0.30	0.35
Central	C6a/C8a	west	2009	2.6E-3	0.32	0.05	0.27	0.30
Central	C7a/C8a	west	2009	2.9E-3	0.31	0.04	0.36	0.33
Central	C15a/C16a	west	2009	1.9E-3	0.35	0.04	0.31	0.33
Central	C15b/C16b	west	2009	1.8E-3	0.36	0.04	0.30	0.33
Central	C15a/C17a	west	2009	4.1E-3	0.27	0.05	0.26	0.27
Central	C16a/C17a	west	2009	7.1E-3	0.22	0.07	0.18	0.20
Barelas	B5a/B4a	east	2009	2.2E-3	0.33	0.04	0.32	0.33
Barelas	B14a/B13a	east	2009	8.8E-4	0.45	0.03	0.40	0.43
Barelas	B14b/B13b	east	2009	1.3E-3	0.40	0.03	0.46	0.43
Barelas	B14a/B12a	east	2009	1.1E-3	0.42	0.03	0.45	0.44

Table 4. Annual flux between individual time-series pairs and depths in the Rio Grande inner valley alluvial aquifer, Albuquerque, New Mexico, 2009–10. Transducers were set about 10 feet below land surface in shallow ("a") wells and were set at about 20 feet in mid-depth ("b") wells.—Continued

[Site locations shown in figures 3*A–H*; a temperature time-series pair consists of concurrent daily mean water-temperature data from two piezometers or from a surface-water gage and a piezometer; a, temperature wave attenuation parameter (eq. 12); ft, foot; q_a, flux determined using value of a and curve a on figure 5; ft/d, foot per day; b, spatial frequency parameter (eq. 13); rad/ft, radians per foot; q_b, flux determined using value of b and curve b on figure 5; q_{heat}, average of q_a and q_b; —, not reported]

Transect location	Temperature time-series pair	Time series location (relative to river)	Year	a (1/ft)	q_a (ft/d)	b (rad/ft)	q_b (ft/d)	q_{heat} (ft/d)
Barelas	B14b/B12b	east	2009	7.4E-4	0.48	0.04	0.31	0.40
Barelas	B13a/B12a	east	2009	1.3E-3	0.40	0.03	0.49	0.45
Barelas	B13b/B12b	east	2009	2.1E-4	0.73	0.03	0.49	0.61
Barelas	BS2/B5a	east	2009	1.4E-3	0.39	0.06	0.21	0.30
Barelas	BS2/B4a	east	2009	6.4E-3	0.23	0.09	0.12	0.18
Barelas	BS2/B3b	east	2009	8.8E-3	0.20	0.06	0.20	0.20
Barelas	BS2/B14a	east	2009	2.2E-3	0.33	—	—	0.33
Barelas	BS2/B14b	east	2009	7.4E-3	0.22	0.08	0.15	0.18
Barelas	BS2/B13a	east	2009	1.5E-3	0.38	0.05	0.27	0.32
Barelas	BS2/B13b	east	2009	3.5E-3	0.28	0.05	0.24	0.26
Barelas	BS2/B12a	east	2009	1.4E-3	0.39	0.04	0.33	0.36
Barelas	BS2/B12b	east	2009	1.9E-3	0.35	0.04	0.33	0.34
Barelas	B16a/B17a	west	2009	1.9E-3	0.35	0.04	0.33	0.34
Barelas	B16b/B17b	west	2009	1.4E-3	0.39	0.04	0.35	0.37
Barelas	B6a/B7a	west	2009	7.7E-4	0.48	0.03	0.46	0.47
Barelas	BS2/B6a	west	2009	1.5E-2	0.17	0.06	0.22	0.19
Barelas	BS2/B6b	west	2009	3.7E-2	0.10	0.06	0.20	0.15
Barelas	BS2/B7a	west	2009	2.4E-3	0.32	0.05	0.24	0.28
Barelas	BS2/B16a	west	2009	3.2E-3	0.29	0.06	0.22	0.26
Barelas	BS2/B16b	west	2009	5.1E-3	0.25	0.06	0.22	0.24
Barelas	BS2/B17a	west	2009	2.6E-3	0.31	0.05	0.28	0.29
Barelas	BS2/B17b	west	2009	3.1E-3	0.30	0.05	0.27	0.28
Rio Bravo	R13a/R12a	east	2009	6.3E-3	0.52	0.29	0.48	0.50
Rio Bravo	R15a/R16a	west	2009	1.7E-2	0.38	1.05	0.10	0.24
Pajarito	PJS2/PJ5a	east	2009	3.2E-3	0.29	0.01	1.57	0.93
Pajarito	PJS2/PJ5b	east	2009	3.2E-3	0.29	0.01	1.39	0.84
Pajarito	PJS2/PJ4a	east	2009	6.6E-4	0.50	0.04	0.32	0.41
Pajarito	PJS2/PJ4b	east	2009	6.6E-4	0.50	0.04	0.32	0.41
Pajarito	PJS2/PJ3a	east	2009	7.2E-4	0.49	0.02	0.60	0.54
Pajarito	PJS2/PJ14a	east	2009	8.0E-3	0.21	0.02	0.67	0.44
Pajarito	PJS2/PJ14b	east	2009	4.8E-2	0.08	0.03	0.40	0.24
Pajarito	PJS2/13a	east	2009	1.8E-4	0.78	0.03	0.38	0.58
Pajarito	PJS2/PJ13b	east	2009	3.0E-3	0.30	0.03	0.38	0.34
Pajarito	PJS2/PJ12a	east	2009	1.7E-3	0.36	0.03	0.41	0.39
Pajarito	PJ5a/PJ4a	east	2009	3.9E-4	0.60	0.05	0.26	0.43
Pajarito	PJ5b/PJ4b	east	2009	2.0E-4	0.75	0.05	0.26	0.50
Pajarito	PJ5a/PJ3a	east	2009	1.2E-3	0.41	0.04	0.34	0.38

Table 4. Annual flux between individual time-series pairs and depths in the Rio Grande inner valley alluvial aquifer, Albuquerque, New Mexico, 2009–10. Transducers were set about 10 feet below land surface in shallow ("a") wells and were set at about 20 feet in mid-depth ("b") wells.—Continued

[Site locations shown in figures 3*A–H*; a temperature time-series pair consists of concurrent daily mean water-temperature data from two piezometers or from a surface-water gage and a piezometer; a, temperature wave attenuation parameter (eq. 12); ft, foot; q_a, flux determined using value of a and curve a on figure 5; ft/d, foot per day; b, spatial frequency parameter (eq. 13); rad/ft, radians per foot; q_b, flux determined using value of b and curve b on figure 5; q_{heat}, average of q_a and q_b; —, not reported]

Transect location	Temperature time-series pair	Time series location (relative to river)	Year	a (1/ft)	q_a (ft/d)	b (rad/ft)	q_b (ft/d)	q_{heat} (ft/d)
Pajarito	PJ4a/PJ3a	east	2009	1.6E-3	0.37	0.03	0.40	0.39
Pajarito	PJ14a/PJ13a	east	2009	7.8E-4	0.47	0.04	0.36	0.41
Pajarito	PJ14a/PJ12a	east	2009	2.0E-3	0.35	0.05	0.28	0.31
Pajarito	PJ13a/PJ12a	east	2009	2.8E-3	0.31	0.06	0.23	0.27
Pajarito	PJS2/PJ6a	west	2009	4.0E-3	0.27	0.01	1.25	0.76
Pajarito	PJS2/PJ6b	west	2009	4.0E-3	0.27	0.01	1.06	0.66
Pajarito	PJS2/PJ7a	west	2009	1.7E-3	0.36	0.03	0.43	0.40
Pajarito	PJS2/PJ7b	west	2009	1.7E-3	0.36	0.03	0.42	0.39
Pajarito	PJS2/PJ8a	west	2009	2.0E-3	0.34	0.04	0.37	0.35
Pajarito	PJS2/PJ15a	west	2009	1.6E-3	0.37	0.10	0.09	0.23
Pajarito	PJS2/PJ15b	west	2009	5.4E-3	0.24	0.10	0.09	0.16
Pajarito	PJS2/PJ16a	west	2009	1.3E-3	0.40	0.04	0.31	0.36
Pajarito	PJS2/PJ16b	west	2009	2.1E-3	0.34	0.04	0.30	0.32
Pajarito	PJS2/PJ17a	west	2009	3.0E-3	0.30	0.05	0.29	0.29
Pajarito	PJ6a/PJ7a	west	2009	2.1E-3	0.34	0.05	0.29	0.31
Pajarito	PJ6b/PJ7b	west	2009	1.9E-3	0.35	0.03	0.41	0.38
Pajarito	PJ6a/PJ8a	west	2009	2.2E-3	0.34	0.04	0.34	0.34
Pajarito	PJ7a/PJ8a	west	2009	2.2E-3	0.33	0.04	0.36	0.35
Pajarito	PJ15a/PJ16a	west	2009	2.3E-3	0.33	0.03	0.39	0.36
Pajarito	PJ15b/PJ16b	west	2009	1.5E-3	0.38	0.03	0.38	0.38
Pajarito	PJ15a/PJ17a	west	2009	3.7E-3	0.28	0.04	0.29	0.29
Pajarito	PJ16a/PJ17a	west	2009	4.1E-3	0.27	0.05	0.26	0.26
I-25	IS2/I3a	east	2009	3.0E-3	0.30	0.04	0.31	0.30
I-25	IS2/I14a	east	2009	1.0E-3	0.44	0.03	0.49	0.46
I-25	IS2/I13a	east	2009	5.8E-3	0.24	0.06	0.20	0.22
I-25	I14a/I13a	east	2009	6.3E-3	0.23	0.08	0.15	0.19
I-25	IS2/I6a	west	2009	6.9E-4	0.49	0.03	0.40	0.45
I-25	IS2/I7a	west	2009	2.4E-3	0.32	0.05	0.25	0.29
I-25	IS2/I8a	west	2009	8.7E-4	0.46	0.03	0.49	0.47
I-25	IS2/I8b	west	2009	1.6E-3	0.37	0.03	0.49	0.43
I-25	IS2/I16b	west	2009	2.2E-3	0.33	0.05	0.24	0.29
I-25	IS2/I17a	west	2009	9.5E-4	0.44	0.03	0.45	0.45
I-25	I6a/I7a	west	2009	3.4E-3	0.29	0.04	0.30	0.30
I-25	I6a/I8a	west	2009	1.1E-3	0.42	0.03	0.39	0.40

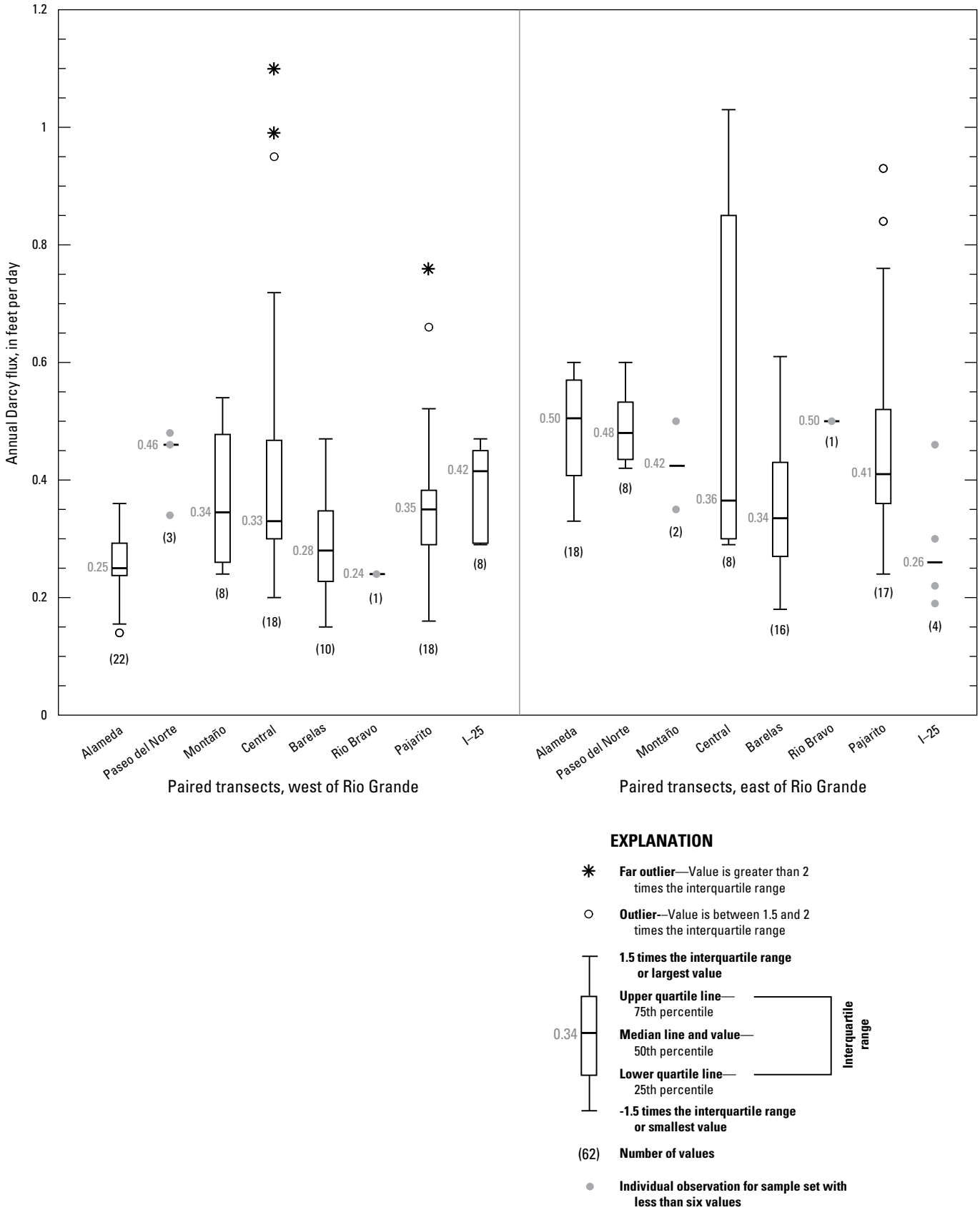

Figure 11. Summary of annual Darcy flux through the Rio Grande inner valley alluvial aquifer, Albuquerque, New Mexico, calculated using the Suzuki-Stallman method.

Horizontal Groundwater-Flux Model Comparison

Annual median q_{slug} flux values computed from Darcy's Law ranged from about 0.10 ft/d at Montaño West to 0.82 ft/d at Alameda East (table 5); annual median q_{heat} flux values computed using the Suzuki-Stallman method ranged from 0.24 ft/d at Rio Bravo West to 0.50 ft/d at Alameda East and Rio Bravo East (table 5). The two methods of computing flux agreed reasonably well (table 5). By using annual mean gradients (table 2) and annual median q_{heat} fluxes computed by using the Suzuki-Stallman method (table 4), the horizontal hydraulic conductivity of the alluvial aquifer was estimated at each paired transect by using equation 4 and solving for hydraulic conductivity. Hydraulic-conductivity values from this analysis ranged from 28 ft/d (Alameda East) to 109 ft/d (I-25 East). The hydraulic conductivities calculated from the results of temperature analysis are very similar to the median hydraulic-conductivity results (30 to 120 ft/d) from the slug tests (fig. 9). The results computed using Darcy's Law and results computed using the Suzuki-Stallman method (table 5) showed that while a majority of transects had greater groundwater fluxes east of the Rio Grande than those west of the river, groundwater fluxes are generally variable throughout the inner valley alluvial aquifer.

Riverside Drain Seepage Investigations

Riverside drain seepage investigations were conducted to compute changes in flow within the drains and to evaluate results from Darcy's Law and Suzuki-Stallman method flux calculations. The seepage investigations were conducted by measuring discharge in the east riverside drain between the

Table 5. Comparison of Darcy's Law and Suzuki-Stallman method results for horizontal-groundwater flux in the Rio Grande inner valley alluvial aquifer, Albuquerque, New Mexico.

[Site locations shown in figures 3*A–H*; q, horizontal groundwater flux; ft/d, foot per day; q_{slug}, flux determined from slug tests and Darcy's Law; q_{heat}, flux determined by using the Suzuki-Stallman method]

Transect location	Annual median q (ft/d)	
	Darcy's Law (q_{slug})[1]	Suzuki-Stallman method (q_{heat})
Alameda		
East	0.82	0.50
West	0.27	0.25
Paseo del Norte		
East	0.49	0.48
West	0.24	0.46
Montaño		
East	0.31	0.42
West	0.10	0.34
Central		
East	0.75	0.36
West	0.53	0.33
Barelas		
East	0.52	0.34
West	0.47	0.28
Rio Bravo		
East	0.19	0.50
West	0.28	0.24
Pajarito		
East	0.46	0.41
West	0.23	0.35
I-25		
East	0.12	0.26
West	0.25	0.42

[1]Calculated by using median value of hydraulic conductivity (fig. 9) from results of slug-test analyses.

Barelas Bridge and the I-25 bridge and in the west riverside drain between the Central bridge and the I-25 bridge (fig. 1) during a period of low flow on February 10–12, 2010 (table 6). On the east drain, measurements were made near the Barelas Bridge (east drain mile 0), near the Rio Bravo bridge (east drain mile 3), between the Rio Bravo bridge and Pajarito (east drain mile 4), at Pajarito (east drain mile 6), and near the I-25 bridge (east drain mile 9). Two seepage investigations were conducted on the west drain. The first seepage measurements were taken near the Central bridge (west drain mile 0) to near the Rio Bravo bridge (west drain mile 4). The second seepage measurements were taken at Pajarito (west drain mile 7) and near the I-25 bridge (west drain mile 10). The flow in the Rio Grande was not measured while seepage was measured. Estimates of the portion of river leakage returned to the drains could not be constrained in the absence of measurements of river flow through this reach.

The accuracy of each seepage measurement was assessed according to hydrographer evaluations of streamflow conditions at the time of measurement for each measured location. The accuracy of measurements for the east and west drain-seepage investigations was estimated to be "fair" (Anthony Cox, U.S. Geological Survey, written commun., 2013). Sauer and Meyer (1992) indicate that the uncertainty of a measurement rated as fair is ±8 percent or less of the total measured streamflow. Using ±8 percent, the uncertainty calculated for the individual seepage measurements ranged from ±0.85 to ±4.0 (table 6). Uncertainty (Taylor, 1997, p. 60) for two or more seepage measurements was calculated as:

$$CU = \sqrt{u_1^{\,2} + u_2^{\,2} + \ldots + u_n^{\,2}} \qquad (15)$$

where

CU is the cumulative uncertainty, in cubic feet per second; and

u_n is the uncertainty for an individual seepage measurement, in cubic feet per second.

The east and west riverside drains had similar average increases in flow during the seepage investigation. The east riverside drain increased in flow from 10.6 cubic feet per second (ft^3/s) (east drain mile 0) to 40.9 ft^3/s (east drain mile 9) over a distance of about 8.8 mi. The increase in flow between east drain mile 0 and east drain mile 9 was 30.3 ft^3/s

Table 6. Seepage investigation discharge measurements and estimated uncertainty in Rio Grande riverside drains, Albuquerque, New Mexico, February 10–12, 2010.

[DDMMSS, degrees minutes seconds; NAD 83, North American Datum of 1983; ft^3/s, cubic feet per second; $ft^3/d/ft$, cubic feet per day per foot; ft, foot; ±, plus or minus; NA, not applicable]

Measurement location[1] (fig. 1)	Latitude (DDMMSS; NAD 83)	Longitude (DDMMSS; NAD 83)	Discharge at measurement location and estimated uncertainty[2] (ft^3/s)		Gain and estimated cumulative uncertainty[3] (ft^3/s)		Flux and estimated cumulative uncertainty[4] ($ft^3/d/ft$)		Distance between measurement points (ft)
east drain mile 0	350407.9	-1063925.1	10.6	±0.85	NA	NA	NA	NA	NA
east drain mile 3	350135.5	-1064008.9	16.2	±1.3	5.6	±1.6	29.5	±8.4	16,418
east drain mile 4	350043.6	-1064015.0	17.8	±1.4	1.6	±1.9	26.1	±31	5,305
east drain mile 6	345905.0	-1064105.8	31.2	±2.5	13.4	±2.9	96.8	±21	11,961
east drain mile 9	345703.9	-1064040.9	40.9	±3.3	9.7	±4.1	66.1	±28	12,680
east drain mile 0 to mile 9	**NA**	**NA**	**NA**	**NA**	**30.3**	**±4.6**	**56.5**	**±8.6**	**46,364**
west drain mile 0	350450.2	-1064032.2	10.6	±0.85	NA	NA	NA	NA	NA
west drain mile 4	**350132.2**	**-1064028.4**	**24.8**	**±2.0**	**14.2**	**±2.2**	**53.8**	**±8.3**	**22,825**
west drain mile 7	345907.7	-1064125.2	43.2	±3.5	NA	NA	NA	NA	NA
west drain mile 10	**345656.2**	**-1064105.8**	**50.4**	**±4.0**	**7.2**	**±5.3**	**44.9**	**±33**	**13,864**

[1]Mile marker location is approximate. Actual distance between measurement points is shown in final column.

[2]Measurement uncertainty was estimated to be 8 percent or less of measured discharge (Anthony Cox, U.S. Geological Survey Hydrologic Technician, written commun., 2013).

[3]Cumulative estimated uncertainty is computed as the square root of the sum of the squares of the individual flow measurement estimated uncertainty terms (eq. 15 in text).

[4]Uncertainty in flux is computed by converting the estimated cumulative uncertainty in gain to units of cubic feet per day and dividing the result by the distance between measurement points.

over 46,364 ft, or an average of 56.5 $ft^3/d/ft$ of drain. The west riverside drain increased in flow from 10.6 ft^3/s (west drain mile 0) to 24.8 ft^3/s (west drain mile 4) over a distance of 4.3 mi. In a 2.6-mi reach, the flow in the west riverside drain increased from 43.2 ft^3/s (west drain mile 7) to 50.4 ft^3/s (west drain mile 10). The increase in flow between west drain mile 0 and west drain mile 4 was 14.2 ft^3/s over 22,825 ft, or an average of 53.8 $ft^3/d/ft$ of drain. The increase in flow between west drain mile 7 and west drain mile 10 was 7.2 ft^3/s over 13,864 ft, or an average of 44.9 $ft^3/d/ft$ of drain. On the dates of measurement, the measured flow increases in the east and west riverside drain reaches could only be attributed to groundwater inflow from the river or from areas outside the drain; no surface-water inputs or overlapping drains were observed.

Temperature profiles at Rio Bravo East (fig. 8) indicate that seasonal transport of heat from the Rio Grande during the nonirrigation period (November-February) is primarily within the upper 40 ft of the inner valley alluvial aquifer. Using (1) the median Darcy flux (q_{slug}) for Rio Bravo East of 0.19 ft/d (table 5), (2) a 1-ft width of aquifer measured parallel to the river, and (3) an assumption that 100 percent of leakage from the Rio Grande is contained in the upper 40 ft of the aquifer at Rio Bravo East, the total flux was calculated to be 7.6 $ft^3/d/ft$ of river. Under the same assumptions and using the median flux calculated from the Suzuki-Stallman method (q_{heat}) for Rio Bravo of 0.50 ft/d (table 5), the total flux is 20 $ft^3/d/ft$ of river. On February 10, 2010, discharge at east drain mile 0 was 10.6 ft^3/s and at east drain mile 3 was 16.2 ft^3/s, an increase of 5.6 ft^3/s, or 483,840 ft^3/d over a distance of 16,418 ft (table 6); in this section, the drain was gaining 29.5 ft^3/d /ft of drain. If the east riverside drain intercepted all of the river leakage from the upper 40 ft of the aquifer, and considering the cumulative uncertainty in the flux between miles 0 and 3 (table 6), the calculated q_{slug} and q_{heat} fluxes would account for 20–36 percent or 53–95 percent, respectively, of the total flow in the drain on February 10, 2010. Given an average annual gradient of 0.0048 at Rio Bravo East (table 2) and considering the cumulative uncertainty in the flux between miles 0 and 3 (table 6), the hydraulic conductivity of the 40 ft of alluvium would have to be in the range of 110 to 197 ft/d for river leakage to account for 100 percent of the gain in flow in the riverside drain during the seepage investigation. At Rio Bravo transect 1, the east drain gains water from river leakage west of the drain and from the alluvial aquifer east of the drain. However, at Rio Bravo transect 2 and Barelas transect 1, the east drain gained water from river leakage west of the drain and lost water to the alluvial aquifer to the east; therefore, it is possible that some of the flow increase in the east drain between Barelas and Rio Bravo could be attributed to seepage from the alluvial aquifer on the east side of the drain and river leakage from the west. Alternatively, if the east drain loses water to the alluvial aquifer to the east for a majority of the reach studied during the seepage investigation, the flux estimated from q_{slug} and q_{heat} would account for even less than 20–36 percent or 53–95 percent, respectively, of the flow increase observed in the drain.

At Rio Bravo West, the q_{slug} and q_{heat} fluxes were 0.28 and 0.24 ft/d, respectively. Temperature profiles at Rio Bravo West during the nonirrigation period (November-February) indicate seasonal transport of heat from the Rio Grande extends to depths greater than 50 ft. The total flux through a vertical slice of the inner valley alluvial aquifer of 1-ft width and 50-ft depth using q_{slug} or q_{heat} would be 14 ft^3/d and 12 ft^3/d, respectively. If the west riverside drain intercepted all of the flow from the upper 50 ft of aquifer and considering the cumulative error in the flux between miles 0 and 4 (table 6), total q_{slug} or q_{heat} flux would only account for 22–31 or 19–26 percent, respectively, of the flow in the drain on February 10, 2010. Given an annual mean horizontal hydraulic gradient of 0.0070 at Rio Bravo West (table 2) and considering the cumulative error in the flux between miles 0 and 4 (table 6), the hydraulic conductivity of the upper 50 ft of aquifer would have to be in the range of 130 to 177 ft/d for river leakage to account for 100 percent of the increase in flow in the west riverside drain during the seepage investigation. At Rio Bravo transects 1 and 2, the west riverside drain gains water from river leakage from the east and the alluvial aquifer to the west; therefore, it is likely that the increase in flow measured during the seepage investigation is because of river leakage and seepage from the alluvial aquifer.

On the east and west sides of the Rio Grande, groundwater outside of the riverside drains can flow towards or away from the drains, depending on the transect location, season, and irrigation operations. However, it is likely that discharge to the riverside drains occurs primarily from the river through the riparian area. Veenhuis (2002) determined that leakage from the river accounts for 79 percent of the flow in the riverside drains between Bernalillo and Rio Bravo. The present estimates of only 20–36 percent or 22–31 percent of the riverside drain flow being accounted for by the q_{slug} flux through the alluvial aquifer indicates that either (1) the estimates provided by Veenhuis (2002) are too high because they include all sources of seepage, not just river seepage, and additional water is entering the drains from the alluvial aquifer outside the drains, (2) hydraulic-conductivity values estimated from slug tests in this study are too low, (3) the estimates provided by Veenhuis (2002) were calculated over a larger distance in an area that extended further north than the present study, or (4) the assumed aquifer thickness in the riparian area that transmits river water to the drains is greater than that indicated by vertical temperature profiles. Increasing hydraulic conductivities by a factor of 2 or 3 would result in the q_{slug} flux still being within the plausible range of $q_{Tiedeman}$ flux values determined using Tiedeman and others (1998) hydraulic conductivities (fig. 10).

For all locations, annual median q_{slug} and q_{heat} fluxes ranged from 0.10 to 0.82 ft/d (table 5). Assuming a uniform aquifer thickness through the Albuquerque area of 40 ft, the range of leakage from the river through the alluvial aquifer is

from 4.0 to 32.8 $ft^3/d/ft$ of aquifer. At Rio Bravo, Roark (2001) calculated river leakage to be from 0.47 to 2.1 $ft^3/d/ft$ of aquifer, and at Paseo del Norte, Moret (2007), using the Suzuki-Stallman method, estimated river leakage to be from 12.9 to 17.2 $ft^3/d/ft$. Previous seepage investigations indicate river leakage to average 74 $ft^3/d/ft$ (Thorn, 1995) and 123 $ft^3/d/ft$ (Veenhuis, 2002) along river reaches of 12.4 and 21.9 mi, respectively. The large variations in river leakage found in this study and previous investigations suggest that estimates of flux through the inner valley alluvial aquifer are strongly dependent on scale, location, and time.

Variability of Horizontal Hydraulic Gradients and Groundwater Fluxes

The volume of water seeping from the Rio Grande into the inner valley alluvial aquifer that is intercepted by the riverside drains depends on the local gradient, aquifer properties, and configuration of the groundwater-flow field. In the Albuquerque area, the hydrology of the alluvial aquifer beneath the Rio Grande riparian area is complicated by heterogeneous aquifer properties and anthropogenic influences on the system. Groundwater data collected at each transect in this study were used to evaluate geologic and anthropogenic influences and present a general understanding of groundwater flow in the riparian area.

Water-level and temperature data have been collected at these eight paired transects for varying lengths of time since 2003. Report 1 (Rankin and others, 2013) included data from 2003 to 2009 and Report 2 (this report) presents data from 2009 to 2010. Table 7 compares the annual mean horizontal hydraulic gradients and annual median fluxes calculated in both reports. Annual mean horizontal hydraulic gradients calculated in Report 1 and in Report 2 were similar, and the range of horizontal hydraulic gradients calculated for each transect were similar over the two time periods (table 7). The q_{slug} and q_{heat} fluxes calculated in Report 1 were similar to the q_{slug} and q_{heat} fluxes calculated in Report 2 on both sides of the river (table 7). At transects where the fluxes calculated in the two reports were different, the fluxes from one report (and time period) were not consistently greater or less than the other. Water-level fluctuations in all piezometers in both reports were more variable during irrigation season (March-October) than during the nonirrigation season (November-February).

Spatial variability in the horizontal hydraulic gradients and fluxes (table 2 and table 7) can be primarily attributed to variability in distances between the river and riverside drains throughout the study area and geologic heterogeneities of the alluvial aquifer. Transects where the river and riverside drains are close together will have steeper horizontal hydraulic gradients than transects where the river and riverside drains are farther apart, assuming other conditions are constant. The inner valley alluvial aquifer is composed of heterogeneous deposits overlying the better cemented and coarser material of the Santa Fe Group aquifer (Hawley and Haase, 1992). In general, core descriptions from the Rio Grande riparian area indicate the inner valley alluvium grades from cobbles, gravels, sands, and silts to gravels, sands, silts, and clays in a downstream direction through the Albuquerque area. Clay layers can be hydrologically influential between the Barelas and Rio Bravo bridges (Bartolino and Sterling, 2000) where clay-layer thicknesses of 13 ft have been observed (Roark, 2001). The influence of these local-scale heterogeneities is dependent on the continuity of the deposit and its location within the groundwater-flow system. Whereas highly permeable sands and gravels may facilitate infiltration from the river, low-permeability sediment can locally impede the rates of horizontal flow or reduce the rates of horizontal flow through the alluvial aquifer. In addition, the orientation of high- and low-permeability sediment deposits with respect to the direction of groundwater flow can influence the rate of groundwater flow (Engdahl and Weissman, 2010). Because of these complicating factors and their variable effects on groundwater flow, there is no clear pattern to the spatial variability of horizontal hydraulic gradients or fluxes.

Temporal variability in the water levels which control the horizontal hydraulic gradients (table 2 and table 7) and fluxes between the Rio Grande and the riverside drains can be primarily attributed to seasonal fluctuations. Water levels in the Rio Grande increase in spring because of snowmelt runoff and in the summer because of monsoon-season storms. Water levels in the riverside drains increase markedly at the beginning of the irrigation season in March and decrease markedly at the end of irrigation season in October. Water levels in the riverside drains may also be influenced by monsoon-season storms and by local irrigation practices. River stages are generally higher than riverside drain stages except where the drains were designed to maintain water-level elevation above the river. Following Darcy's Law, and given constant hydraulic-conductivity values, the horizontal fluxes at each transect will be greatest when the difference between water levels in the Rio Grande and riverside drains produce the greatest hydraulic gradients.

The Rio Grande generally loses water to the surrounding alluvial aquifer, but the drains have more complicated hydraulic interactions with the alluvial aquifer because of the way they were designed to facilitate irrigation practices. Drains capture river leakage, transport water for irrigation, and capture return flows from nearby irrigation. At all transects, water seeps away from the river into the inner valley alluvial aquifer as indicated by the water-level data (fig. 6*A–P*). However, the water levels and hydraulic gradients exhibit spatial and temporal variability near both the east and west riverside drains. Water-level data at the transects indicate that drains gain water from the river side of the alluvial aquifer, although there are exceptions at some transects (I-25 East, Central West, Montaño West, and Alameda West). Most transects exhibit short periods each year when they do not gain water from the river side of the alluvial aquifer. There

Table 7. Comparison of annual mean horizontal hydraulic gradient and annual median flux at selected locations calculated for Report 1 (2003–9) and Report 2 (the current report, 2009–10).

[Site locations shown in figures 3*A*–*H*; ft/ft, foot per foot; q, horizontal-groundwater flux; ft/d, foot per day; q_{slug}, flux determined from slug tests and Darcy's Law; q_{heat}, flux determined by using the Suzuki-Stallman method; —, not calculated, insufficient data]

	West					East				
	Annual mean horizontal hydraulic gradient (ft/ft)	Range of daily horizontal hydraulic gradients (ft/ft)	Downstream direction relative to Rio Grande (range) (degrees)[1]	Annual median q (ft/d)		Annual mean horizontal hydraulic gradient (ft/ft)	Range of daily horizontal hydraulic gradients (ft/ft)	Downstream direction relative to Rio Grande (range) (degrees)[1]	Annual median q (ft/d)	
Report				Darcy's Law (q_{slug})	Suzuki-Stallman method (q_{heat})				Darcy's Law (q_{slug})	Suzuki-Stallman method (q_{heat})
					Alameda					
2	0.0045	0.004–0.006	76 (72–80)	0.27	0.25	0.0137	0.010–0.024	87 (79–92)	0.82	0.50
					Paseo del Norte					
1	0.0050	0.005–0.006	—	0.23	—	0.0130	0.009–0.049	—	0.36	0.52
2	0.0053	0.004–0.010	81 (73–95)	0.24	0.46	0.0109	0.009–0.012	57 (47–93)	0.49	0.48
					Montaño					
1	0.0030	0.003–0.004	—	0.09	0.24	0.0100	0.008–0.015	—	0.30	0.34
2	0.0033	0.003–0.006	64 (32–86)	0.10	0.34	0.0103	0.008–0.015	95 (91–101)	0.31	0.42
					Central					
2	0.0040	0.003–0.006	88 (81–94)	0.53	0.33	0.0062	0.005–0.011	78 (75–80)	0.75	0.36
					Barelas					
1	0.0100	0.007–0.013	—	0.66	0.47	0.0090	0.007–0.013	—	0.54	0.34
2	0.0078	0.007–0.009	73 (70–78)	0.47	0.28	0.0087	0.007–0.011	83 (78–87)	0.52	0.34
					Rio Bravo					
1	0.0070	0.004–0.013	—	0.25	0.27	0.0050	0.003–0.007	—	0.18	0.40
2	0.0070	0.005–0.008	81 (78–83)	0.28	0.24	0.0048	0.004–0.007	70 (61–82)	0.19	0.50
					Pajarito					
2	0.0072	0.006–0.009	77 (71–83)	0.23	0.35	0.0144	0.012–0.019	100 (97–101)	0.46	0.41
					I-25					
1	0.0050	0.004–0.008	—	0.25	0.34	0.0030	0.001–0.005	—	0.10	0.23
2	0.0050	0.003–0.009	60 (41–70)	0.25	0.42	0.0024	0.002–0.004	69 (58–85)	0.12	0.26

is also considerable variability in the horizontal hydraulic gradients on the outside of the drains (east of the east riverside drain and west of the west riverside drain) as indicated by the water-level data (fig. 6*A–P*). At some transects, the east and west drains almost always lose water to the east and west, respectively (Barelas West and Rio Bravo East). At other transects, the riverside drains usually gain water from both sides (Central East, Rio Bravo West, Pajarito East and West). There are two transects (Central West and I-25 East) where the drain loses water to both the east and west sides because of the way the drains are constructed. In addition, at Alameda West and Montaño West, it appears that the drains are above the elevation of the water table and so have little interaction with groundwater. The spatial and temporal variability in the horizontal gradients around the riverside drains makes it very difficult to generalize the interaction of the riverside drains with the surrounding alluvial aquifer.

Summary

The Albuquerque area is the major population center in New Mexico and has two principal sources of water for municipal, domestic, commercial, and industrial uses in this area: (1) groundwater from the Santa Fe Group aquifer system, and (2) surface water from the Rio Grande. Estimates indicated that from 1960 to 2002, pumping from the Santa Fe Group aquifer system caused groundwater levels in eastern Albuquerque to decline more than 120 feet (ft) while water-level declines along the Rio Grande in Albuquerque were generally less than 40 ft. These differences in water-level declines in the Albuquerque area have resulted in a great deal of interest in quantifying the river-aquifer interaction associated with the Rio Grande.

The Santa Fe Group aquifer system in the Albuquerque area consists of the middle Tertiary to Quaternary-age Santa Fe Group and the Quaternary-age post-Santa Fe Group alluvium (inner valley alluvial aquifer). The inner valley alluvial aquifer consists of river-valley and basin-fill sediments that underlie the present-day Rio Grande flood plain with an average thickness of 80 ft. The alluvium consists of unconsolidated to poorly consolidated, fine- to coarse-grain sand and rounded gravel with subordinate, discontinuous lens-shaped interbeds of fine-grain sand, silt, and clay. The underlying Santa Fe Group is composed primarily of gravel, sand, silt, and clay deposits and is approximately 14,000-ft thick in parts of the basin.

In 2003, the U.S. Geological Survey, in cooperation with the Bureau of Reclamation, acting as fiscal agent for the Middle Rio Grande Endangered Species Collaborative Program, and the U.S. Army Corps of Engineers, began a study to characterize the hydrogeology of the Rio Grande inner valley alluvial aquifer in the Albuquerque area of New Mexico. Previous researchers have used streambed permeameters, the transient response of the aquifer to a flood pulse, vertical profiles of temperature measurements, and calibrated numerical models to estimate the flux between the Rio Grande and the Santa Fe Group aquifer system. As compared to previous more regional-scale studies, this study was designed to provide spatially detailed information about the amount of water that discharges from the Rio Grande to the adjacent aquifer. Study results provide hydrologic data and enhance the understanding of rates of water leakage from the Rio Grande to the inner valley alluvial aquifer, groundwater flow through the aquifer, and discharge of water from the aquifer to the riverside drains.

The study area extends about 20 miles along the Rio Grande in the Albuquerque area, and the east and west edges of the study area are limited to areas within the inner valley adjacent to the Upper Corrales, Corrales, Albuquerque, and Atrisco Riverside Drains. The riverside drains are ditches located east and west of the river and generally separated from the river by levees. The drains are designed to intercept lateral groundwater flow from the river and prevent waterlogged-soil conditions in the inner valley. Seepage to the riverside drains constitutes one of the main sources of groundwater discharge from the inner valley alluvial aquifer.

Piezometers and surface-water gages were installed in paired transects at eight locations in the Albuquerque area. Each transect included nested piezometers and surface-water gages configured in roughly straight lines and oriented perpendicular to the river and riverside drains. At each location, transects extended from the Rio Grande to just outside the riverside drains on both sides of the river and are spaced about 500 ft apart. The paired-transect configuration was chosen to facilitate definition of horizontal and vertical gradients at each location. Nested piezometers, completed at various depths in the alluvial aquifer, and surface-water gages installed in the Rio Grande and riverside drains were instrumented with pressure transducers, and water-level and water-temperature data were collected from 2009 to 2010. Horizontal groundwater flux from the Rio Grande to the inner valley alluvial aquifer was estimated from Darcy's Law using hydraulic-gradient values estimated from water-level data and hydraulic-conductivity values estimated from slug tests. The Suzuki-Stallman one-dimensional analytical solution to the heat-transport equation also was used to model annual groundwater temperature changes within the aquifer and the results were used to provide additional detail on rates of groundwater flux with depth and distance from the river.

Water levels from the piezometers indicate that groundwater movement was usually away from the river towards the riverside drains. Hourly groundwater temperatures were recorded at 10 and 20 ft below land surface in selected piezometer nests. Large seasonal ranges in surface-water temperature are apparent; surface-water temperatures ranged from 29 degrees Fahrenheit (°F) in the winter to 81 °F in the summer. Surface-water temperatures in the drains typically were similar to temperatures measured in the Rio Grande, but the magnitudes of temperature fluctuations in the river were somewhat larger. Maximum and minimum water temperatures

in piezometers generally indicate a decrease in amplitude and an increase in time lag of the temperature signal with increasing depth and distance from the river.

Monthly vertical temperature profiles qualitatively show that heat transport is primarily within the upper 30 ft of the inner valley alluvial aquifer. Exceptions occur on the east side of the Rio Grande between Paseo del Norte and Barelas where geological heterogeneities and regional pumping may induce groundwater flux from the river to greater depths. Local-scale heterogeneities result in large ranges of groundwater flux and may reduce flux rates where clay- or silt-rich low-permeability sediments are present.

Annual mean horizontal groundwater gradients in the inner valley alluvial aquifer ranged from 0.0024 (I-25 East) to 0.0144 (Pajarito East). The median hydraulic-conductivity values of the inner valley alluvial aquifer determined from slug tests ranged from 30 feet per day (ft/d) (Montaño) to 120 ft/d (Central) for pairs of transects, with a median hydraulic conductivity for all transects of 50 ft/d. These values are close to the range of estimates (from 10 to 150 ft/d) determined by previous investigations. Daily mean groundwater fluxes computed using Darcy's Law and the slug-test results ranged from about 0.01 ft/d (Montaño West) to between 1.0 and 2.0 ft/d (Central East). By using the Suzuki-Stallman method, median annual groundwater flux was determined to be greatest at Alameda East (0.50 ft/d) and lowest at Alameda West (0.25 ft/d). The results from both methods agreed reasonably well.

Seepage investigations conducted by measuring discharge in the east and west riverside drains provided information for computing changes in flow within the drains and for evaluating results from Darcy's Law and Suzuki-Stallman method flux calculations. Discharge measured in the east riverside drain between the Barelas Bridge (east drain mile 0) and the I-25 bridge (east drain mile 9) indicated that the flow in the east riverside drain increased by an average of 56.5 cubic feet per day per linear foot ($ft^3/d/ft$) of drain. Discharge measured in the west riverside drain between the Central bridge (west drain mile 0) and the I-25 bridge (west drain mile 10) indicated that flow increased between west drain miles 0 and 4, an average of 53.8 $ft^3/d/ft$ of drain, and that flow increased between west drain mile 7 and mile 10, an average of 44.9 $ft^3/d/ft$ of drain. In comparison to the seepage measurement results, the groundwater fluxes from the river through the inner valley alluvial aquifer calculated from Darcy's Law (q_{slug}) and by the Suzuki-Stallman method (q_{heat}) would account for 20–36 percent or 53–95 percent, respectively, of the total flow in the east riverside drain and 22–31 percent or 19–26 percent, respectively, of the total flow in the west drain. These results indicate that the drains likely also receive water from outside the inner valley.

The spatial variability of horizontal hydraulic gradients and groundwater fluxes can be primarily attributed to variability in the distances between the river and riverside drains throughout the study area and geologic heterogeneities in the alluvial aquifer. Temporal variability in the water levels, which control the horizontal hydraulic gradients and fluxes between the Rio Grande and the riverside drains, can be primarily attributed to seasonal fluctuations in river stage and irrigation practices.

References

Anderholm, S.K., and Bullard, T.F., 1987, Description of piezometer nests and water levels in the Rio Grande Valley near Albuquerque, Bernalillo County, New Mexico: U.S. Geological Survey Open-File Report 87–122, 51 p.

Anderson, M.P., 2005, Heat as a ground water tracer: Ground Water, v. 43, no. 6, p. 951–968.

Barroll, Peggy, 2001, Documentation of the administrative groundwater model for the Middle Rio Grande Basin: Santa Fe, New Mexico, Office of the State Engineer, Hydrology Bureau Report 99–3, 22 p.

Bartolino, J.R., 2003, Chapter 2—the Rio Grande—Competing demands for a desert river, *in* Stonestrom, D.A., and Constantz, J., eds., Heat as a tool for studying the movement of ground water near streams: U.S. Geological Survey Circular 1260, p. 8–16.

Bartolino, J.R., and Cole, J.C., 2002, Ground-water resources of the Middle Rio Grande Basin, New Mexico: U.S. Geological Survey Circular 1222, 132 p.

Bartolino, J.R., and Niswonger, R.G., 1999, Numerical simulation of vertical ground-water flux of the Rio Grande from ground-water temperature profiles, central New Mexico: U.S. Geological Survey Water-Resources Investigations Report 99–4212, 34 p.

Bartolino, J.R., and Sterling, J.M., 2000, Electromagnetic surveys to detect clay-rich sediment in the Rio Grande inner valley, Albuquerque, New Mexico: U.S. Geological Survey Water-Resources Investigations Report 00–4003, 45 p.

Bexfield, L.M., and Anderholm, S.K., 2000, Predevelopment water-level map of the Santa Fe Group aquifer system in the Middle Rio Grande Basin between Cochiti Lake and San Acacia, New Mexico: U.S. Geological Survey Water-Resources Investigations Report 00–4249, 1 sheet.

Bexfield, L.M., and Anderholm, S.K., 2002, Estimated water-level declines in the Santa Fe Group aquifer system in the Albuquerque area, central New Mexico, predevelopment to 2002: U.S. Geological Survey Water-Resources Investigations Report 02–4233, 1 sheet.

Bexfield, L.M., and McAda, D.P., 2003, Simulated effects of ground-water management scenarios on the Santa Fe Group aquifer system, Middle Rio Grande Basin, New Mexico, 2001–40: U.S. Geological Survey Water-Resources Investigations Report 03–4040, 39 p.

Blasch, K.W., Constantz, Jim, and Stonestrom, D.A., 2007, Thermal methods for investigating ground-water recharge, *in* Stonestrom, D.A., Constantz, Jim, Ferré, T.P.A., and Leake, S.A., eds., Ground-water recharge in the arid and semiarid southwestern United States: U.S. Geological Survey Professional Paper 1703, appendix 1, p. 351–373.

Bouwer, Herman, and Rice, R.C., 1976, A slug test for determining hydraulic conductivity of unconfined aquifers with completely or partially penetrating wells: Water Resources Research, v. 12, no. 3, p. 423–428.

Butler, J.J., 1998, The design, performance, and analysis of slug tests: Boca Raton, Florida, Lewis Publishers, 252 p.

Carslaw, H.S., and Jaeger, J.C., 1959, Conduction of heat in solids (2d ed.): New York, Oxford University Press, 510 p.

Connell, S.D., Love, D.W., and Dunbar, N.W., 2007, Geomorphology and stratigraphy of inset fluvial deposits along the Rio Grande Valley in the central Albuquerque Basin, New Mexico: New Mexico Geology, v. 29, no. 1, p. 31.

Constantz, Jim, Thomas, C.L., and Zellweger, G.W., 1994. Influence of diurnal variations in stream temperature on streamflow loss and groundwater recharge: Water Resources Research, v. 30, no. 12, p. 3253–3264.

Constantz, Jim, Tyler, S.W., and Kwicklis, Edward, 2003, Temperature-profile methods for estimating percolation rates in arid environments: Vadose Zone Journal, v. 2, p. 12–24.

Constantz, J.E., Niswonger, R.G., and Stewart, A.E., 2008, Analysis of temperature gradients to determine stream exchanges with ground water, *in* Rosenberry, D.O., and LaBaugh, J.W., eds., Field techniques for estimating water fluxes between surface water and ground water: U.S. Geological Survey Techniques and Methods, book 4, chap. D2, 128 p.

Engdahl, N.B., Vogler, E.T., and Weissmann, G.S., 2010, Evaluation of aquifer heterogeneity effects on river loss using a transition probability framework: Water Resources Research, v. 46, no. 1, 13 p.

Engdahl, N.B., and Weissmann, G.S., 2010, Anisotropic transport rates in heterogeneous porous media: Water Resources Research, v. 46, issue 2, 12 p.

Falk, S.E., Bexfield, L.M., and Anderholm, S.K., 2011, Estimated 2008 groundwater potentiometric surface and predevelopment to 2008 water-level change in the Santa Fe Group aquifer system in the Albuquerque area, central New Mexico: U.S. Geological Survey Scientific Investigations Map 3162, 1 sheet.

Fetter, C.W., 1994, Applied hydrogeology (3d ed.): New Jersey, Prentice-Hall, 690 p.

Freeman, L.A., Carpenter, M.C., Rosenberry, D.O., Rousseau, J.P., Unger, Randy, and McLean, J.S., 2004, Use of submersible pressure transducers in water-resources investigations: U.S. Geological Survey Techniques of Water-Resources Investigations, book 8, chap. A, 65 p.

Google Inc., 2011, Google Earth (version 6.1) [Software]: Available at http://www.google.com/earth/index.html.

Gould, Jaci, 1994, Middle Rio Grande channel permeameter investigations: Albuquerque Area Office, Bureau of Reclamation Middle Rio Grande Water Assessment Supporting Document No. 11, variously paged.

Hawley, J.W., and Haase, C.S., 1992, Hydrogeologic framework of the northern Albuquerque Basin: New Mexico Bureau of Mines and Mineral Resources, Open-File Report 387, 176 p.

Hawley, J.W., and Whitworth, T.M.,1996, Hydrogeology and potential recharge areas for the basin and valley-fill aquifer systems and hydrogeochemical modeling of proposed artificial recharge of the Upper Santa Fe aquifer, northern Albuquerque Basin, New Mexico: New Mexico Bureau of Mines and Mineral Resources, Open-File Report 402–D, 68 p.

Heath, R.C., 1983, Basic ground-water hydrology: U.S. Geological Survey Water-Supply Paper 2220, 86 p.

Kernodle, J.M., McAda, D.P., and Thorn, C.R., 1995, Simulation of ground-water flow in the Albuquerque Basin, central New Mexico, 1901–1994, with projections to 2020: U.S. Geological Survey Water-Resources Investigations Report 94–4251, 114 p.

Kues, Georgianna, 1986, Ground-water levels and direction of ground-water flow in the central part of Bernalillo County, New Mexico, summer 1983: U.S. Geological Survey Water-Resources Investigations Report 85–4325, 24 p.

Lapham, W.W., Wilde, F.D., and Koterba, M.T., 1997, Guidelines and standard procedures for studies of ground-water quality—Selection and installation of wells, and supporting documentation: U.S. Geological Survey Water-Resources Investigations Report 96–4233, 110 p.

McAda, D.P., 1996, Plan of study to quantify the hydrologic relations between the Rio Grande and the Santa Fe Group aquifer system near Albuquerque, central New Mexico: U.S. Geological Survey Water-Resources Investigations Report 96–4006, 58 p.

McAda, D.P., 2001, Simulation of a long-term aquifer test conducted near the Rio Grande, Albuquerque, New Mexico: U.S. Geological Survey Water-Resources Investigations Report 99–4260, 58 p.

McAda, D.P., and Barroll, Peggy, 2002, Simulation of ground-water flow in the middle Rio Grande Basin between Cochiti and San Acacia, New Mexico: U.S. Geological Survey Water-Resources Investigations Report 02–4200, 81 p.

Moret, G.J.M., 2007, Annual variations in groundwater temperature as a tracer of river-aquifer interactions: State College, Pennsylvania State University, Ph.D. dissertation, 153 p.

National Climatologic Data Center, various dates, NCDC climate data online: accessed on various dates at http://www7.ncdc.noaa.gov/CDO/cdopoemain.cmd?datasetabbv=DS3505&countryabbv=&georegionabbv=&resolution=40.

Peter, K.D., 1987, Ground-water flow and shallow-aquifer properties in the Rio Grande inner valley south of Albuquerque, Bernalillo County, New Mexico: U.S. Geological Survey Water-Resources Investigations Report 87–4015, 29 p.

Powell, R.I., and McKean, S.E., 2014, Estimated 2012 groundwater potentiometric surface and drawdown from predevelopment to 2012 in the Santa Fe Group aquifer system in the Albuquerque metropolitan area, central New Mexico: U.S. Geological Survey Scientific Investigations Map 3301, 1 sheet. (Available at http://dx.doi.org/10.3133/sim3301.)

.Rankin, D.R., McCoy, K.J., Moret, G.J.M., Worthington, J.S., and Bandy-Baldwin, K.M., 2013, Groundwater hydrology and estimation of horizontal groundwater flux from the Rio Grande at selected locations in Albuquerque, New Mexico, 2003–09: U.S. Geological Survey Scientific Investigations Report 2012–5007, 75 p.

Reiter, Marshall, 2001, Using precision temperature logs to estimate horizontal and vertical groundwater flow components: Water Resources Research, v. 37, no. 3, p. 663–674.

Roark, D.M., 2001, Estimation of hydraulic characteristics in the Santa Fe Group aquifer system using computer simulations of river and drain pulses in the Rio Bravo study area, near Albuquerque, New Mexico: U.S. Geological Survey Water-Resources Investigations Report 01–4069, 52 p.

Sanford, W.E., Plummer, L.N., McAda, D.P., Bexfield, L.M., and Anderholm, S.K., 2003, Use of environmental tracers to estimate parameters for a predevelopment-ground-water-flow model of the Middle Rio Grande Basin, New Mexico: U.S. Geological Survey Water-Resources Investigations Report 03–4286, 102 p.

Sauer, V.B., and Meyer, R.W., 1992, Determination of error in individual discharge measurements: U.S. Geological Survey Open-File Report 92–144, 21 p.

Silliman, S.E., and Booth, D.F., 1993, Analysis of time-series measurements of sediment temperature for identification of gaining vs. losing portions of Juday Creek, Indiana: Journal of Hydrology, v. 146, p. 131–148.

Smerdon, J.E., Pollack, H.N., Cermak, Vladimir, Enz, J.W., Kresl, Milan, Safanda, Jan, and Wehmiller, J.F., 2004, Air-ground temperature coupling and subsurface propagation of annual temperature signals: Journal of Geophysical Research, v. 109, no. D21, 10 p.

Stallman, R.W., 1965, Steady one-dimensional fluid flow in a semi-infinite porous medium with sinusoidal surface temperature: Journal of Geophysical Research, v. 70, no. 12, p. 2821–2827.

Stonestrom, D.A., and Constantz, Jim, 2003, Heat as a tool for studying the movement of ground water near streams: U.S. Geological Survey Circular 1260, 96 p.

Suzuki, S., 1960, Percolation measurements based on heat flow through soil with special reference to paddy fields: Journal of Geophysical Research, v. 65, no. 9, p. 2883–2885.

Taylor, J.R., 1997, An introduction to error analysis—The study of uncertainties in physical measurements (2d ed.): Sausalito, Calif., University Science Books, 332 p.

Thorn, C.R., 1995, Surface-water discharge and evapotranspiration rates for grass and bare soil along a reach of the Rio Grande, Albuquerque, New Mexico, 1989–95: U.S. Geological Survey Open-File Report 95–419, 23 p.

Tiedeman, C.R., Kernodle, J.M., and McAda, D.P., 1998, Application of nonlinear-regression methods to a ground-water flow model of the Albuquerque Basin, New Mexico: U.S. Geological Survey Water-Resources Investigations Report 98–4172, 90 p.

U.S. Census Bureau, 2000, Census of population and housing—New Mexico 2000: Summary population and housing characteristics, PHC–1–33, 114 p.

Veenhuis, J.E., 2002, Summary of loss between selected cross sections on the Rio Grande in and near Albuquerque, New Mexico: U.S. Geological Survey Water-Resources Investigations Report 02–4131, 30 p.

Vennard, J.K., and Street, R.L., 1982, Elementary fluid mechanics (6th ed.): New York, N.Y., John Wiley & Sons, Inc., 700 p.

Publishing support provided by
Lafayette Publishing Service Center

ISSN 2328-0328 (online)
http://dx.doi.org/10.3133/sir20165021